ORGANIC DYES AS COLORIMETRIC SENSORS FOR ANIONS: SPECTRAL ANALYSIS

A DISSERTATION

Submitted in partial fulfillment of the requirements for the award of the degree of

MASTER OF TECHNOLOGY

in

ADVANCED CHEMICAL ANALYSIS

By

KARNISHA SHRIVASTAVA

DEPARTMENT OF CHEMISTRY
INDIAN INSTITUTE OF TECHNOLOGY ROORKEE
ROORKEE - 247 667 (INDIA)

JUNE, 2011

INDIAN INSTITUTE OF TECHNOLOGY ROORKEE, ROORKEE

CERTIFICATE

It is certified that the dissertation report entitled **"ORGANIC DYES AND CALORIMETRIC SENSORS FOR ANION: SPECTRAL ANALYSIS"** is the result of work carried out during the period of **July, 2010** to **June, 2011** by **Ms. KARNISHA SHRIVASTAVA**, Department of Chemistry, Indian Institute of Technology Roorkee, Roorkee under my supervision. Her work neither in part nor in whole has been submitted for any other degree.

Dr. K. R. JUSTIN THOMAS
Assistant Professor
Department of Chemistry
IIT Roorkee-247 667

Date: 30-6-2011
Place: ROORKEE

INDIAN INSTITUTE OF TECHNOLOGY ROORKEE, ROORKEE

CANDIDATE'S DECLARATION

I hereby certify that the work which is being presented in the thesis entitled **"ORGANIC DYES AND CALORIMETRIC SENSORS FOR ANION: SPECTRAL ANALYSIS"** in partial fulfillment of the requirements for the award of the Degree of **MASTER OF THECHNOLOGY** and submitted in the **Department of Chemistry, Indian Institute of Technology Roorkee, Roorkee,** is an authentic record of my own work carried out during a period from **July, 2010** to **June, 2011** under the supervision of **Dr. K. R. Justin Thomas, Assistant Professor, Department of Chemistry, Indian Institute of Technology Roorkee, Roorkee.**

The matter presented in the thesis has not been submitted by me for the award of any other degree of this or any other Institute.

Date: 30-6-2011

Place: ROORKEE

KARNISHA SHRIVASTAVA

ACKNOWLEDGEMENT

Apart from the efforts of me, the success of any thesis work depends largely on the encouragement and guidelines of many others. I take this opportunity to express my gratitude to the people who have been instrumental in the successful completion of this thesis work.

At first, I wish to express my deep sense of gratitude to my supervisor **Dr. K. R. Justin Thomas** for his invaluable supervision, advices and guidance from the very beginning of this research as well as giving me extraordinary experiences throughout the work. I am very thankful to him for his inspiring encouragement and kind cooperation. His unparallel guidance had changed my vision towards life, for which I will be ever grateful to him.

I would also like to thank **Professor V. K Gupta**, Head of the Department of chemistry, Indian Institute of Technology Roorkee and **Professor Kamaluddin**, former Head of the department for extending the instrumental facilities in the department and moral support to carry out these investigations.

This is a great opportunity to express my respect to **Dr. R. K. Dutta** (co-ordinator M.Tech), for his encouragement and support.

I would like to thank Mr. Dhirendra Kumar for his assistance in finalizing the research problem. I am truly in debt to you for always offering a helping hand and going that extra mile to do whatever you can do. One of the most important person Miss Neha Kapoor for lifting me up and encouraging me when I needed it the most. Thank you very much for your love and support.

I would even thanks to my other lab mates Mr. Sushil Kumar, Mr. Abhishek Baheti, Mr. B.M.N.K Prasad, Mr. A. Venkateswararao for their assistance, criticisms and useful insights. I am thankful to all the other Master students of IIT Roorkee with whom I share tons of fond memories. Those presences has always kept me cheerful and motivated me to achieve the highest and best in life.

Finally, I express my heartfelt gratitude to my highly respectable and adorable to my parents for their unconditional love, encouragement and blessings. They have been a guiding force throughout my life and I tried to measure up to their expectations. I would like to acknowledge the support and encouragement of my friends Mr. Ravi and Miss. Beenu. I humbly dedicate this work to them.

At last thanks to the almighty *God* who has given me the spiritual support and courage to carry out this work.

KARNISHA SHRIVASTAVA

Abstract

A new class of organic dyes containing hydrazone or imidazole chromophores have been synthesized and characterized as new colorimetric and ratiometric optical sensors for fluoride and acetate anions. These receptors show a unique selectivity and reactivity for fluoride and acetate in CH_3CN by deprotonation process leading to a colorimetric response which we can detect by naked eye. The binding between dye and anions have been confirmed by quantitative NMR analysis. In the NMR, signal corresponding to hydroxyl and imidazoles NH hydrogens disappeared after the addition of anions to the dye, moreover other signals shifted upfield, which confirms the binding of -OH and -NH hydrogen by the anion. This type of receptor binds fluoride and acetate *via* electrostatic interaction (anion-π and charge/electron transfer). The presence of strong electron withdrawing group (NO_2) enhanced the acidity of –OH and –NH, and the reactivity of fluoride and acetate towards the dyes. These sensors exhibited high selectivity for fluoride and acetate anions over other anions with more pronounced change in absorption characteristics. The binding properties of the dyes with the anions were evaluated by Job's, Benesi-Hildebrand and Scott methods.

Table of contents

List of Figure

List of Tables

Chapter 1

Colorimetric and Ratiometric Anion Sensors: Aim and Scope

Anions play an important role in many biological processes and pathological events and also in bulk materials such as fertilizers and industrial raw materials, all of which necessitate the development of sensitive anion sensors that use either optical or electrochemical outputs. The detection of fluoride anions is important for a wide range of applications such as medical diagnostics, environmental and chemical processing monitoring and even chemical warfare agent alerts, drinking water analysis [1].

In recent years, anion sensing and recognition has grown into an area of great interest in supramolecular and biological chemistry. As anion receptor interactions mainly of a hydrogen bonding and electrostatic nature, are different than the metal ligand coordination for cation receptor interactions, the design of anion receptors differs substantially from that of cation receptors. Among the several widely used fluoride and acetate detecting and sensing techniques including electrochemical colorimetric (UV) and fluorescence responses, UV and fluorescence detections have attracted the most attention since they have been demonstrated high sensitivities with detecting limit as low as sub-ppm (parts per million) [2].

A number of compounds capable to bind fluoride ion have been reported. It is often difficult to control selectivity and sensitivity among anions because of their wide range of geometries, low charge to radii ratios, sensitivities to pH, and high solvation energies. Among the anions, fluoride ions are one of the most attractive targets because of their considerable significance for health and environmental issues. As an essential element of the body, the U.S. Public Health

Service affirmed the optimal level to be 1 mg of consumed fluoride per day. On the other hand, unnecessary and inappropriate fluoride ingestion can result in fluorosis, urolithiasis, or even cancer. The EPA (United States Environmental Protection Agency) gives an enforceable drinking water standard for fluoride of 4 mgL^{-1} to prevent osteofluorosis and a secondary fluoride standard of 2 mgL^{-1} to protect against dental fluorosis [3].

To date, the ion-selective electrode, ion chromatography, and standard Willard and Winter methods are generally used for quantitative fluoride analysis. However, all these methods involve disadvantages, such as complicated procedures, high costs, or low mobility. Therefore, it is important to develop highly selective, sensitive, convenient, and rapid fluoride detection methods.

Optical chemosensors with high specificity and sensitivity, ease, and safety of handling have received considerable attention, and a number of fluorescence sensors have been reported that are capable of detecting fluoride ions. The recognition proceeded mostly through hydrogen bonding or Lewis acid coordination, and the sensors could only be operated in organic solvents to detect tetrabutylammonium (TBA) fluoride rather than inorganic fluoride salts [4].

In order to selectively differentiate between biologically interesting anionic substrates of similar basicity and surface charge density, such as fluoride ,acetate ,and hydrogen phosphate , considerable efforts have been made to develop hydrogen-bonding donors/receptors containing urea, thiourea, amide, phenol imidazole ion, or pyrrole subunits and to utilize different kinds of signaling mechanisms including internal charge transfer (ICT), photoinduced electron transfer (PET), metal-to-ligand charge transfer (MLCT), excimer/exciplex formation, and tuning proton transfer for fluorescence chemosensors. But the differentiation is always poor due to the same spectral outputs for the anion receptor interactions [5].

We have utilized the approach for the synthesis of colorimetric anion sensors which have been applied previously to attach the different chromophores (a signaling unit) such as nitrophenyl, anthraquinone, and nitrobenzene azo groups and other electron-withdrawing moieties to an anion receptor. In our recent efforts to develop chromogenic anion sensors for use in imidazole based sensor assays, we realized the need for anion sensors with varying substrate selectivity and different colorimetric response patterns. Inspired by our sensor's, which showed dramatic changes in color in the presence of inorganic anions Figure 1.1, we designed and synthesized sensors utilizing imidazole moieties, hoping that these would provide improved sensing performance (both binding and signaling). The selectivity of an anion sensor is related to the structure of the hydrogen bond complex and the basicity of the anions. Among anions, fluoride and oxygen in acetate are the most electronegative atoms and, as such, usually forms the strongest H-bond interaction with an -NH or -OH groups [6].

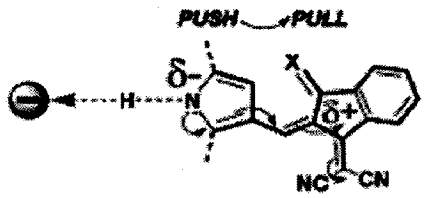

Figure 1.1 Anion hydrogen bonding results in partial charge transfer from electron-rich pyrrole to electron-poor indanylidene.

In this work our main approach to enhance the quality towards sensing of the fluoride and acetate over other anions. Reported sensors, in this work we are expecting the hydrogen bonding between anions and compound will take place by the deprotonation from -OH and -NH group present in the compounds and to increase the acidity of the hydrogen for good interaction we have introduced an electron deficient group in the structure.

1.1 References

1. Bhosale, S.V.; Bhosale, S.V.; Kalyankar, M. B.; Langford, S. J. *Org.Lett.* **2009**, *11*, 5418.

2. Ding, J.; Day, M. *Macromolecules* **2006**, *39*, 6054.

3. Zhao, Y.; Lin, Z.; Ou, S.; Duan, C.; Liao, H.; Bai, Z. *Inorg. Chem. Commun.* **2006**, *9*, 802.

4. Wu, Y.; Peng, X.; Fan, J.; Gao, S.; Tian, M.; Zhao, J.; Sun, S. *J. Org. Chem.* **2007**, *72*, 62.

5. Hu, R.; Feng, J.; Hu, D.; Wang, S.; Li, S.; Li, Y.; Yang, G. *Angew .Chem. Int. Ed.* **2010**, *49*, 4915.

6. Nishiyabu, R.; Anzenbacher, P. *Org. Lett.* **2006**, *8*, 359-362.

Chapter 2

Colorimetric and Ratiometric Anion Sensors: A Review

2.1 Introduction

Supramolecular chemistry is a highly interdisciplinary field of science. It covers the chemical, physical, and biological features of chemical species of greater complexity than individual molecules themselves which are held together and organized by means of intermolecular interactions. Traditional chemistry focuses on the covalent bonds where as supramolecular chemistry examines the weaker and reversible noncovalent interactions between molecules. There are number of such interactions that can be utilized. They include: hydrogen bonding, metal coordination, hydrophobic or solvatophobic effects, Van der Waals forces, electrostatic effects and π- π stacking interactions. Supramolecular chemists can be thought of as architects, who combine individual non-covalently bonded molecular building blocks, designed to be held together by intermolecular forces in order to create functional architectures. As supramolecular chemistry is a multidisciplinary field; a range of basic principles is required to obtain an understanding of a particular system.

Biological systems often provide inspiration, while organic and inorganic chemistry is required for the synthesis of the pre-designed supramolecular components, and physical chemistry is used to fully understand their properties. Finally, technical advances can lead to functioning devices ready for application to the real world. Perhaps the most important assets of a supramolecular chemist, however, are imagination and creativity, which have given rise to a wide range of beautiful and functional systems. Important concepts that have been demonstrated

by supramolecular chemistry include molecular self assembly, molecular folding, molecular recognition, host-guest chemistry, mechanically interlocked molecular architectures, and dynamic covalent chemistry.

2.1.1 Electrostatic interactions

Electrostatic interactions are based on the coulombic attraction between opposite charges. Ion-ion interactions are non-directional, while for ion-dipole interactions the dipoles must be suitably aligned for optimal binding efficiency. The high strength of electrostatic interactions has made them a prized tool amongst supramolecular chemists for achieving strong binding.

2.1.2 Hydrogen bonding

Hydrogen bonds have been utilized in receptors designed to coordinate neutral organic species, short chain alcohols, amides, and anions. The directional nature of hydrogen bonds, combined with the precision with which the individual components can be built into molecular systems has made them especially attractive to supramolecular chemists.

2.1.3 π- π stacking forces

These forces occur between systems containing aromatic rings. Attractive interactions can occur in either a 'face-to-face' or 'edge-to-face' manner. π-π interactions are caused by intermolecular overlapping of p-orbitals in π-conjugated systems, so they become stronger as the number of π-electrons increases.

2.1.4 Dispersion forces

Dispersion forces are due to an induced dipole - induced dipole interaction. Their strength depends on the polarizability of the interacting molecules. These van der Waals forces are believed to provide additional enthalpic stabilization to the coordination of a hydrophobic guest into a hydrophobic cavity.

2.1.5 The hydrophobic effect

The hydrophobic effect is the specific driving force for the association of apolar binding partners in aqueous solution. Water molecules around apolar surfaces of a hydrophobic cavity arrange themselves to form a structured array. Upon guest complexation water molecules are released and become more disordered, resulting in an increase in entropy. The hydrogen bonds between water molecules are stronger than the interactions between the water molecules and a polar solutes, thereby also providing an enthalpic force for apolar guest coordination in some cases.

2.1.6 Classical coordination chemistry

The interaction between metal centers and ligands is described as a dative bond, whereby, the ligand donates two electrons to form a Lewis acid-base interaction. Although not strictly a non covalent interaction itself, this "classical bond" is widely employed in supramolecular chemistry. The geometric requirements of metal ions combined with the design of specific ligands have permitted the construction of complex and eye-catching molecular topologies, often by a self assembled process.

2.2 Chemical sensor

The forces described above can be used individually, but in reality more than one type of interaction is usually utilized in concert to maximize the selectivity and tunability of the new receptor, and also to increase the strength of the complex formed. Chemical sensors from Figure 2.1 we can generally understood to be devices that transform chemical information into analytically useful signals.

The term chemosensor has been defined as a molecule of abiotic origin that signals the presence of matter or energy. Chemosensors are able to bind selectively and reversibly with the analyte of

interest. This results in a concomitant change in one or more properties of the system, such as redox potentials, absorption, or fluorescence spectra. Because of the two different processes occurring during analyte detection, i.e., molecular recognition and signal transduction, chemosensors are usually designed based on the classic reporting unit-spacer-receptor principle. The receptor is responsible for the selective binding of analyte, while the reporting unit e.g. chromophore or luminophore changes its properties upon complexation. The spacer can establish the geometry of the system and tune the electronic interaction between the two active moieties.

A sensor is a device, which responds to an input quantity by generating functionally related output; use the development of sensors to meet the need is referred to as sensor technology and is applicable in a very broad domain including the environment, medicine, commerce and industrially in the form of an electrical or optical signal [1].

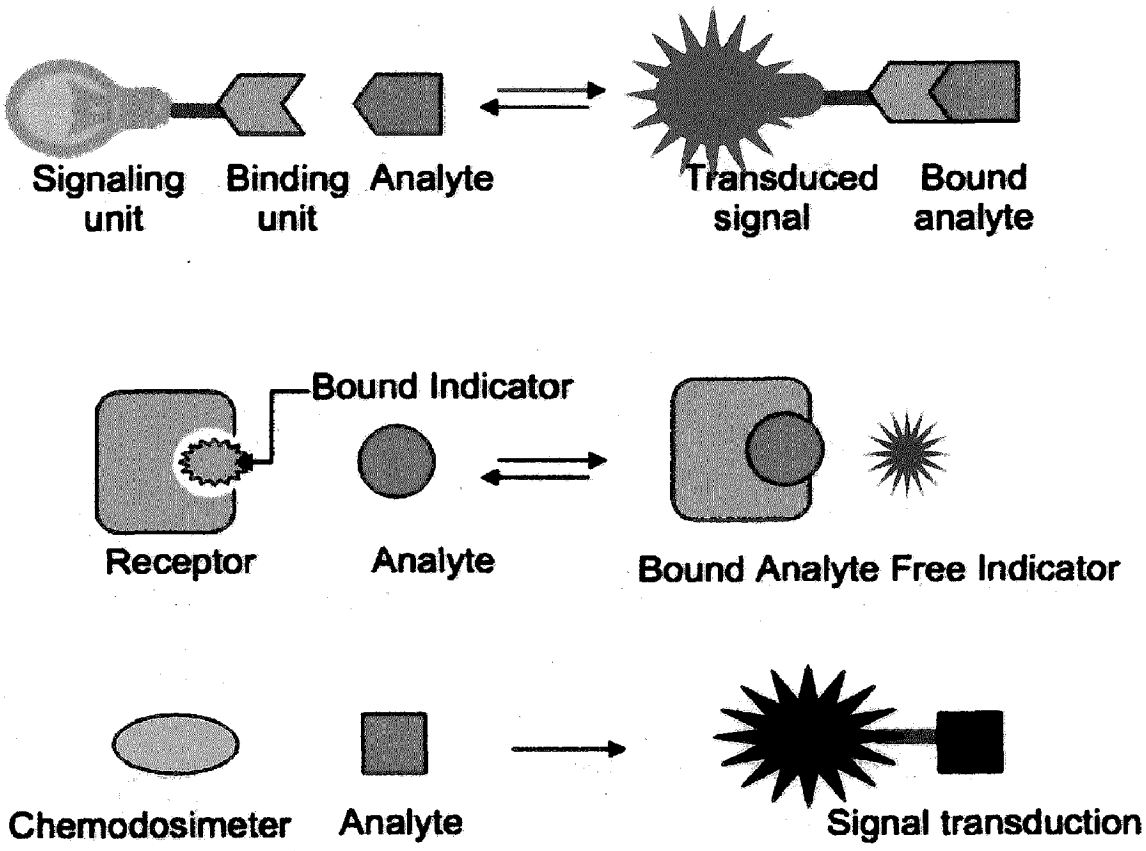

Figure 2.1 Different types of chemosensor designs.

2.2.1 ***Thermal Sensor***- The thermocouple is widely used temperature measuring instrument which can give the temperature value by converting into electrical signal.

2.2.2 ***Pressure sensor***- A pressure sensor measures pressure, typically of gases or liquids. Pressure is an expression of the force required to stop a fluid from expanding, and is usually stated in terms of force per unit area.

2.2.3*Potentiometric sensor*- This is the type of chemical sensor that may be used to determine the analytical concentration of some components of the analytical gas or solution.

2.2.4 ***Infra red sensor***-Infra red radiation consist of electromagnetic wave in the wavelength region of 0.75μm to 1000μm, lying between visible light and Microwave light. In order to cover this broad spectrum of wavelengths a variety of infra red detectors have been developed and produced.

2.2.5 ***Electrochemical Sensor***- Electrochemical Sensors are used to determine the concentration of various analytes in testing samples such as fluids and dissolved solid materials. So basically this type of sensor converts chemical property into electrical signal.

2.2.6 ***Optical Sensor***- Optical Sensors are used in numerous research and commercial applications today. These sensors are used for quality and process control, metrology, imaging, and remote sensing to mention a few uses. Today there are many types of optical sensors; many based on the use of lasers, imagers, and/or fibers. In this meeting, papers reporting the development of devices to implement the various sensor types and their configuration into sensing elements will be presented. Some of the enabling technologies to be discussed include advances in short pulse high power fiber lasers, super-continuum fiber lasers, semiconductor detectors and imagers, novel fiber sensor types such as micro-structured optical fibers of glass or polymer materials and micro-processors. This topical meeting will address various sensor types

including optical fiber, laser, and imaging sensors, and include all aspects of optical sensors from the component employed, their configuration through detection schemes and algorithms, and applications [2].

2.3 Types of optical sensor

It is based chemosensor by which we can sense the particular chemical species present in the solution:

2.3.1*Colorimetric Sensor*- If a system with a large color change can be developed. It could be incorporated into a diagnostic test paper for D-glucose, similar to universal indicator paper for pH.

2.3.2 *Ratiometric Sensor*- Ratiometric sensor measurements can increase the selectivity and the sensitivity of the detection, because the ratio of the fluorescent intensities at two wavelengths is independent of the concentration of the sensor, the fluctuation of source-light intensity, and the sensitivity of instrument.

2.3.3 *Cation Sensor*-Most conventional chemosensor development relied on rational design and the synthesis of a target ion recognition moiety. A recent alternative approach is configuring a dye array consisting of several non specific sensors to attain suitable responses and analyze their pattern as a fingerprint. Metal cation was the most extensively studied targets in this area.

2.3.4 *Anion Sensor*- Anion sensor is basically consists of an anion receptor and one sensing unit. The receptor binds the anion via the electrostatic force. The neutral anion receptor can be molecules containing urea, thiourea, Lewis acid and etc [3].

This type of unit usually binds an anion by hydrogen bonding. The sensory unit can give a signal transduction such as electrochemical signals or optical signals. Upon binding of an anion to the

receptor unit, the sensory part will give a signal change which can be detected by a special instrument or by naked eyes [4].

In this area, different types of chromogenic anion sensors are described, namely, NH-based hydrogen bonding, Lewis acid, metal-ion template, transition metal complexes, and chromogenic guest displacement. The first four types possess anion receptors attached directly to the chromophores, while the guest displacement techniques employ indicators that are replaced by specific anions. The last type has emerged recently and uses specific reactions between chromogenic hosts or indicators and particular anions to cause dramatic color changes [5].

In the field of supramolecular chemistry, the progress in synthetic receptors for anions has attracted considerable attention in recent decades due to the fact that a large number of biological processes involve molecular recognition of anionic species. It is thus important to develop techniques for quantifying or sensing such anions [6]. Nowadays, the development of colorimetric anion sensing is particularly challenging, since visual detection can give immediate qualitative information and is becoming increasingly appreciated in terms of quantitative analysis [7].

One approach to reach an effective, from Figure 2.2 anion sensor for biological anions involves the construction of optical anion sensors. Such a system generally consists of two parts:-

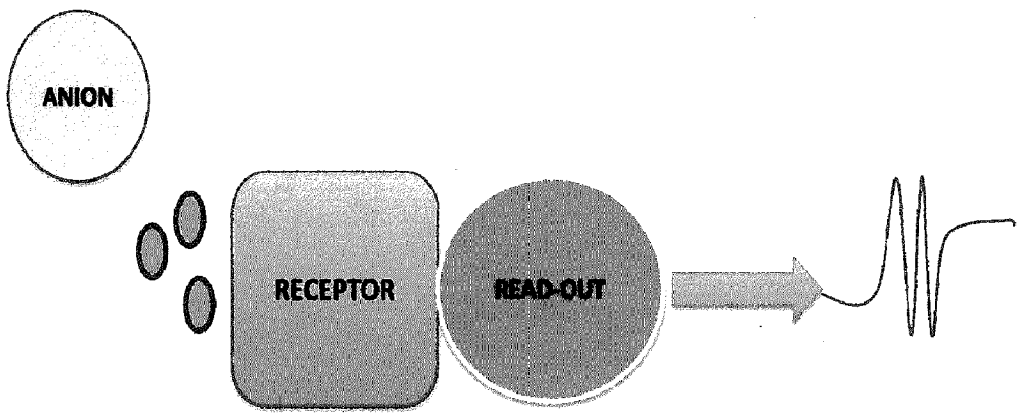

Figure 2.2 Operating principle of chromogenic anion sensors.

One part is an anion binding site employing various combinations of anion receptor units. Receptors can be mainly divided into two categories: neutral anion receptors and positive-charge anion receptors. Neutral anion receptors employed hydrogen bonding NH-based donors such as pyrroles, amides, and urea/thioureas or Lewis acids. Positive charge anion receptors use ammonium derivatives or guanidinium centers for binding negative-charge anions. The other is the chromophore part, which converts the binding events or recognition phenomena to optical signals. These two parts can be either covalently attached or intermolecularly linked to each other.

The concept of chromogenic anion sensors is illustrated in Figure 2.2. The crystal in the figure can be compared to analytes such as anions, and one unit acts like a receptor that is connected to readout. When the anion goes through the receptor unit that bind with the binding unit present in the receptor, then the signal produces from the readout this is the signal of the interaction between the anion and the receptor unit [8].

2.4 Host material

Receptor is a structure of molecule which can bind the particular ligand or ion. It can bind the particular species with different type of forces like electrostatic or ionic forces [14]. There should be some important quality in the receptor:

1. It should be very selective
2. It should be ultra sensitive
3. The sensor should be colorimetric & ratiometric for good results.

Among the reported sensors in this regard, fluorescent chemosensors attract particular attention because of their high selectivity, sensitivity, and simplicity. Some fluorescent

chemosensors for fluoride ion have been reported. Moreover, it is still difficult to recognize fluoride ion over oxygen-containing anion especially the acetate or dihydrogen phosphate ion (or both the two anions) due to their similar basicity and surface charge density. Only in recent years, there are few fluorescent sensors reported that can fully distinguish fluoride ion from the acetate and dihydrogen phosphate ion. So, it is significant to develop the "turn on"-type fluorescent sensor that can recognize fluoride ion with high selectivity.

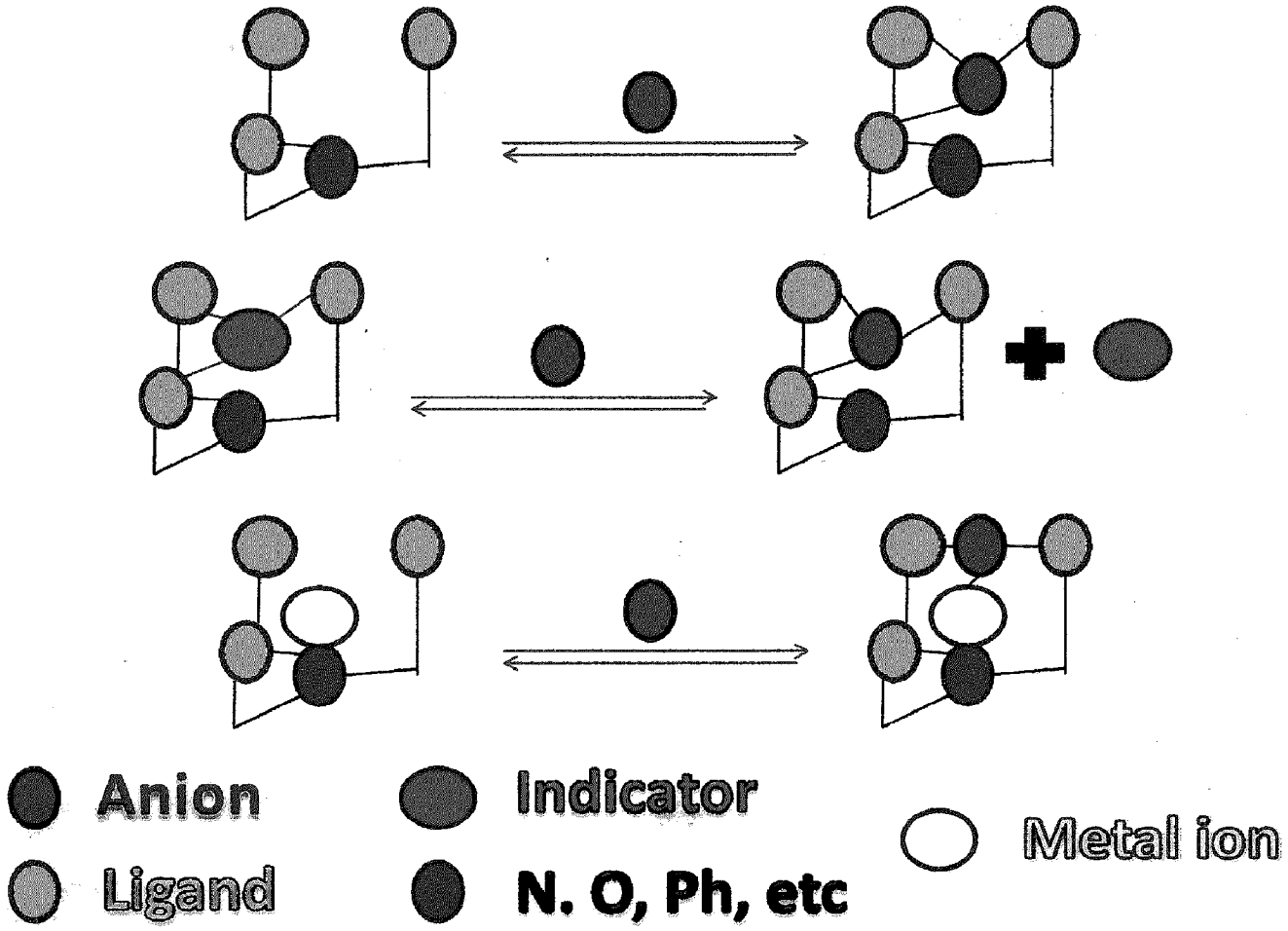

Figure 2.3 Binding of anion with different type of receptors.

Typically there are three from FIigure 2.3 approaches used by chemists in developing chemosensors for the detection of analytes. These are classified according to the arrangement of binding sites or reactive sites, and the signaling subunit in the sensor system. In the first

approach, the binding site and the signaling motif are both appended in the same molecule by a covalent bond. Once the analyte is bound to the binding site it induces a change in the electronic properties of the signaling unit indicating the sensing of the target anion. The second approach is the Indicator Displacement Approach or the Indicator Displacement Assay (IDA). This strategy represents a binding subunit-signaling subunit as "molecular ensembles". Once the analyte is bound to the receptor, the signaling subunit is released to the solution with a concomitant change in their optical characteristics. A third approach is called as "chemodosimeter approach. The chemodosimeter strategy is based on the use of a selective reaction, generally irreversible, that is induced by the target species and gives rise to some observable signal in fluorescence or in color. When designing sensors for various types of analytes chemists usually utilize one of the three approaches cited above.

Chromogenic anion sensors can be divided into two main categories: metal and nonmetal chromogenic hosts. For metal involved chromogenic hosts, the changing color comes from the Color of metals or metal complexes, especially transition metal ions, as their electronic properties are perturbed upon coordination to anions. The other way to generate a chromogenic sensor is to displace the coordinated chromophore by specific anions. Besides coordination aspects, the color changes can stem from reactions between chromogenic hosts or indicators and anions. This type of chromogenic anion sensor can be called a "chromoreactand". When the reaction occurs, the conformed host will definitely change its electronic properties. This results in an observable color change.

2.5 OH and NH-based hydrogen bonding chromogenic hosts

These hosts include simple anion sensor systems containing urea, thiourea, amine, amide, alcohol, and pyrrole groups linked to chromophores. Chromophores used in this type of

chromogenic anion sensors are mainly organic dyes such as azobenzene, nitrobenzene, indoaniline, and anthraquinone or extensively conjugated aromatic compounds such as quinoxaline, oxadiazole, and porphyrin. The color change occurs upon binding of anion guests that affect the electronic properties of the chromophores [15].

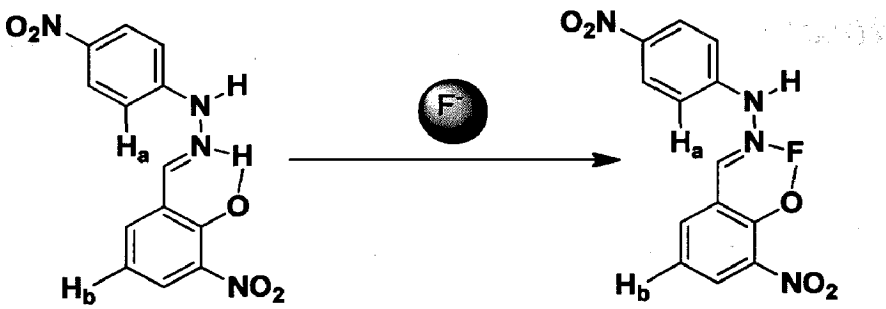

Figure 2.4 Interaction of fluoride ion with hydrogen through electrostatic force.

A number of commercially available compounds such as diaminoanthraquinone, nitroaniline, nitrophenylenediamine, nitrophenyl, thiourea, nitrophenol, alizarin, hydroxynaphthoquinone, naphthol, acridone as anion sensors in organic solvents such as dichloromethane. We can see from Figure 2.4 compounds contain hydrogen bond donors such as amine, amide, alcohol, and urea as anion binding sites. The compounds also contained chromophore subunits (acting as an electron acceptor) whose electronic properties were modified as a result of interactions with a bound anionic substrate (acting as an electron donor). The OH and NH-based hydrogen bonding chromogenic hosts can be classified as follows.

2.6 Hosts containing nitrophenyl unit

Thiourea is an especially good hydrogen bond donor and is an excellent anion receptor for carboxylate anions. From Figure 2.5 thiourea based chromophores with p-nitrophenyl units, C_1 and C_2 has reported in the previous work. As a result, compounds C_1 and C_2 were found to be

more highly selective for acetate than other anions in 1% water: MeCN. The binding properties of C_1 and C_2 with acetate showed that increasing the concentration of acetate produced a significant bathochromic shift in the UV–vis spectra. The stability constant of the acetate complex of C_1 was $5.6\times10^3\ M^{-1}$, much weaker than that of C_1 ($K_a=3.5\times10^5\ M^{-1}$). It was evident that introducing a p-nitrophenyl group into the (p-nitrophenyl) thiourea moiety enhanced the hydrogen bonding ability. Likewise, chromophore C_2 was then applied to the colorimetric determination of acetic acid in commercially available brands of vinegar [16].

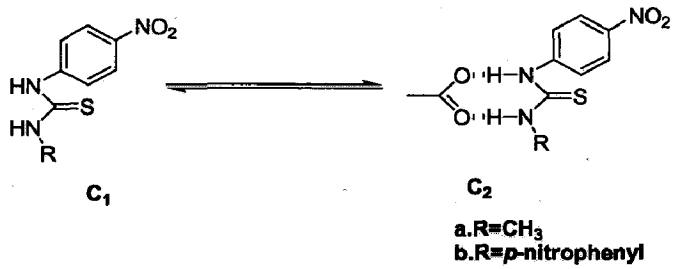

Figure 2.5 Hosts containing nitrophenyl unit.

From Figure 2.6 besides urea and thiourea, amide groups can also form effective chromogenic anion sensors. It has demonstrated the use of amide groups containing nitrophenyl-macrocycle C_3 as a selective colorimetric sensor for fluoride. DMSO solution of compound C_3 showed dramatic color changes upon addition of fluoride, acetae, and hydrogen phosphate ions. It was found that a colorless solution of C_3 turned dark blue (λ_{max}=593, 708 nm), yellow (λ_{max}=375 nm), and yellow (λ_{max}=384 nm) when exposed to fluoride, hydrogen phosphate, and acetate, respectively. However, compound C_4 formed a substantially stable 2:1 anion-to-ligand ratio with fluoride in DMSO-d_6 and CD_3CN with Ka values of 7.8×10^6 and $7.5\times10^6\ M^{-1}$ respectively [18]. The 3, 5-dinitrophenyl derivatives of pyrrole 2, 5-diamide C_4 acted as a selective naked-eye sensor for fluoride in MeCN solution, which gives rise to a deep blue color (λ_{max}=598 nm). This color change was due to a deprotonation process caused by fluoride acting

as a base and subsequent charge-transfer interactions between the deprotonated pyrrole and the nitroaromatic groups [17].

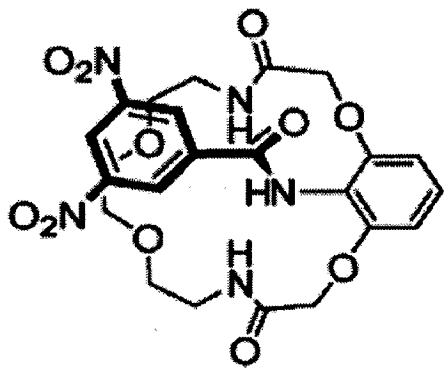

C_3

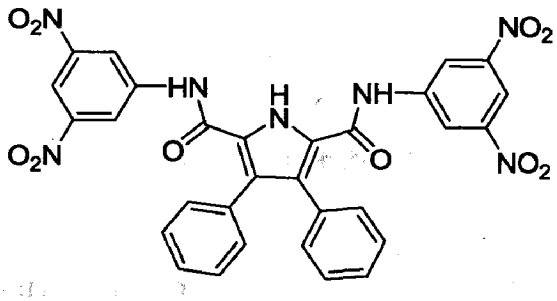

C_4

Figure 2.6 Hosts containing urea, thiourea and amide group.

From Figure 2.7 the pyrroles functionalized with nitrobenzene C_5 and C_6 can act as fluoride sensors. These systems bear an appended chromophore directly linked to the pyrrole skeleton through a conjugated C≡C triple bond. Upon addition of tetrabutylammonium fluoride, solutions of C_5 and C_6 in CH_2Cl_2 turned from pale yellow (λ_{max}=391 nm) to intense yellow (λ_{max}=433 nm) for C_5 and from yellow (λ_{max}=441 nm) to red (λ_{max}=498 nm) for C_6. In addition, the color changed from yellow (λ_{max} =441 nm) to orange when Cl^- (λ_{max}=483 nm) and $H_2PO_4^-$ (λ_{max}=478 nm) were added to a solution of C_6 [19].

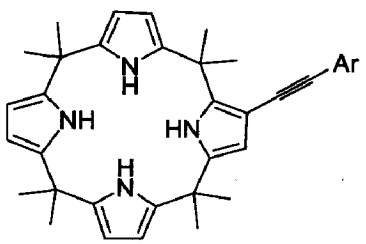

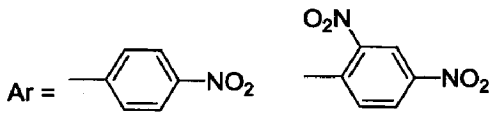

C_5 C_6

Figure 2.7 Hosts containing pyrrole functionalized with nitrobenzene.

2.7 Chromogenic hosts containing azo dye unit

From Figure 2.8 It has recently reported anion coordination with a nitro-azophenol thiourea-based sensor, compound C_7 .Association constants for anion binding were determined by ^1H NMR and UV–vis titrations in $CDCl_3$. Hydrogen phosphate ($Ka=2.6\times10^4\ M^{-1}$) and acetate ($Ka=1.9\times10^4\ M^{-1}$) gave stronger complexes with C_7 than other anions due to their high basicity [20].

Moreover, hydrogen phosphate with four oxygens makes the strongest complexes via multitopic hydrogen-bonding interactions and these results agreed with those obtained by ^1H NMR. The large downfield shifts of thiourea -NH resonances (>2.5 ppm) were detected upon complexation with hydrogen phosphate and acetate. Broadening of the phenol OH resonance was also observed, indicating its participation in hydrogen-bonding interactions with anions.

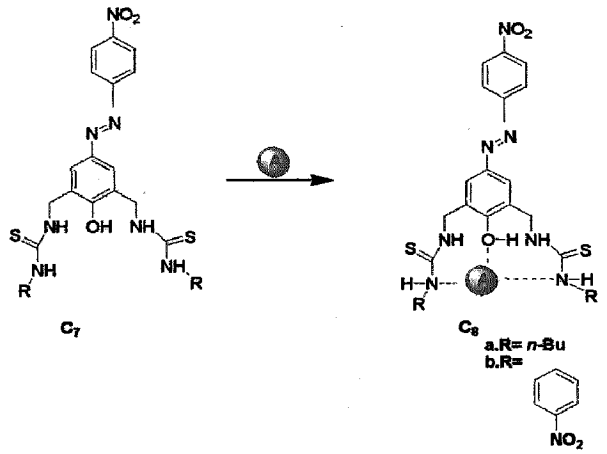

Figure 2.8 Hosts containing azo dye unit.

In the absence of anions, the UV–Vis absorption spectrum of C_7 showed an absorption λ_{max} =376 nm. Upon addition of hydrogen phosphate, the peak at 376 nm decreased while a new peak appeared at 529 nm, concomitant with a solution color change from light yellow to deep red [21].

This may be due to electronic excitation through charge transfer from the oxygen donor of the phenol to an acceptor substituent ($-NO_2$) of the chromophore. The excited state would be more stabilized by anion binding, resulting in a bathrochromic shift in the absorption maxima as well as a color change. Changing the substituent at the thiourea moiety of 1 from butyl groups to nitrobenzene groups in compound C_7 allowed the easy colorimetric differentiation of fluoride, hydrogen phosphate, and acetate which have similar basicity. The degree of red shift for C_8 was determined to be hydrogen phosphate ≥ acetate ≈ fluoride > bromide ≈ choride >hydrogen phosphate ≈ iodide in $CHCl_3$. The maximum red-shift value (λ_{max} =538 nm) for hydrogen phosphate can be understood on the basis of the guest basicity and the structure of the complex.

Hong and coworkers changed the signaling unit in compound C_9 from nitroazobenzene to indoaniline. From Figure 2.9 the compound C_9, a new chromogenic indoaniline–thiourea-based sensor, showed or hydrogen phosphate, the color of the $CHCl_3$ solution changed from blue-green (λ_{max} =678 nm) to deep significant color and UV–vis spectral changes upon binding anions. Upon the addition of hydrogen phosphate blue (λ_{max} =632 nm). The association constants obtained from UV–vis titrations for complexes of C_9 with hydrogen phosphate and hydrogen phosphate in $CHCl_3$ are 1.1×10^4 and 2.5×10^4 M^{-1},respectively. However,addition of acetate or fluoride ,which are more basic anions, caused a less intense color change. In addition, in the case of chloride, bromide, and iodide, no detectable color changes were observed. In the same manner as in compound C_9, compound C_9 possesses four NH urea moieties and allows the selective colorimetric detection of tetrahedral oxoanions such as hydrogen phosphate [22].

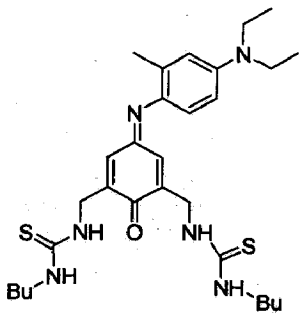

C_9

Figure 2.9 Host containing indoaniline thiourea based anion sensor.

2.8 Chromogenic host containing naphthalimide units

From Figure 2.10 the receptors C_{10}–C_{13}, which contain naphthalimide groups, can act as chromophores and show recognition of anion especially fluoride in DMSO. Upon addition of fluoride to the solution of C_{10}, 1:2 complexes was found concomitant with the color change from light yellow to deep purple, while receptors from C_{11}. C_{11}- C_{13} showed color changes from green to purple. These results can be attributed to strong hydrogen-bonding interactions between the 4-amino moiety of the naphthalimide group and fluoride, or more likely a complete deprotonation. Surprisingly, color changes of receptors from Figure 2.10 C_{11}-C_{13} reversed gradually with time due to the fixation of CO_2 (as HCO_3^-) by the receptors as 1:1 adducts. This was confirmed by X-ray crystallography [23].

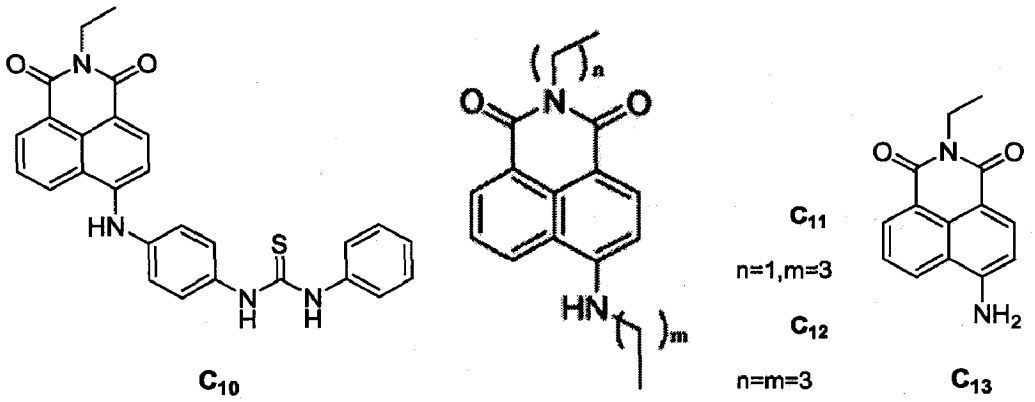

C_{10} C_{11} n=1,m=3 C_{12} n=m=3 C_{13}

Figure 2.10 Hosts containing naphthalimide unit based anion sensors.

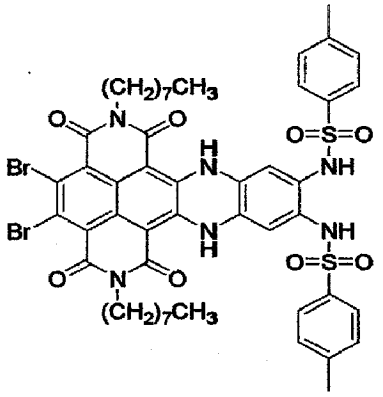

C_{14}

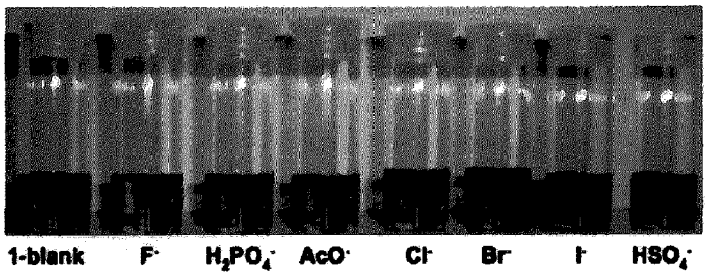

Figure 2.11 Color changes after addition of the different anions in naphthalimide based anion sensor.

The synthesis and characterization of a highly fluorescent core-substitutedfrom Figure 2.11 naphthalene diimide sensor C_{14} bearing a bis-sulfonamide group is described. The compound shows a unique selectivity and reactivity for the fluoride ion over other anions in $CHCl_3$ by a two-stage deprotonation process leading to a colorimetric response. In DMSO solution, the sensor is shown to be highly selective for fluoride (Ka ~ 10^6M^{-1}) over other anions with more pronounced changes in absorption characteristics [25].

On addition of Bu_4NF from 0 to 2.0 equiv in compound 3, the intensity bands at 559 and 609 In the presence of 3 equivalent of fluoride, the bands at 570 and 622 nm predominate with three clear isosbestic points observed.

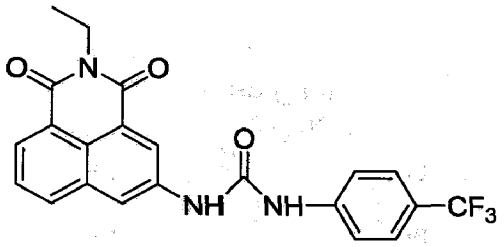

C_{15}

Figure 2.12 Host based on naphthalimide unit.

From Figure 2.12 the 1, 8-naphthalimide sensor C_{15} in Figure 2.12 was developed as a colorimetric and fluorescent sensor for anions. Being the first example of such anion sensors, where the 3-position of the naphthalimide ring is used to incorporate the anion recognition moiety, in this case a triflurомethyl derived aryl urea moiety, the sensors gave rise to significant changes in both the absorption and the emission spectra, which were both red shifted upon interacting with anions. The changes were most pronounced for fluoride, and to a lesser extent for acetate and hydrogen phosphate, in DMSO, making C_{15} a highly selective sensor for fluoride.

2.9 Chromogenic hosts containing naphthalene units

The fluoride-selective chromogenic and fluorescent sensor containing naphthalene urea was synthesized. From UV–visible studies, from Figure 2.13 the sensor C_{16} showed a characteristic band at 325 nm. Upon addition of fluoride, a new peak at 379 nm occurred in MeCN: DMSO (9:1 v/v). Furthermore, λ_{em} of compound C_{16} at 379 nm was shifted to 445 nm upon addition of (Ka=14,200 M^{-1}).

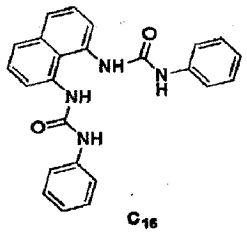

Figure 2.13 Host containing naphthalene.

Addition of other anions showed the same λ_{em} as free Figure 2.13 ^{1}H NMR results suggested that fluoride bound four urea -NH protons via hydrogen-bonding interactions, which resulted in the downfield shift of the -NH proton signals.

From Figure 2.14 the other dual-sensing receptor based on binaphthalene skeleton C_{16} bearing two thiourea groups showed sensing abilities toward fluoride, acetate, and hydrogen phosphate in MeCN. A bathochromic shift with unique isosbestic points was observed upon addition of these [28] anions. From fluorescence titrations, the intensity of λ_{em} of 15 at 459 nm decreased and a weak broad emission band around 650 nm occurred upon addition of fluoride ($Ka=2.1\times10^6\ M^{-1}$), acetate ($Ka=1.1\times10^5 M^{-1}$), and hydrogen phosphate ($Ka=5.5\times10^4\ M^{-1}$). X-ray crystallography showed that two naphthyl rings are placed in the same plane and two thiourea groups are located in the anti position. The thiourea groups are in the *syn–anti* conformation due to formation of intermolecular hydrogen bonds in the solid state. In the solution state, two naphthyl rings can freely rotate.

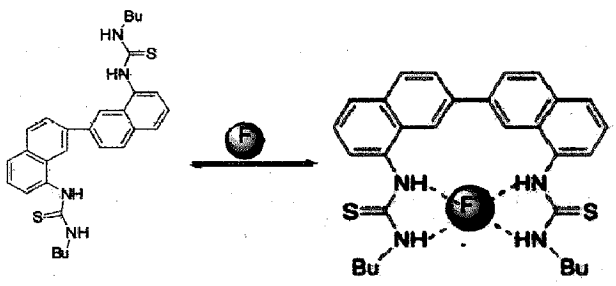

Figure 2.14 Hydrogen bonding interaction containing .naphthalene unit

2.10 Chromogenic hosts containing anthraquinone units

From Figure 2.15 anthraquinone based derivatives C_{17} and C_{18} showed potential as offluoridethe-shelf anion sensors. It was found that C_{17} had a more dramatic color change than C_{18} upon addition of anions. The solution of C_{17} in CH_2Cl_2 changed from yellow (λ_{max} =478 nm) to dark purple (λ_{max} =555 nm), red (λ_{max} =519 nm), reddish orange (λ_{max} =513 nm), orange (λ_{max} =499 nm), purple (λ_{max} =548 nm), and orange (λ_{max} =493 nm) when exposed to fluoride, chloride, bromide, iodide, hydrogen hosphate, and hydrogen sulphate respectively [15].

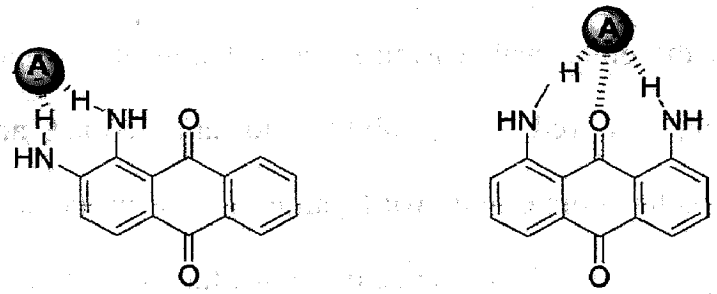

C_{17} C_{18}

Figure 2.15 Hosts containing anthraquinone unit.

Author have synthesized receptors 1,5-bis-*N*-(9,10-dioxo-9,10-di-hydroanthracen-1-yl)-*N'*-butylthiourea and its urea analogue, 1,5-bis-*N*-(9,10-dioxo-9,10-dihydroanthracen-1-yl)-*N'*-butylurea 2, by condensation of 1,5-diaminoanthraquinone with butyl isothiocyanate and butyl isocyanate, respectively [29].

From Figure 2.16 compound C_{20} showed a remarkable color change from orange to brown (λ_{max} =670 nm) in DMSO upon adding fluoride. Color changes are most probably due to a charge-transfer process and electron-rich formation of hydrogen bonds between thiourea-bound fluoride and the electron-deficient anthraquinone moiety. The anion was believed to form a 2:1 anion-to-ligand ratio as shown in compound C_{20} [29].

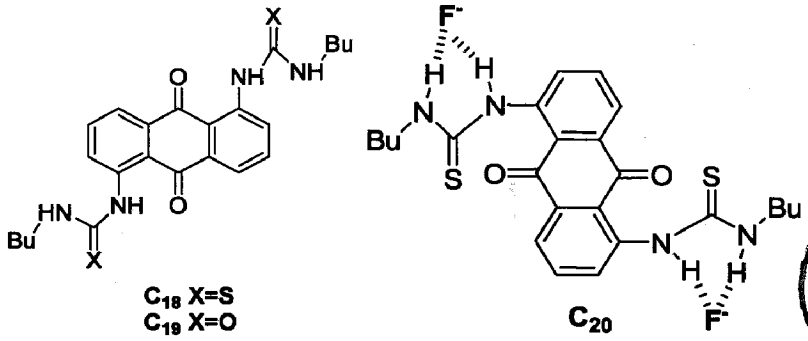

Figure 2.16 Proposed hydrogen bond formation between fluoride and sensors.

Similar to compounds C_{21} and C_{22} from Figure 2.17 , anthraquinone-functionalized [30] pyrroles C_{21} and C_{22} can act as fluoride sensors .Upon adding fluoride to solutions of C_{21} and C_{22} in CH_2Cl_2, the color of compound C_{21} changed from yellow (λ_{max} =467 nm) to red (λ_{max} =518 nm),

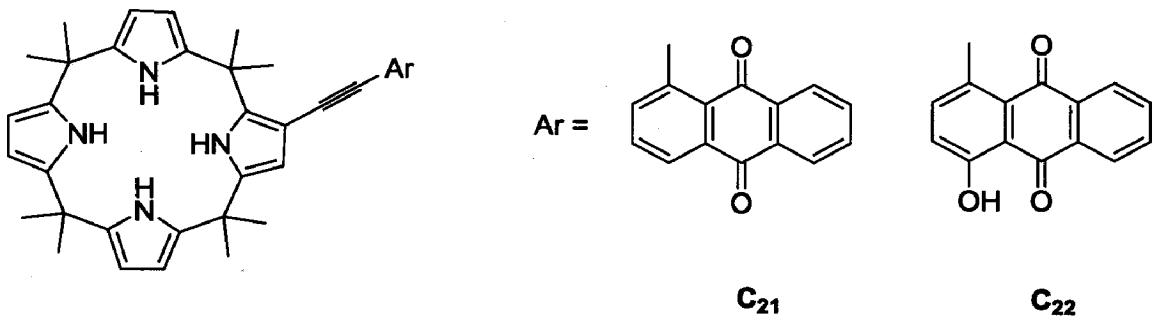

Figure 2.17 Hosts containing anthraquinone-fuctionalized pyrroles.

while C_{22} turned from red (λ_{max} =526 nm) to blue (λ_{max} =613 nm).The dramatic color changes were tentatively ascribed to charge-transfer interactions between electron-rich pyrrole-bound anions and electron-deficient anthraquinone moieties [6].

2.11 Chromogenic hosts containing oxadiazole and benzoxazole units

Wang and colleagues has synthesized two derivatives Figure 2.18 of oxadiazole C_{23} and C_{23} that were used as anion-fluorescent and -colorimetric sensors. The two compounds showed high

selectivity for hydrogen phosphate and fluoride over chloride in DMF. It was found that compounds C_{23} and C_{24} changed their color from colorless (λ_{max} =376 nm) to yellow (λ_{max} =400 nm) upon addition of fluoride and hydrogen phosphate in DMF. Association constants of C_{23} with fluoride and hydrogen phoshate are 8.6×10^4 and 7.9×10^5 M^{-1} respectively. Furthermore, compound C_{24} showed high selectivity toward hydrogen phosphate with $K_a=1.8\times10^6$ M^{-1}

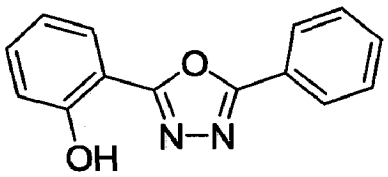

C_{23}

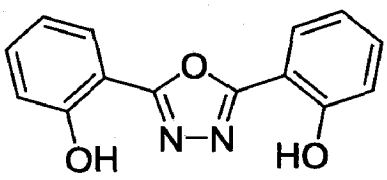

C_{24}

Figure 2.18 Hosts containing oxadiazole and benzoxazole units.

In DMF solution, Figure 2.19 the hydroxybenzoxazole-based polymer C_{25} showed selective colorimetric sensing ability for fluoride over hydrogen phosphate, chloride, and hydrogen sulphate [32]. Upon addition of fluoride to the solution of C_{25}, the color changed from colorless (λ_{max} =333 nm) to yellow (λ_{max} =420 nm) due to the binding of fluoride to this polymer. Therefore, compound C_{25} can act as a naked-eye detector for fluoride anion [31].

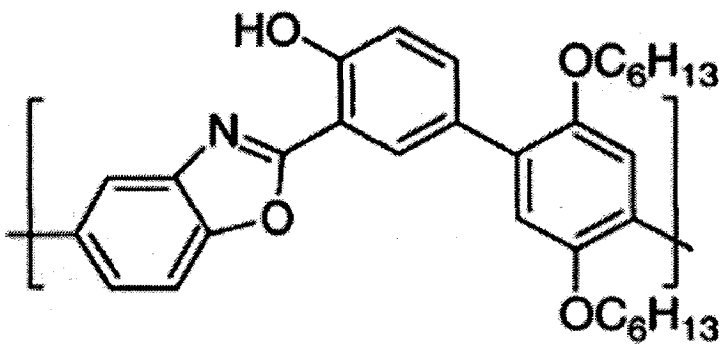

C_{25}

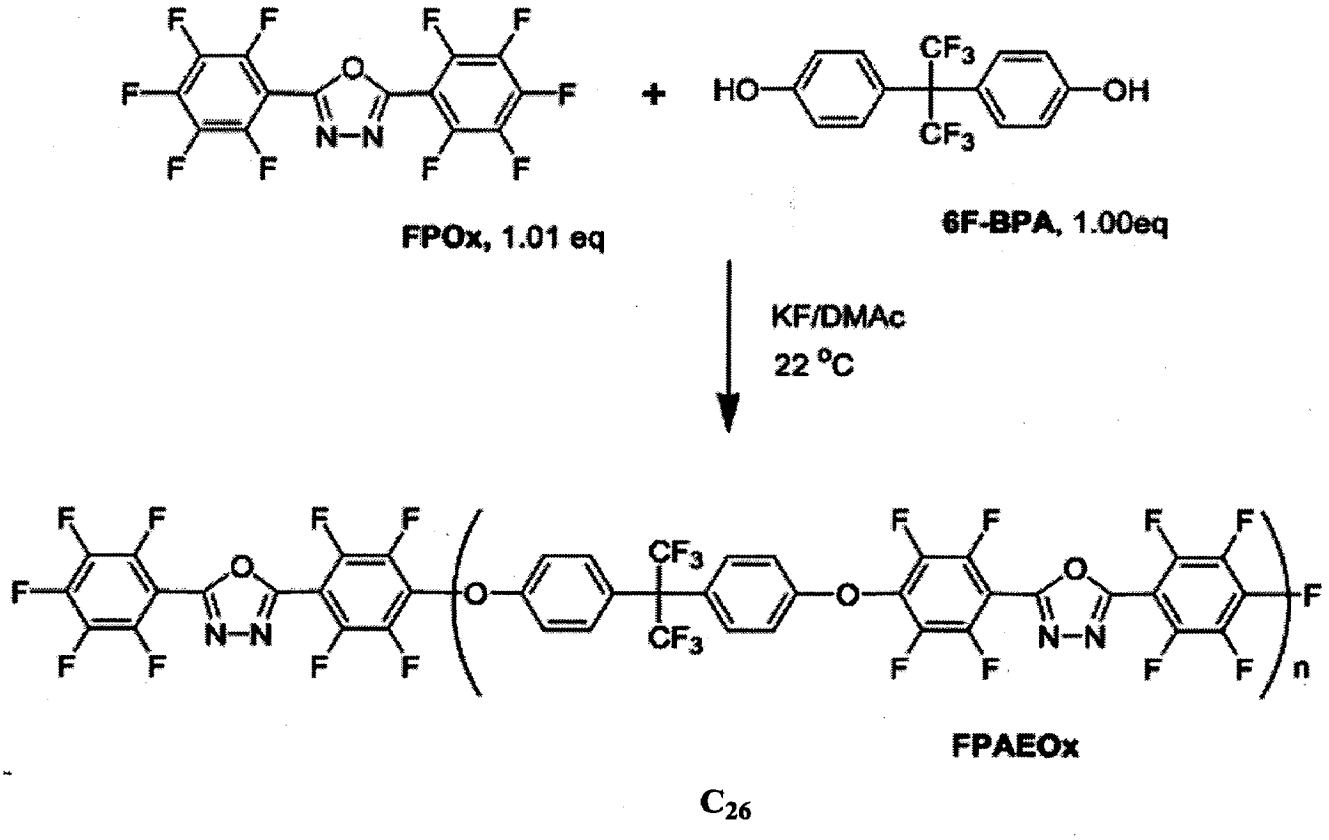

Figure 2.19 Polycondensation of FPOx with 6F BPA.

The polycondensation of FPOx with 6F BPA Figure 2.19 can be easily conducted at room temperature in the presence of KF to produce polymers with high molecular weights and well-defined linear chain structures. During the reaction, KF not only acts as a catalyst and as a base as found for other bis- (pentafluorophenyl) monomers, but also interacts with oxadiazole group in FPOx unit. This interaction consumed additional C_{27} equiv of KF. Therefore, compared to the reaction of otherbis (pentafluorophenyl) monomers, the reaction of FPOx required C_{27} equiv more KF so that the reaction can be completed. This interaction was confirmed by UV studies, which revealed a new strong absorption in the spectrum upon the addition of KF into the FPOx solution. This change in the UV spectrum upon the addition of KF has been further investigated to determine the possible use of FPOx as a sensory material for the detection of fluoride anion in solution. The results of this investigation suggest that this molecule has a very high sensitivity

and selectivity in both UV and fluorescence detection for sensing fluoride anion with a lower detection limit of about 0.1 ppm. The FPOx-containing polymer, FPAEOx, showed a similar sensitivity and selectivity in sensing fluoride anion in acetonitrile solutions. However, due to the poor solubility, the polymer in actonitrile showed a tendency of aggregation of the FPOx unit, which caused a lower sensitivity to the solution with low fluoride concentrations, (concentrations lower than 0.0135 mM) [33].

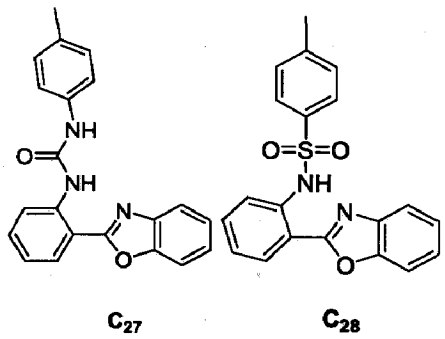

C_{27} C_{28}

Figure 2.20 Hosts containing oxadiazole and benzoxazole units.

From Figure 2.20 condensation of 2-(2′-aminophenyl) benzoxazole with p-toluenesulfonyl chloride and phenyl isocyanate yield new anion sensors, which can undergo excited-state intramolecular proton transfer (ESIPT) upon excitation. For the acid receptor C_{27}, the ESIPT process can be readily disturbed by basic anions such as fluoride , acetate , and hydrogen phosphate by deprotonating the sulfonamide unit, whereas in the case of C_{28}, a good hydrogen-bonding donor, from Figure 2.21 the ESIPT process is inhibited either by the fluoride induced deprotonation of the urea unit or by the formation of a strong acetate urea intermolecular hydrogen bond complex, and these two types of inhibition mechanisms consequently result in different ratiometric responses. But other anions with less hydrogen-bonding acceptor abilities cannot inhibit the ESIPT [38]. Interestingly, the different inhibition abilities of fluoride, acetate,

and hydrogen phosphate produce different spectral behaviors in C_{28}, so this new sensor successfully distinguishes the subtle difference in these three anionic substrates of similar basicity and surface charge density.

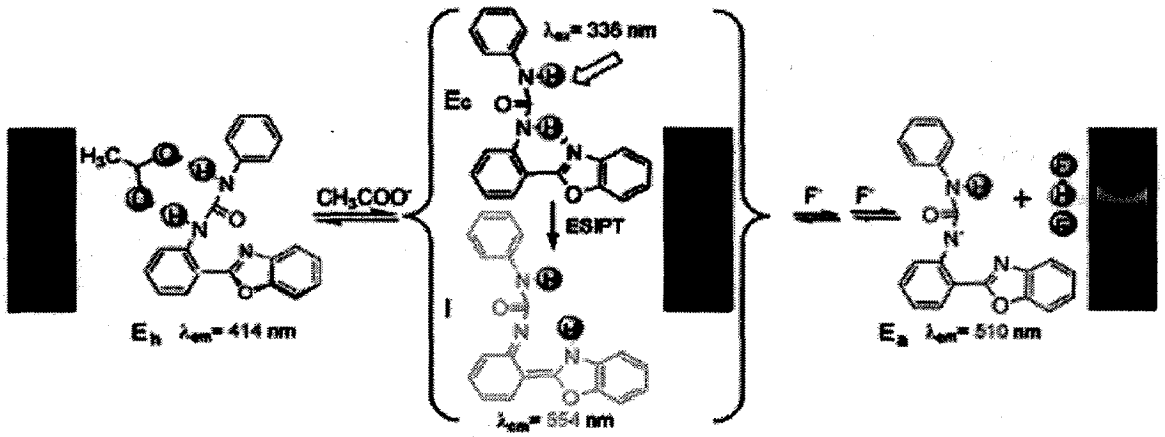

Figure 2.21 the fluoride induced deprotonation of the urea unit by the formation of strong intermolecular hydrogen bonding.

The absorption spectra of C_{27} and C_{28} were measured in different solvents. Their spectra are structured regardless of the solvent polarity which is indicative of the rigidity of the molecular frameworks. Their absorption band maxima undergo slight blue shifts with the increasing of the polarity and hydrogen-bonding capacity of the solvents, which is the result of the partial breaking of the IHB (intermolecular hydrogen bonding) with the formation of the -NH solvent hydrogen bond complex . Another interesting feature is the appearance of a weak absorption band above 350 nm in polar protic solvents. A similar weak absorption band has also been observed in 2-(2′-tosylamino phenyl) benzimidazole. This can be ascribed to the presence of small amounts of deprotonated ground-state anion. The acidic property of sulfonamide in TABO has made it easy to be deprotonated by the solvents with strong hydrogen-bonding acceptor

abilities. The interactions of sensors with anions were investigated through spectrophotometric titrations by adding a standard solution of the tetrabutylammonium salt of anions to a dry DMSO solution of sensors. The UV vis spectral changes of C_{27} during the titration with fluoride. Addition of fluoride induces the formation of a new red-shifted absorption band at 360 nm with the decrease of the band at 320 nm.

2.12 Chromogenic hosts containing dipyrroylquinoxaline units

Sessler and coworkers Figure 2.22 has investigated 2, 3-dipyrrol-2′-ylquinoxaline derivatives C_{29}- C_{31} as potential anion receptors and sensors [35]. The electronic influence of the functional groups present in the receptor played a crucial role in its recognition and sensing ability. It was found that receptor C_{30} had a higher affinity for fluoride (K_a=1.2×10^5 M^{-1}) than C_{29} (K_a=2×10^4 M^{-1}) in CH_2Cl_2.The solution of C_{30} underwent a dramatic color change from yellow to purple in the presence of fluoride. Furthermore, receptor C_{30} showed the lack of a complete -NH hydrogen bond donor. It then displayed a slight change in the optical spectrum.

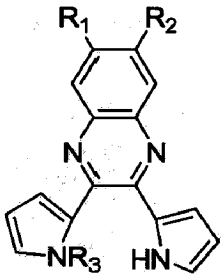

C_{29} R_1=R_2=R_3=H
C_{30} R_1=R_3=H,R_3=NO_2
C_{31} R_1=R_2=H,R_3=SEM

Figure 2.22 Hosts containing dipyrroylquinoxaline units.

The fluorinated dipyrrolylquinoxaline Figure 2.23 C_{32} underwent a sharp yellow to orange color change in the presence of both fluoride (K_a= 61,600 M^{-1}) and hydrogen phoshate (K_a=17,300 M^{-1}) anions in CH_2Cl_2 [36]. No changes in color were observed upon addition of chloride (K_a=180 M^{-1}).

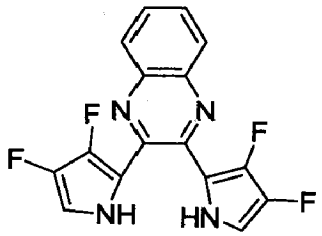

C_{32}

Figure 2.23 Hosts containing dipyrroylquinoxaline units.

Sessler has synthesized Figure 2.24 two novel quinoxaline derivatives bearing dipyrromethane C_{33} and tripyrromethane C_{34}. Both compounds were found to be much better anion receptors not only for fluoride (for C_{33} and C_{34}, K_a=32,000 M^{-1} and >1,000,000 M^{-1}), but also for hydrogen phosphate (C_{33} and C_{34}, Ka= 4,300 $M^{-1}$and 300,000 M^{-1}) in CH_2Cl_2.The substantial increase in affinities seen in the case of hydrogen phosphate was ascribed to the greater number of pyrrole -NH donors required to bind a larger anion.

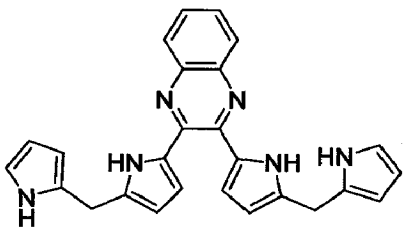

C_{33}

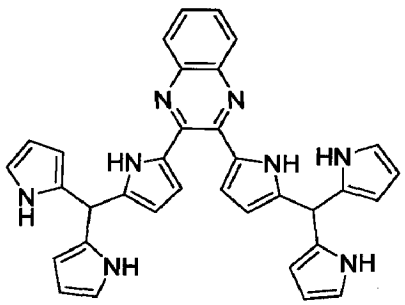

C_{34}

Figure 2.24 Two novel quinoxaline derivatives bearing dipyrromethane.

2.13 Chromogenic hosts containing quinolinium units

From figure 2.25 C_{35} and C_{35}, quinolinium-derived anion sensors have been synthesized which shows a turn-off fluorescence response in the presence of anions, with selectivity for acetate. The compound exhibits complex anion binding comprising of a host dimer, 2:1 and 1:1 host: guest species. Fluorescent quenching is due to both dynamic and static processes with charge transfer being the dominant mechanism [37].

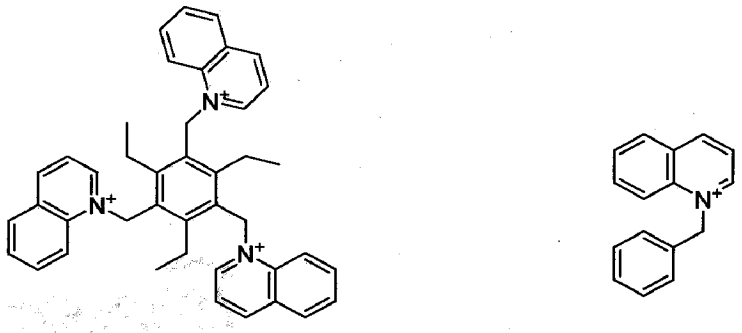

C_{35} C_{36}

Figure 2.25 Chromogenic hosts containing quinolinium units.

Significant chemical shift changes in the resonances assigned to the protons ortho and meta to the quinolinium nitrogen atom were observed, with very small shifts for the other signals. In all cases, infections in the isotherms occur before the addition of one equivalent of anion, suggesting more a complicated series of binding equilibria than a 1: 1 host: guest stoichiometry.

2.14 Nanoparticles containing NH-based hydrogen bonding chromogenic host

Nowadays, fabrication of chromophore-functionalized gold nanoparticles has emerged as one of the most exiting research areas, and their possible applications as anion sensors were also presented [38]. Figure 2.26, the amide-functionalized gold nanoparticle C_{37} was used for optical sensing of hydrogen phosphate, hydrogen sulphate, acetate, chloride, bromide, and iodide. In

CH_2Cl_2, nanoparticle C_{37} showed a red-wine color with a characteristic band centered at 520 nm [39]. When 0–0.5 equivalent of the anions were added to the solution of C_{37}, and then at 520 nm band decreased in intensity with a slight red shift in wavelength. This marked decrease in the intensity of the band was ascribed to an anion-induced aggregation of C_{37} through hydrogen bond formation between anions and the inter particle amide groups. Further addition of anions to C_{37} solution caused an increase in intensity of this plasmon band, which reflected the desegregation of the nanoparticle built by C_{37} and the corresponding anions.

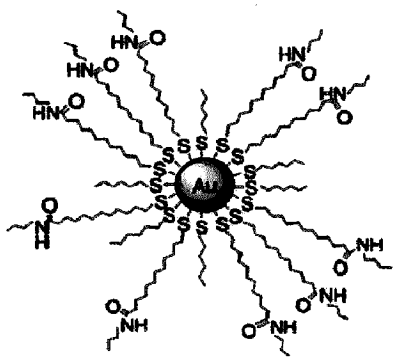

C_{37}

Figure 2.26 Nanoparticles containing NH-based hydrogen bonding chromogenic host.

This nanoparticle was capable of optically sensing changes in anion concentration at a level of 10^{-6}M.

2.15 Lewis acid chromogenic host

This section involves a type of receptor that requires the incorporation of a defined number and type of Lewis acids, such as Zn, and Hg, into a molecular skeleton with their electron deficient sites exposed for interaction Figure 2.27 with the lone electron pair of anions. Authors have synthesized an azo dye molecule with boronic acid, receptor C_{38}, which can act as a colorimetric sensor for detection of fluoride.

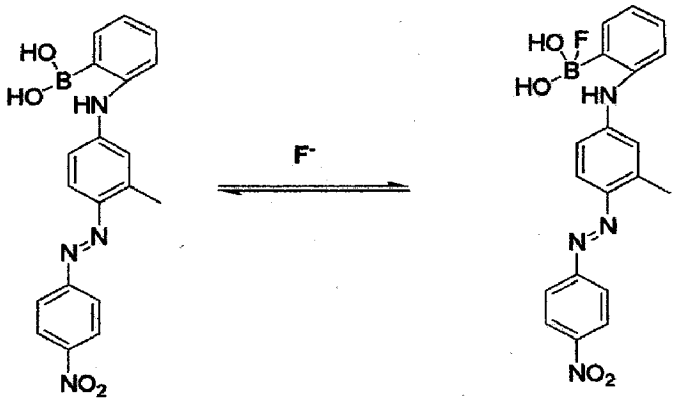

C_{38}

Figure 2.27 Lewis acid chromogenic hosts.

Upon addition of KCl, KBr, and KI in MeOH solution of 40 the orange absorbance at 450 nm increased in intensity, while KF caused a dramatic color change from orange (λ_{max}=450 nm) to claret (λ_{max} =563 nm) with K_a=130 M^{-1} [40].

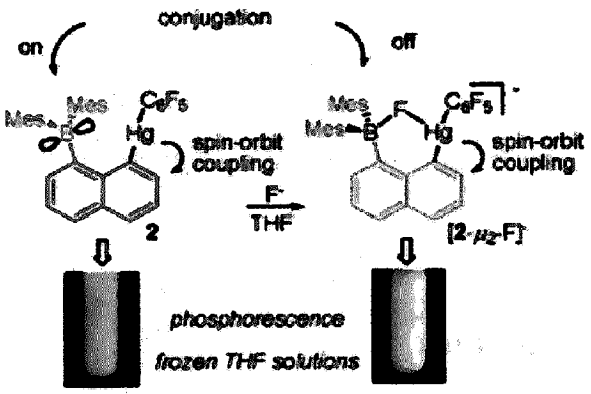

C_{39}

Figure 2.28 Lewis acid chromogenic hosts.

From Figure 2.28, it has reported a heteronuclear bidentate Lewis acid which serves as a highly selective and sensitive phosphorescent C_{39} fluoride sensor [41]. The proximity of the two Lewis acidic sites enforced by the 1, 8-naphthalenediyl backbone promotes fluoride anion

chelation and is responsible for the high binding constant. The interplay of conjugative and spin orbit coupling effects mediated by the boron and mercury atoms, respectively, results in the phosphorescent signaling of fluoride binding. To our knowledge, C_{39} is the first example of a *phosphorescent* anion sensor.

2.16 Transition metal complexes as chromogenic host

This type of chromogenic sensor utilizes the coordination chemistry of transition metal complexes, which have vacant binding sites to bind specific anions or have pendant arms containing anion receptor units. From Figure 2.29 C_{40} transition metal complexes already have their own specific colors due to their different electronic structures. Coordinating directly to anions or binding of anions by the pendant arms results in perturbations of their electronic structures and causes color changes [42].

A highly selective fluorogenic signaling fluoride-sensor Ru-HL, comprised of Ru-bipy moiety (bipy = 2, 2′-bipyridine) and 3-hydroxyl-2-naphthoylhydrazine was prepared and structurally characterized. The fluorescence spectra titration revealed the high selectivity and sensitivity of Ru-HL for fluoride through an excited-state intermolecular proton transfer (ESPT) signaling transduction mechanism.

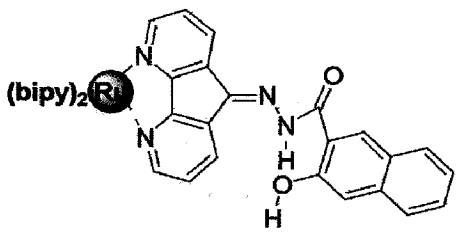

C_{40}

Figure 2.29 Transition metal complexes as chromogenic host.

2.17 Conclusions

We have summarized many different types of chromogenic anion sensors. Many anion receptors containing different anion binding sites and a plethora of chromophores have been described. Each type has its own advantages and drawbacks. The NH-based hydrogen bonding-type and Lewis acid-type sensors are simple and easy to use, but they have a limited use in some media such as water. The metal ion template type can be alternatively employed as a switchable "on" or "off" sensor utilizing a metal ion as a switch. The transition metal complex chromogenic hosts are still waiting for new discoveries. The indicator displacement method is a powerful approach in terms of analytical aspects, but it is sometimes complicated to use. Therefore, this type of chromogenic sensor, in particular, needs more development. There should be a lot of space to fill in this area .The chromoreactand has only recently emerged and definitely needs more investigation. Overall, chromogenic anion sensing is still a young field waiting for new disclosures. It is yet a long way to bring these synthetic sensors or systems to practical use. We optimistically believe that there is a way to combine the aforementioned approaches to fabricate an ultimate chromogenic sensor for a particular anion.

2.18 Reference

1. Shao, J. *J. Inclusion. Phenom. Macrocyclic Chem.* **2011**, *70*, 91.
2. Sokkalingam, P.; Lee, C. H. *J. Org. Chem.* **2011**, *76*, 3820.
3. Lehn, J. M. *Angew. Chem. Int. Ed. Engl.* **1988**, *27*, 90.
4. Schmidtchen, F. P.; Berger, M. *Chem. Rev.* **1997**, *97*, 1609.
5. Harley, J. H.; James, T. D.; Ward, C. J. *J.Chem. Soc. Perkin Trans. 1.* **2000**, 3155.
6. Gale, P. A. *Coord. Chem. Rev.* **2000**, *199*, 181.
7. Gale, P. A. *Coord. Chem. Rev.* **2001**, *213*, 79.

8. Gale, P. A. *Coord. Chem. Rev.* **2003**, *240*, 191.

9. Beer, P. D.; Gale, P. A. *Angew. Chem. Int. Ed.* **2001**, *40*, 486.

10. Lavigne, J. J.; Anslyn, E. V. *Angew. Chem. Int. Ed.* **2001**, *40*, 3118.

11. Fabbrizzi, L.; Poggi, A. *Chem. Soc. Rev.* **1995**, *24*, 197.

12. Suksai, C.; Tuntulani, T. *Chem. Soc. Rev.* **2003**, *32*, 192.

13. Martínez-Máñez, R.; Sancenón, F. *Chem. Rev.* **2003**, *103*, 4419.

14. Miyaji, H.; Sessler, J. L. *Angew. Chem. Int. Ed.* **2001**, *40*, 154.

15. Nishizawa, K. R.; Hayashita, S. T.; Teramae, N. *Tetrahedron Lett.* **2001**, *42*, 5053.

16. Piatek, P.; Jurczak, J. *Chem. Commun.* **2002**, 2450.

17. Camiolo, S.; Gale, P. A.; Hursthouse, M. B.; Light, M. E. *Org. Biomol. Chem.* **2003**, *1*, 741.

18. Miyaji, H.; Sato, W.; Sessler, J. L.; Lynch, V. M. *Tetrahedron Lett.* **2000**, *41*, 136.

19. Lee, D. H.; Lee, K. H.; Hong, J. I. *Org. Lett.* **2001**, *3*, 5.

20. Lee, D. H.; Lee, H. Y.; Lee, K. H.; Hong, I.-J. *Chem Commun.* **2001**, 1188.

21. Lee, D. H.; Lee, H. Y.; Hong, J.-J. *Tetrahedron Lett.* **2002**, *43*, 7273.

22. Gunnlaugsson, T.; Kruger, P. E.; Lee, T. C.; Parkesh, R.; Pfeffer, F. M.; Hussey, G. M. *Tetrahedron Lett.* **2003**, *44*, 6575.

23. Gunnlaugsson, T.; Kruger, P. E.; Jenson, P.; Pfeffer, F. M.; Hussey, G. M. *Tetrahedron Lett.* **2003**, *44*, 8909.

24. Bhosale, S. V.; Bhosale, S. V.; Kalyankar. M. B.; Langford. S. J. *Org. Lett.* **2009**, *11*, 5418.

25. Duke, R. M.; Gunnlaugsson, T. *Tetrahedron Lett.* **2011**, *52*, 1503.

26. Xu, G.; Tarr, M. A. *Chem. Commun.* **2004**, 1050.

27. Cho, E. J.; Moon, J. W.; Ko, S. W.; Lee, J. Y.; Kim, S. K.; Yoon, J.; Nam, K. C . *J .Am. Chem.* Soc. **2003**, *125*, 12376.

28. Kondo, S.; Nagamine, M.; Yano, Y. *Tetrahedron Lett.* **2003**, *44*, 8801.

29. Jiménez, D.; Martínez-Máñez, R.; Sanceñon, F. ; Soto, J. *Tetrahedron Lett.* **2002**, *43*, 2823.

30. Miyaji, H.; Sato, W.; Sessler, J. L. *Angew. Chem. Int. Ed.* **2000**, *39*, 1777.

31. Tong, H.; Zhou, G.; Wang, L.; Jing, X.; Wang, F.; Zhang, J. *Tetrahedron Lett.* **2003**, *44*, 131.

32. Wu, Y.; Peng, X.; Fan, J.; Gao, J.; Tian, M.; Zhao, J.; Sun, S. *J. Org. Chem.* **2007**, *72*, 6270.

33. Ding, J.; Day, M. *Macromolecules.* **2006**, *39*, 6054.

34. Black, C. B.; Andrioletti, B.; Try, A. C.; Ruiperez, C.; Sessler, J. L. *J. Am. Chem. Soc.* **1999**, *121*, 10438.

35. Anzenbacher, P. J.; Try, A. C.; Miyaji, H.; Jursíková, K.; Lynch, V. M.; Marquez, M.; Sessler, J. L. *J. Am. Chem. Soc.* **2000**, *122*, 10268.

36. Sessler, J. L.; Maeda, H.; Mizuno, T.; Lynch, V. M.; Fututa, H. *Chem. Commun.* **2002**, 862.

37. Thomas, K. G.; Kamat, P. V. *Acc. Chem. Res.* **2003**, *36*, 888.

38. Watanabe, S.; Sonobe, M. ; Arai, M. ; Tazume, Y. ; Matsuo, T. ; Nakamura, T.; Yoshida, K. *Chem. Commun.* **2002**, 2866.

39. Ward, C. J.; Patel, P.; James, T. D. *Chem. Lett.* **2001**, 406.

40. Swinburne, A. N.; Paterson, M. J.; Beeby, A.; Steed, J. W. *Org. Biomol. Chem.* **2010**, *8*, 1010.

41. Melaimi, M.; Gabbai, F. P. *J. Am.* Chem. Soc. **2005**, *127*, 9680.

Chapter 3

Hydrazone and Imidazole based Anion Sensors: Synthesis and Characterization

3.1 Introduction

We have successfully introduced the synthesis and characterization of the Hydrazone and Imidazole based anion sensor. We have also introduced a control molecule introducing the electron withdrawing group.

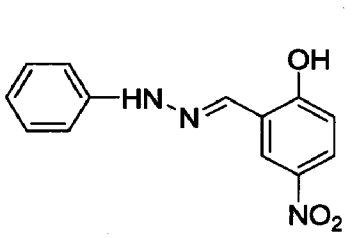

3a

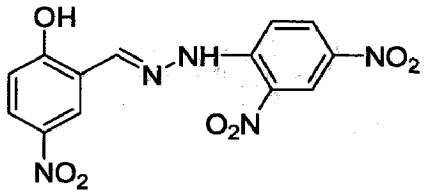

3b

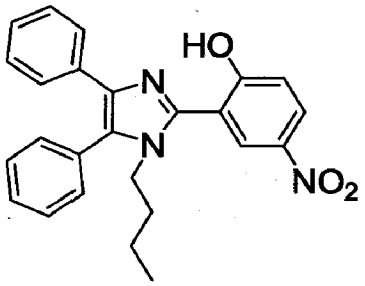

4a

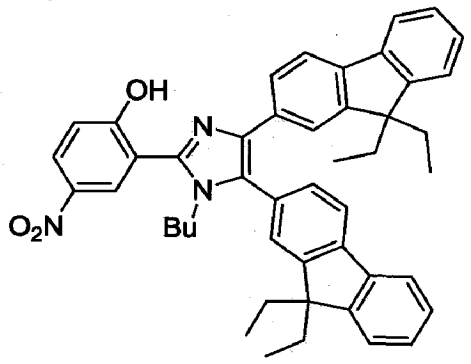

4b

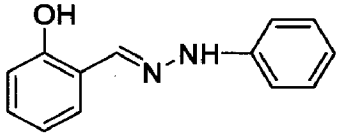

5a

Figure 3.1 Structure of all the dyes (**3a, 3b, 4a** and **4b**).

3.2 Materials and methods

All the chemicals were commercially available and they were used without further purification. All solvents were dried and distilled immediately prior to use by standard procedure. ^{1}H and ^{13}C NMR spectra were recorded on Bruker AV 500 O FT-NMR spectrometer. Deuterated chloroform ($CDCl_3$), dimethylsulphoxide (DMSO-d_6) or acetonitrile-d_3 (CD_3CN) was used as solvent. UV-vis absorption spectra were recorded at room temperature in quartz cuvettes using Shimadzu UV-1800 spectrophotometer for 2.0×10^{-5} M solutions of relevant dyes in acetonitrile. The IR spectra were recorded on NEXUS FT-IR (THERMONICOLET).

3.3 General synthesis of 2-hydroxy-5-nitrobenzaldehyde

To a cold solution of salicylaldehyde (5 mL, 0.049 mol) in acetic acid (30 mL), conc. nitric acid (5 mL) was added dropwise over 3.5 h in such a tempo to keep the temperature below 10° C. After addition, the reaction mixture was heated up to 50° C over 30 min. Then the reaction mixture was cooled to room temperature and poured into ice and left for 8 h. A yellow precipitate was obtained which was filtered out and dissolved in warm aqueous solution of sodium hydroxide (3 g of NaOH 50 mL). The resulted red solution was left to crystallize overnight and the formed sodium salt of 5-nitro-2-hydroxybenzaldehyde was separated by filtration and then hydrolyzed with hydrochloric acid. Crystallization of the resulted solid from acetic acid afforded the creamy needles of 5-nitro-2-hydroxybenzaldehyde.

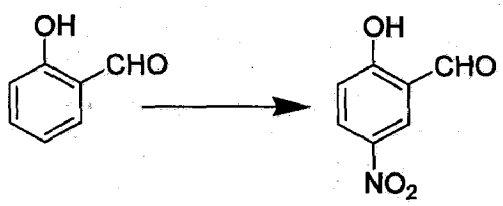

Figure 3.2 Synthetic route of 2-hydroxy-5-nitrobenzaldehyde.

2-hydroxy-5-nitrobenzaldehyde, it was synthesized from the 2-hydroxybenzaldehyde by using general procedure above, White crystals. Yield: 41%.^{1}H NMR ($CDCl_3$, 500 MHz): δ 11.61 (s, 1 H), 10.01 (s, 1 H), 8.57 (d, J = 2.5 Hz, 1 H), 8.42 (dd, J = 6.5 Hz, 1 H), 7.26 (s, 1 H), 7.13 (s, 1 H).

3.4 Synthesis of hydrazone based Anion sensor (3a and 3b)

3.4.1 *General Synthesis of (E)-4 nitro-2-((2-phenyl hydrazono) methyl) phenol (3a)*

A mixture of 2-hydroxy-5nitro benzaldehyde (0.1672 g, 1mmol), 1-phenyl hydrazine (0.1081 g, 1mmol) and ethanol (5ml) was heated at 85° C for 12 h in the round bottom flask. After the completion of the reaction after this the mixture poured into water and then the yellow precipitate was filtered out.

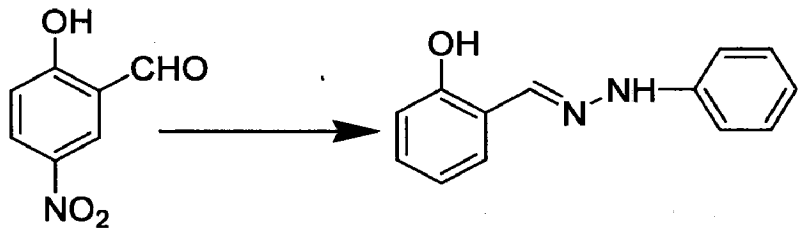

Figure 3.3 Synthetic route of **3a**.

(*E*)-4 nitro-2-((2-phenyl hydrazono) methyl) phenol (3a)

3a it was synthesized from 2-hydroxy-5-nitrobenzaldehyde and got Yellow solid. Yield: 90%. mp: 198-200° C. ^{1}H NMR ($CDCl_3$, 500 MHz): δ 11.72 (s, 1 H), 8.12-8.14 (m, 2 H), 7.90 (s, 1 H), 7.78 (s, 1 H), 7.33-7.36 (m, 2 H), 7.06-7.07 (m, 1 H), 6.98-7.01 (m, 3 H). ^{13}C NMR ($CDCl_3$,125 MHz): δ 162.11, 142.33, 140.40, 138.00, 129.52, 125.19, 124.74, 121.57, 118.40, 117.07, 112.65. FT-IR (KBr, cm^{-1}): 3427, 3328, 3079, 1602, 1338.

3.4.2 *General synthesis of (E)-2-((2, 4-dinitro phenyl)hydrazono) methyl) (3b)*

A mixture of 2-hydroxy-5-nitrobenzaldehyde (0.1672 g, 1mmol), 1-(2,4-dinitrophenyl) hydrazine (0.1081 g, 1mmol) and ethanol (5mL) was heated at 85° C for 12 h in the round bottom flask. The completion of the reaction was analyzed by TLC. After that the mixture was poured into ice water. A orange precipitate formed which was washed many time with ice water, filtered and collected.

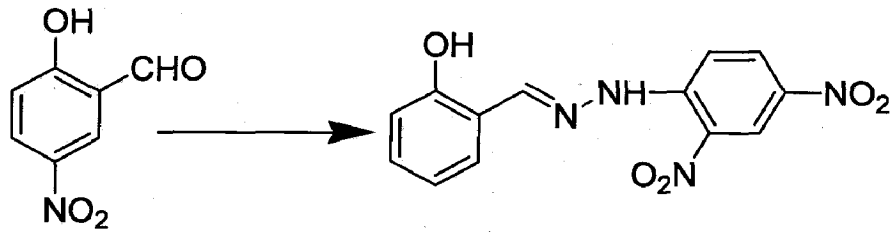

Figure 3.4 Synthetic route of **3b.**

(*E*)-2-((2,4-dinitro phenyl)hydrazono) methyl) (3b) we synthesized from 2-hydroxy-5-nitrobenzaldehyde : Orange solid. Yield: 92%. mp: 290-293° C. ^{1}H NMR ($CDCl_3$, 500 MHz): δ 11.85 (s, 1 H), 9.00 (s, 1 H), 8.86 (d, J = 2.5 Hz, 1 H), 8.65 (d, J = 3.0 Hz, 1 H), 8.46 (dd, J = 2.5, J= 7 Hz, 1 H), 8.19 (dd, J = 3, 6 Hz, 1 H), 8.09 (d, J = 9.5 Hz, 1 H). FT-IR (KBr, cm^{-1}): 3440, 3286, 3079, 1613, 1337.

3.5 Synthesis of imidazole based Anion Sensor (4a and 4b)

3.5.1 *General Synthesis of 2-(1-butyl-4, 5-diphenyl-1H-imidazole-2-yl)-4-nitrophenol (4a)*

A mixture of 2-hydroxy-5-nitrobenzaldehyde (0.1672 g, 1mmol), 1,3-diphenylpropane-1,2-dione, butan-1-amine (0.0878 g, 1.2mmol), ammonium acetate (0.231 g, 3mmol) and acetic acid (5mL) were heated at 125° C for 24 h in the round bottom flask. The completion of the reaction was analyzed by TLC. After that the mixture was poured into ice water. The residue was adsorbed on silica gel. The desired product was purified by column chromatography by using hexane/dichloromethane mixture as eluant.

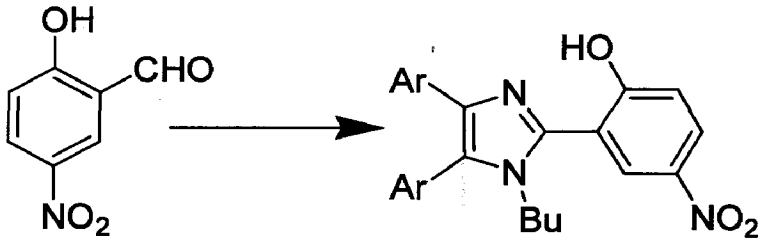

Figure 3.5 Synthetic route of **4a.**

2-(1-butyl-4,5-diphenyl-1*H*-imidazole-2-yl)-4-nitrophenol (4a)

Yellow solid.Yeild:41%. mp:190-192° C. ^{1}H NMR ($CDCl_3$, 500 MHz): δ 8.35 (d, J = 3 Hz, 1 H), 8.27 (dd, J = 3Hz, J = 6Hz, 1 H), 7.53-7.58 (m, 3 H), 7.46-7.48 (m, 2 H), 7.39 (dd, J =1, J =7.5 Hz, 2 H), 7.21-7.23 (m, 3 H), 7.16-7.19 (m, 1 H), 3.85 (dd, J = 8, 7.5 Hz, 2 H), 1.28-1.34 (m, 2 H), 0.93-1.00 (m, 2 H), 0.55 (t, J = 7.5 Hz, 3 H). ^{13}C NMR ($CDCl_3$, 125 MHz): δ 164.59, 142.56, 139.33, 134.70, 132.40, 131.35, 130.75, 129.73, 129.41, 128.40, 127.23, 126.46, 125.60, 121.17, 118.44, 113.10, 45.65, 32.42, 29.72, 19.64, 13.37. FT-IR (KBr, cm^{-1}): 3440, 3062, 2921, 1592, 1331.

3.5.2 *General synthesis of 2-(1-butyl-4, 5-bis(9,9-diethyl-9H-fluoren-2-yl)-4-nitrophenol (4b)*

A mixture of 2-hydroxy-5-nitrobenzaldehyde (0.1672 g, 1mmol), 1-3-bis(9,9-diethyl-9*H*-fluoren-2-yl)propane-1,2-dione (0.5127 g,1mmol),ammonium acetate (0.231 g, 3mmol) and acetic acid (5mL) was heated at 125° C for 24 h in the round bottom flask. After the completion of reaction it was evaporated for dryness in a rotary evaporator and the residue was adsorbed on silica gel. It was purified by column chromatography by using hexane/dichloromethane mixture as eluant.

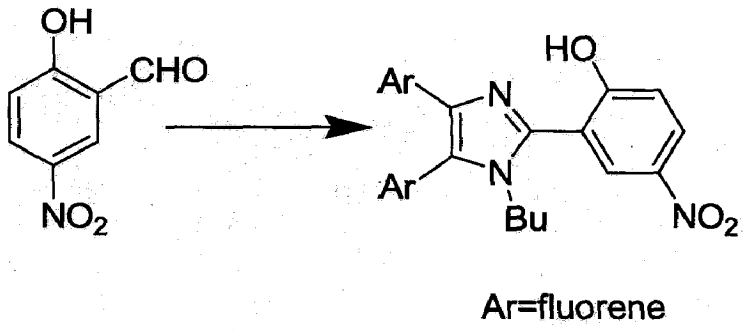

Figure 3.6 Synthetic route of **4b**.

2-(1-butyl-4,5-bis(9,9-diethyl-9*H*-fluoren-2-yl)-4-nitrophenol(4b)

Yellow solid.Yeild:57%.mp: 290° C. ^{1}H NMR ($CDCl_3$, 500 MHz): δ 8.65 (d, J = 3 Hz, 1Hz), 7.81-7.79 (m, 1H), 7.63-7.61 (m, 1H), 7.54 (d, J = 8 Hz, 1H), 7.39-7.42 (m, 4H), 7.36 (dd, J = 1.5, J = 6 Hz, 1H), 7.29-7.26 (m, 1H), 7.25-7.24 (m, 1H), 7.21(d, J =9.5 Hz, 1H) 3.85 (dd, J = 8, 7.5 Hz, 2H), 1.34-1.28 (m, 2H), 1.0-0.93 (m, 2H), 0.55 (t, J = 7.5 Hz, 3H). ^{13}C NMR ($CDCl_3$, 125 MHz): δ 164.66, 150.99, 150.12, 149.99, 143.13, 142.49, 141.11, 140.71, 140.56, 139.38, 135.29, 131.25, 131.14, 131.14, 130.32, 128.23, 128.07, 127.25, 127.01, 126.81, 125.67, 125.62, 125.38, 123.09, 122.85, 121.15, 120.95, 120.63, 120.19, 119.63, 119.56, 118.44, 113.15, 77.32, 77.06, 76.81, 56.48, 55.96, 45.83, 32.82, 32.67, 32.52, 29.74, 26.94, 19.77, 13.46, 8.59, 8.49. FT-IR (KBr, cm^{-1}): 3440, 3050, 2962, 1588, 1335.

3.6 General synthesis of benzaldehyde, 2-hydroxy-, 2-phenylhydrazone (5a)

A mixture of 2-hydroxybenzaldehyde (0.12 g, 1 mmol), 1-phenyl hydrazine (0.11 g, 1mmol) and ethanol (5 mL) was heated at 85° C for 12 h in the round bottom flask. The completion of the reaction was analyzed by TLC. After that the mixture was poured into ice water. The residue was adsorbed on silica gel. The desired product was purified by column chromatography by using hexane/dichloromethane mixture as eluant.

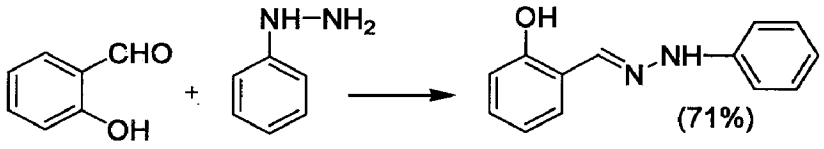

Figure 3.7 Synthetic route of **5a.**

It was synthesized from 2-hydroxybenzaldehyde and 1-phenyl hydrazine by following the general procedure described above Yellow solid. Yield: 71%. mp: 140-142° C. ^{1}H NMR ($CDCl_3$, 500 MHz): δ 10.85 (s, 1 H), 7.88 (s, 1 H), 7.49 (s, 1 H), 7.31(t, J = 8.5, 2 H), 7.23-7.26 (m, 1 H), 7.24 (dd, J = 1.5 Hz, J = 6.5, 1 H), 6.99 (t, J = 8, 3 H), 6.89-6.95 (m, 2 H).

3.7 Conclusion

Synthetic methodologies were developed successfully for the preparation of the two type hydrazone and imidazole based anion sensor. These anion sensors has successfully characterized or confirmed by NMR spectroscopy. They sensor dyes were obtained in moderate yields in pure form suitable for spectroscopic analysis. The structural composition was established without doubt by spectral analysis.

3.8 Reference

1. Yigit, M.; Seckin, T.; Koytepe, S.; Cetinkaya, E. *Turk. J. Chem.*, **2007**, *31*, 113.

Chapter 4

Hydrazone based anion sensors: Spectral analysis

4.1 Introduction

In comparison with the variety of host molecules as cation receptors, the investigation of selective receptors for anions is still less [1]. It has been well documented that anions such as fluoride, acetate, and hydrogen phosphate are important in many biological processes and are known to be present in many commonly used agricultural fertilizers as well as in food additives [2].

Generally, a sensor molecule is be composed of a receptor component that is responsible for binding the analyte and a signaling unit that is capable of translating the analyte binding induced changes into an output signal [3, 4] . In the case of binding modes of the receptor with anions, those are classified basically into electrostatic interactions, hydrogen bond interactions, electron deficient Lewis acid coordination via orbital overlap and interactions with metal centers etc. [5, 6] The hydrogen binding is widely used in anion recognition due its directionality, a feature which allows the design of receptors having ability to differentiate between anions with different geometries and hydrogen-bonding requirements [7, 8].

Many hosts include simple anion sensor systems containing urea, thiourea, amine, and amide, alcohol, and pyrrole groups linked to chromophores. Chromophores used in this type of chromogenic anion sensors are mainly organic dyes such as azobenzene, nitrobenzene, indoaniline, and anthraquinone or extensively conjugated aromatic compounds such as

quinoxaline, oxadiazole, and porphyrin. The color change occurs upon binding of anion guests that affect the electronic properties of the chromophores.

The compounds also contained chromophore subunits (acting as an electron acceptor) whose electronic properties were modified as a result of interactions with a bound anionic substrate (acting as an electron donor). The NH-based hydrogen bonding chromogenic hosts can be classified as follows.

Anion receptor should contain two units one is binding site contain various types of anion receptor .One type is neutral type of anion receptor like –OH and –NH (donor) based on hydrogen bonding. The other part is Chromophore part, which convert the binding event of anion into optical signal. These two parts can be either covalently attached or intermolecularly linked to each other.

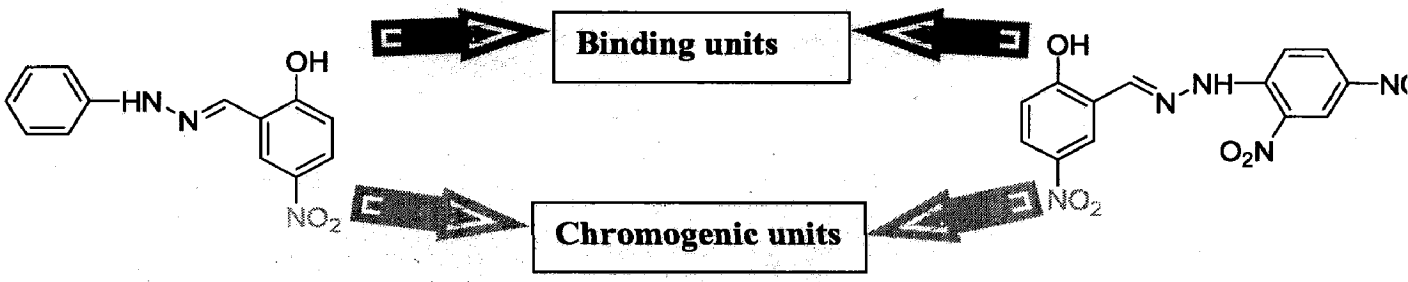

3a **3b**

Figure 4.1 Receptor Dyes (**3a-3b**) for fluoride.

Here, we have reported hydrazones based anion sensors **(3a-3b)**. They contain two binding sites namely –OH and –NH attached with the electron withdrawing (–NO_2) group, which increase the acidity of the receptor unit and the easy deprotonation take place through the binding site. We also report a control molecule without the introduction of the electron withdrawing group to see the affect in binding between the receptor and the anion.

4.2 Synthesis and characterization

The synthetic route leading to the formation of the two new hydrazone based anion sensor dyes is displayed in Figure 4.2.The synthesis began with salicylaldehyde which generated the **2**-hydroxy-5-nitrobenzaldehyde in moderate yield (41%) and in the presence of phenyl hydrazine it produced the (*E*)-4 nitro-2-((2-phenyl hydrazono) methyl) phenol **(3a)** with the moderate yield (90%).The **2**-hydroxy-5-nitrobenzaldehyde with the reaction 1-(2,4-dinitrophenyl) hydrazine produce (*E*)-2-((2, 4-dinitro phenyl) hydrazono) methyl) **(3b)** with a moderate yield (92%).

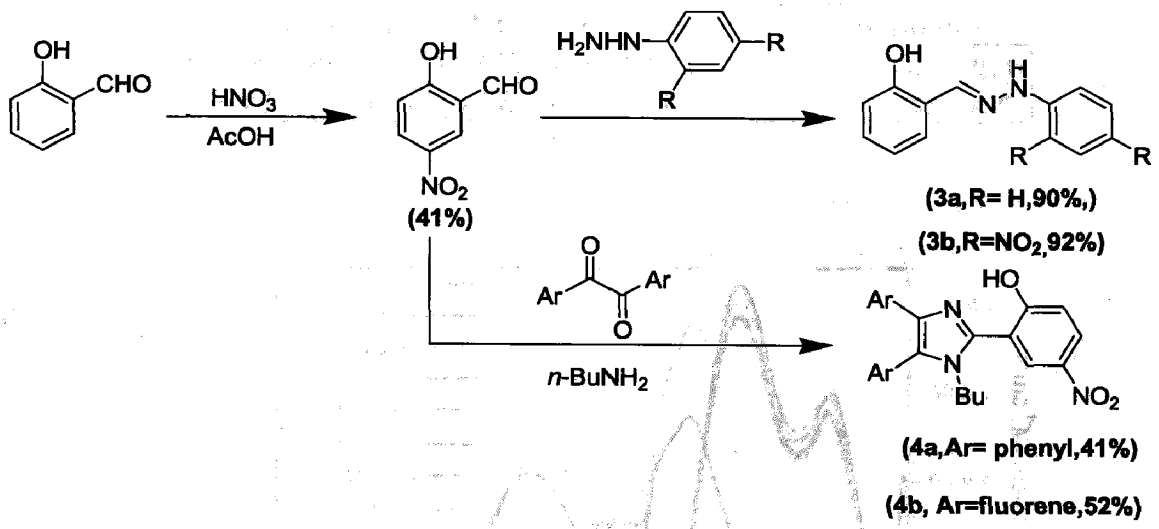

Figure 4.2 Synthetic scheme of the receptors **3a, 3b & 4a, 4b.**

The entire targeted compounds were characterized by NMR & IR spectroscopy. The dyes were yellow **(3a)** and orange **(3b)** and freely soluble in acetonitrile, dimethyl sulphoxide or toluene and chloroform. The analytically pure samples were used for further spectroscopic investigations.

4.3 Optical spectra

Electronic absorption spectra were carried out on a Shimadzu UV-1800 spectrophotometer for solutions of relevant dyes in acetonitrile.

Table 4.1 Absorption spectral data for the host **3a** in the presence of different salts

salts	λ, nm $\epsilon_{max}(M^{-1} cm^{-1} \times 10^3)$
None	301 (19.6), 351 (25.1)
Iodide	301 (18.9), 351 (23.9)
Bromide	301 (19.3), 351 (23.2)
Chloride	301 (18.3), 351 (22.9)
Hydrogen sulphate	301 (18.8), 351 (23.5)
Hexachlorophosphate	301 (18.6), 351 (23.3)
Perchlorate	301 (18.8), 351 (24.1)
Fluoride	301 (8.8), 378 (18.6), 458 (15.6)
Acetate	301 (12.1), 378 (23.4), 458 (16.6)

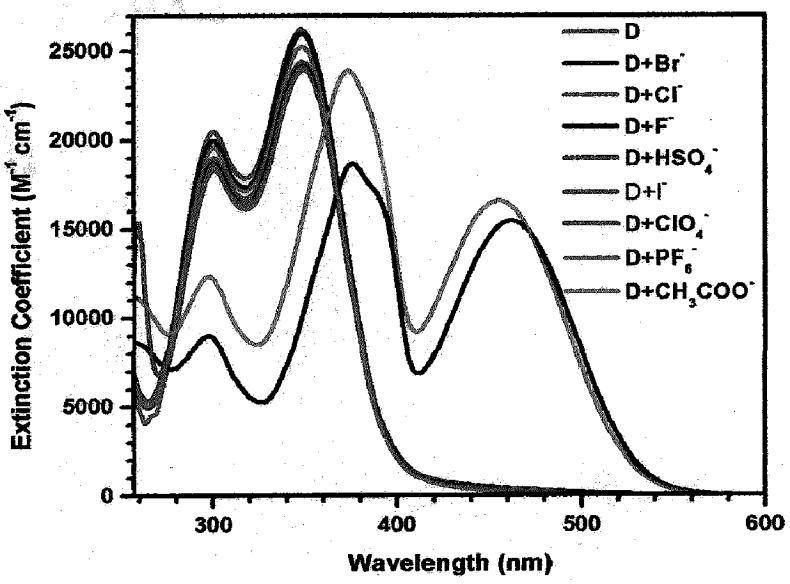

Figure 4.3 UV–Vis absorption spectral changes observed for **3a** in acetonitrile upon addition of 10 equivalents of tetrabutylammonium anion salts.

The absorption spectra of dye **3a** in the solution of acetonitrile with different anions bromide, chloride, flouride, hydrogen phosphate, iodide, chlorate, phosphate' acetate has recorded. There was not any essential change in the absorption spectra of dye with the anions bromide, chloride, hydrogen phoshate, iodide, chlorate and phosphate two peaks same as the spectra of **3a** observed around at 301 and 351 nm because of the π-π^* electron transition. Large bathochromic shifts were observed in absorption spectra Figure 4.3 of **3a** with both anions fluoride and acetate. It is indicating the reorganization property of **3a** towards fluoride and acetate. There were three band observed in case of fluoride, acetate anions ,two band in the absorption spectra at 301 nm because of the π-π^* electron transition (the peak around 351 has shifted on around 378 nm after addition of the fluoride, acetate) and the other is a strong absorption in the visible region around 458 nm, which can be assigned to an intermolecular charge transfer (ICT) between the –OH donating unit and the electron withdrawing group (-NO_2), by the derotonation from –OH donating unit present in the dye after the addition of the anions (fluoride,acetate).

Figure 4.4 Color changes shown by the receptor **3a** in acetonitrile, on addition of 10 equivalents of different salts.

Upon the addition of the anions in Figure 4.4 (fluoride, acetate) the color almost transparent of **3a** turned into dark yellow this was because of the binding between **3a** and these two anions by the deprotonation from the donor unit of the dye. So we can say this is a colorimetric type of anion sensor. In case of other anion there were no color change has observed.

After the addition of the protic solvent the color disappeared because which proton has deprotonated then the protic solvent filled the deficiency of the proton which can clearly visible to necked eye.

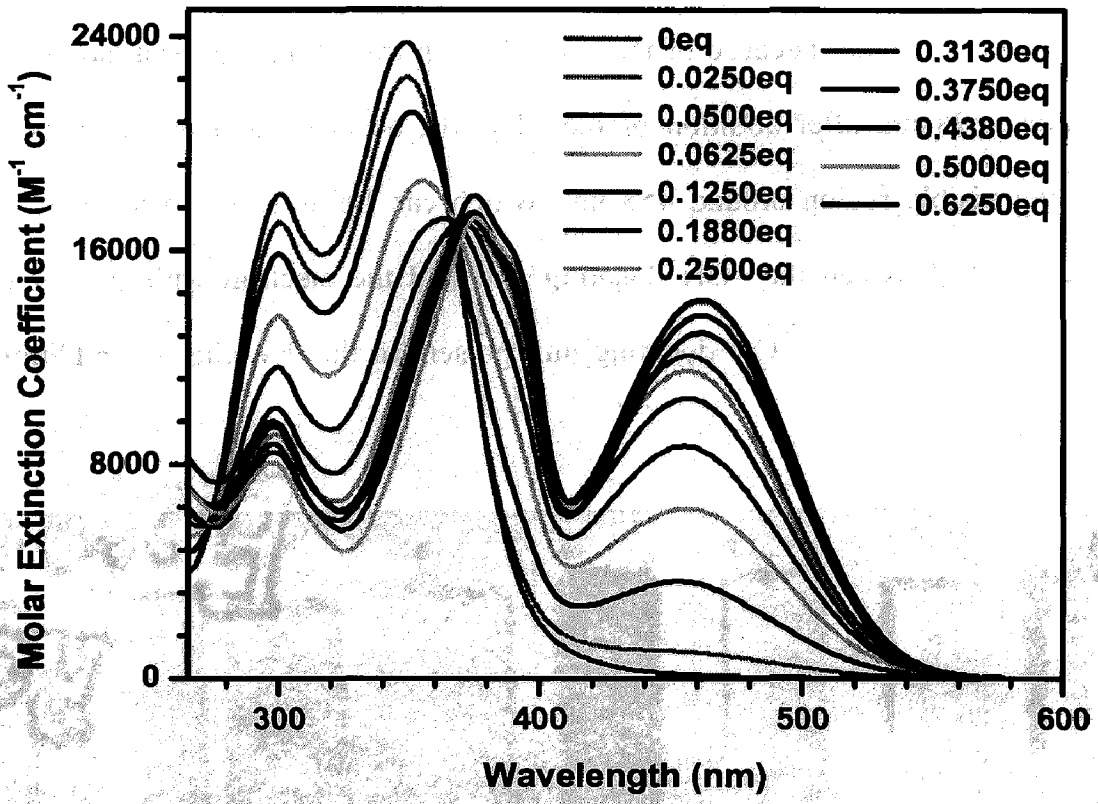

Figure 4.5 UV-Vis titration spectral changes observed for receptor dye **3a** upon addition of tetrabutylammonium fluoride.

After the addition of the fluoride up to 0.6250 equivalents in **3a** in Figure 4.5 the new absorption band at 462 nm increases with the increment in the concentration of fluoride because intramolecular charge transfer transition takes place, because of the deprotonation of dye after

addition of fluoride and peak around 301 generated because of the π-π^* electronic transition, decreased after addition of these fluoride and the peak around 351 nm has shifted around at 358 nm. The selectivity of an anion sensor is related to the structure of the hydrogen bond complex and the basicity of the anions. Among anions, fluoride and acetate is the most electronegative atom.

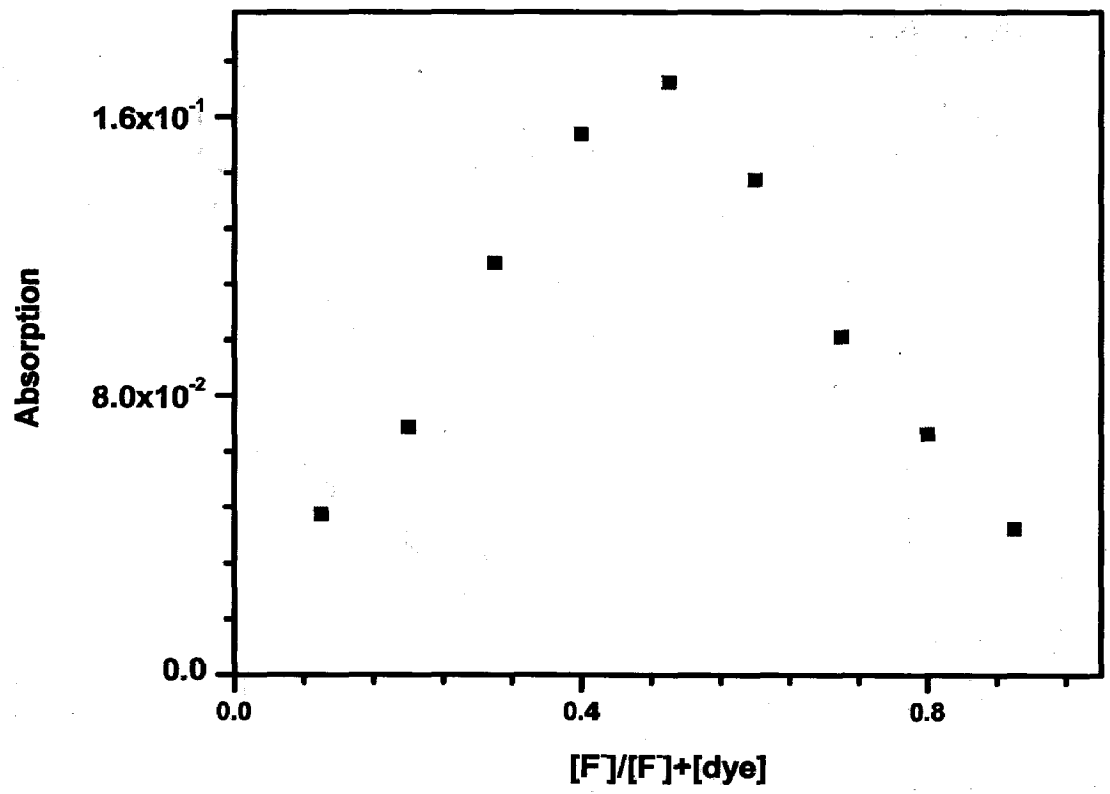

Figure 4.6 Job's plot between **3a** and fluoride, the plot indicates 1:1 binding stoichiometry between **3a** and fluoride.

From the job' s plot Figure 4.6 analysis we got the idea about the 1:1 binding between **3a** and fluoride, one new band generated at around 462 nm, when we started the addition of fluoride in the solution of dye the band at 462 nm increased but after some time starts decreasing.

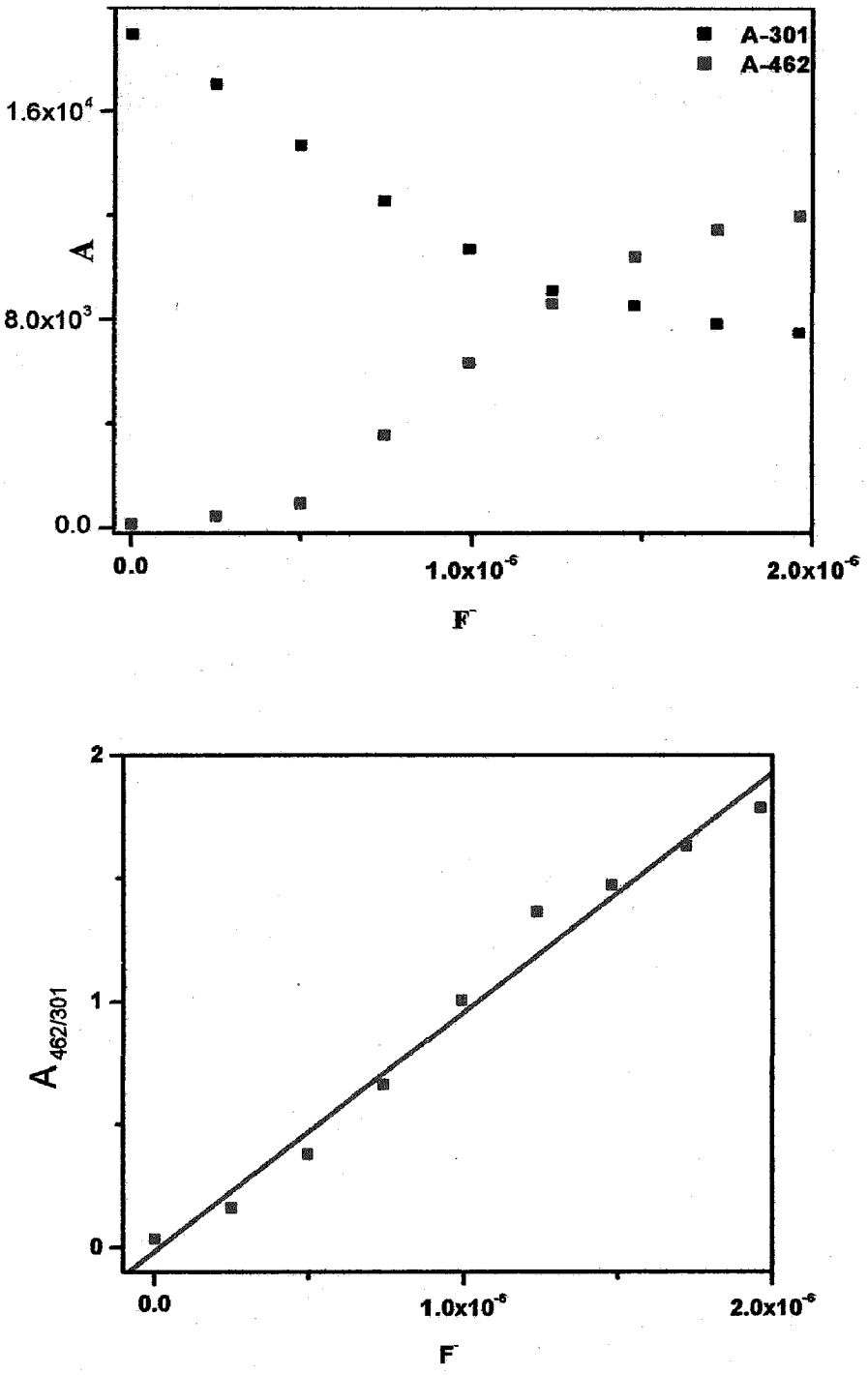

Figure 4.7 Plot of concentration of fluoride vs. absorbance at 301 and 462 and 462/301 of **3a.**

In Figure 4.7 we can see that the peak around 301 nm generated due to π-π^* electronic transition that decreases and the band generated around 462 by the binding between anion and the **3a** that increases after addition of more equivalent of the fluoride.

To see the binding property of the anion and the dye **3a** we have calculated the binding constant of dye **3a** towards fluoride from three methods.

4.4 Benesi-Hildebrand Method

According to this method, $\frac{[H]}{Abs} = \frac{1}{\varepsilon K_b}\frac{1}{[G]} + \frac{1}{\varepsilon}$

Where [H] = concentration of guest (anion), for example the dye, which must be kept constant during the measurements, Abs = absorbance after addition of host (dye), ε = extinction coefficient of the charge transfer absorption of the host-guest complex, K_b = binding constant, [G] = concentration of the guest

A plot of $\frac{1}{[G]}$ versus $\frac{[H]}{Abs}$ will give a slope of $\frac{1}{\varepsilon K_b}$ and intercept $\frac{1}{\varepsilon}$

The ratio $\frac{Intercept}{Slope} = \frac{\varepsilon K_b}{\varepsilon} = K_b$

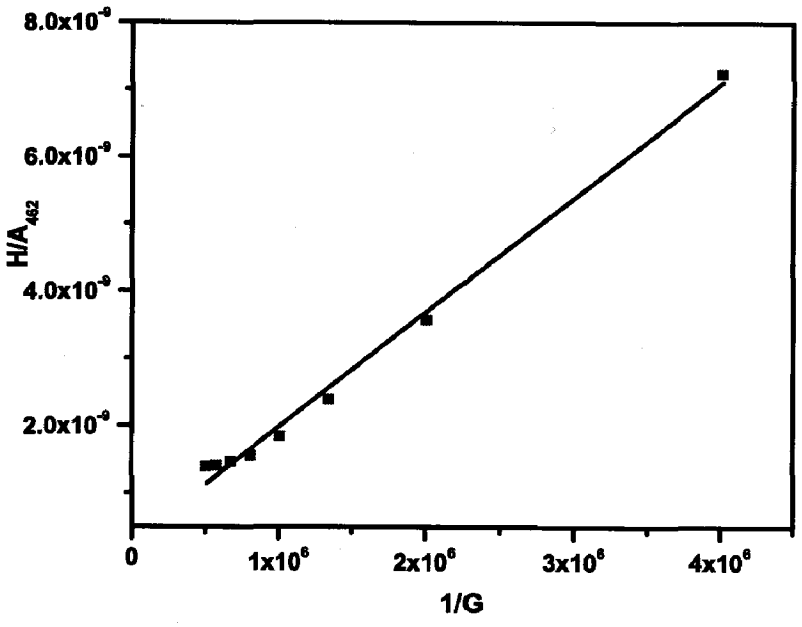

Figure 4.8 Plot of **3a** for binding constant calculation from Benesi-Hildebrand method with fluoride.

From Figure 4.8 we have calculated the value of K_b by using Benesi-Hildbrand method in case of formation of the complex by the interaction between fluoride and **3a** (K_b=1.60×10^5 M^{-1}).

4.5 Alternate method

According to this method

$$\frac{A_0}{A_0 - A} = \left(\frac{A_0}{A_0 - A_{complex}}\right) \times \frac{1}{K} \times \frac{1}{[G]} + \left(\frac{A_0}{A_0 - A_{complex}}\right)$$

The ratio $\frac{Intercept}{Slope} = \frac{1}{1/K \times 1/[G]} = K$

Here the host is dye **3a** and the guest is fluoride.

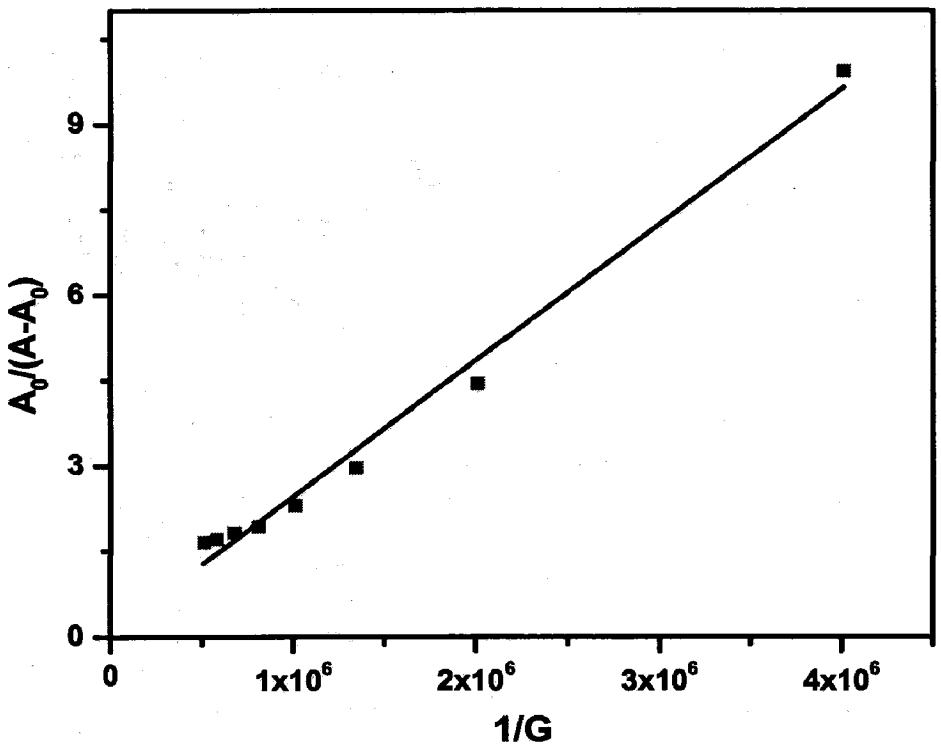

Figure 4.9 Plot of **3a** for binding constant calculation from Alternate method with fluoride

From this method Figure 4.9 we have calculated the value of K (3.00×10^4 M^{-1}).

4.6 Scott equation

The equation is $\frac{[G]}{\Delta A_{obs}} = \frac{[G]}{\Delta A_c} + \frac{1}{K_a \Delta A_c}$

Where ΔA_{obs} is the change in absorbance upon addition of guest, G; ΔA_c = absorption change between pure complex and the free component at the saturation; [G] (fluoride) = concentration of the guest; K_a = association constant

A plot $\frac{[G]}{\Delta A_{obs}}$ versus [G] will give a slope = $\frac{1}{\Delta A_c}$ and intercept = $\frac{1}{\Delta A_c K_a}$

The ratio $\frac{\text{slope}}{\text{intercept}}$ will give the binding constant.

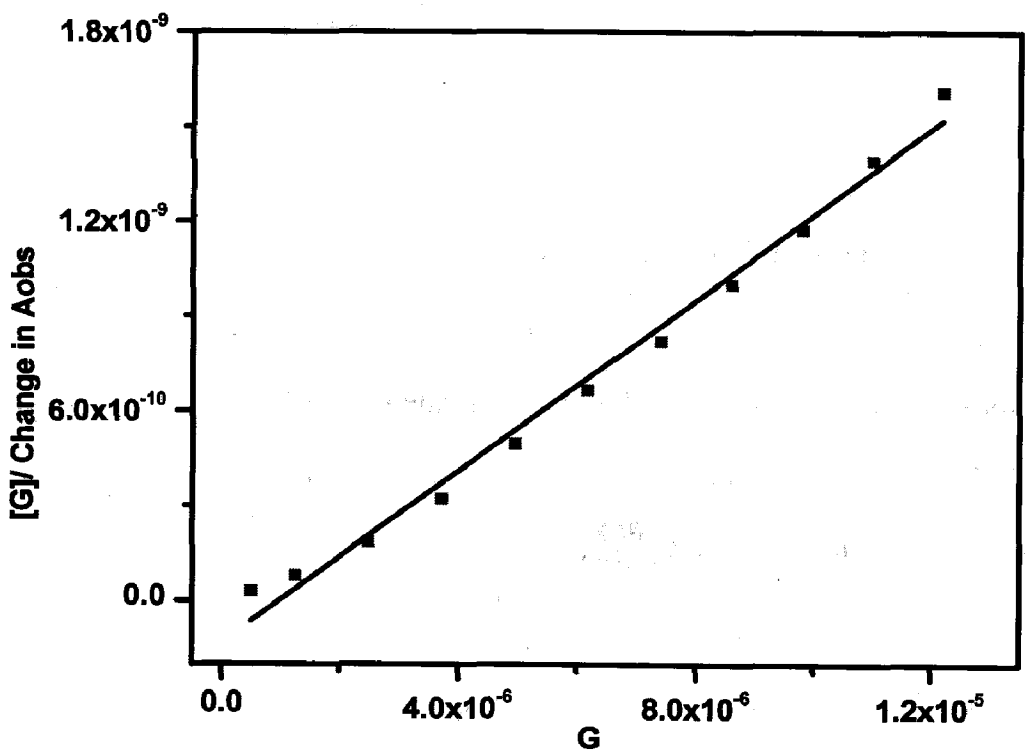

Figure 4.10 Plot of **3a** for binding constant calculation from Scott method with fluoride

From this method we have also calculated the value of K_a that is around $2.10\times10^5\ M^{-1}$.

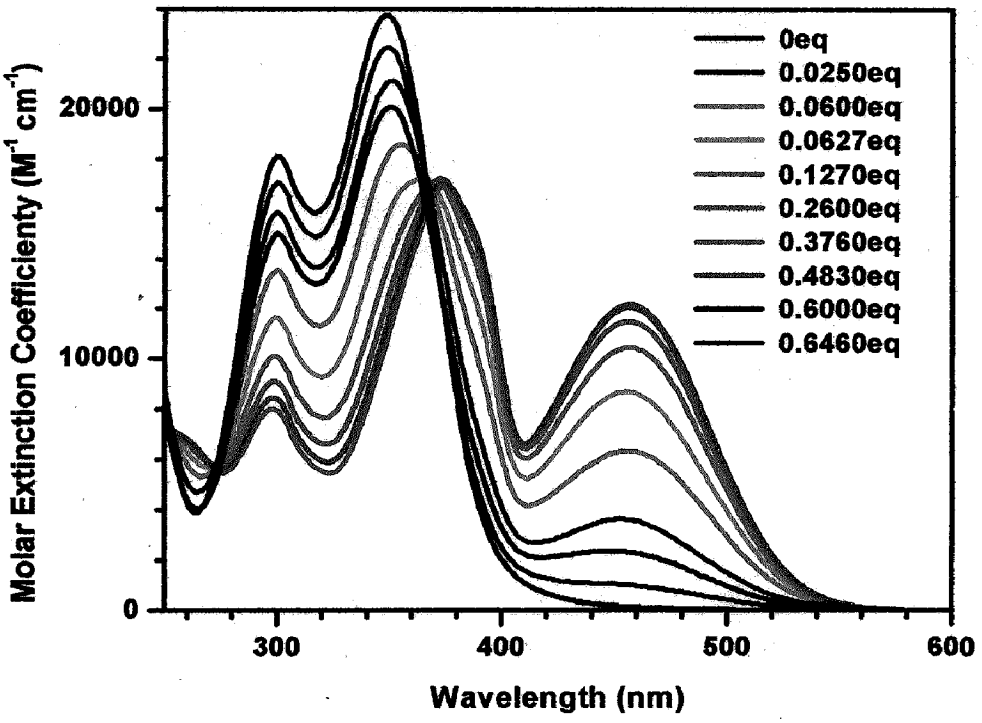

Figure 4.11 UV-Vis titration spectral changes observed for receptor Dye **3a** upon addition of tetrabutylammonium acetate.

After the addition of the $CH_3CO_2^-$ up to 0.6460 equivalent in **3a** in Figure 4.11 the new absorption band at 455 nm increases with the increment in the concentration of fluoride because intramolecular charge transfer transition take place because of the deprotonation of dye after addition of acetate and peak around 301 generated because of the π-π^* electronic transition, decreased after addition of these fluoride and the peak around 351 nm has shifted around at 358 nm. The selectivity of an anion sensor is related to the structure of the hydrogen bond complex and the basicity of the anions. Among anions, fluoride and acetate is the most electronegative atom and, as such usually forms the strongest H-bond interaction with an -NH or -OH groups. In particular reported receptor in this work are selective for both fluoride and acetate.

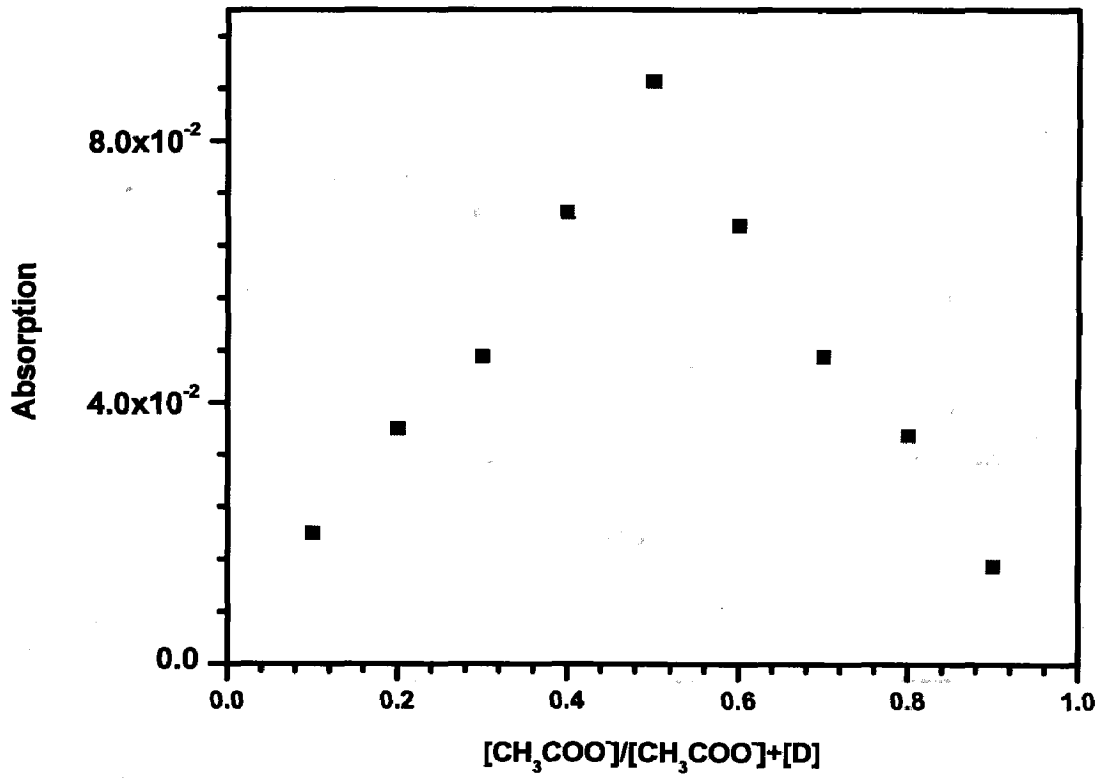

Figure 4.12 Job's plot between **3a** and fluoride, the plot indicates 1:1 binding stoichiometry acetate.

From the job' s plot Figure 4.12 analysis we got the idea about the 1:1 binding between **3a** and fluoride, one new band generated at around 455 nm. When we started the addition of acetate in the solution of dye the band at 455 nm increased but after some time start decreasing.

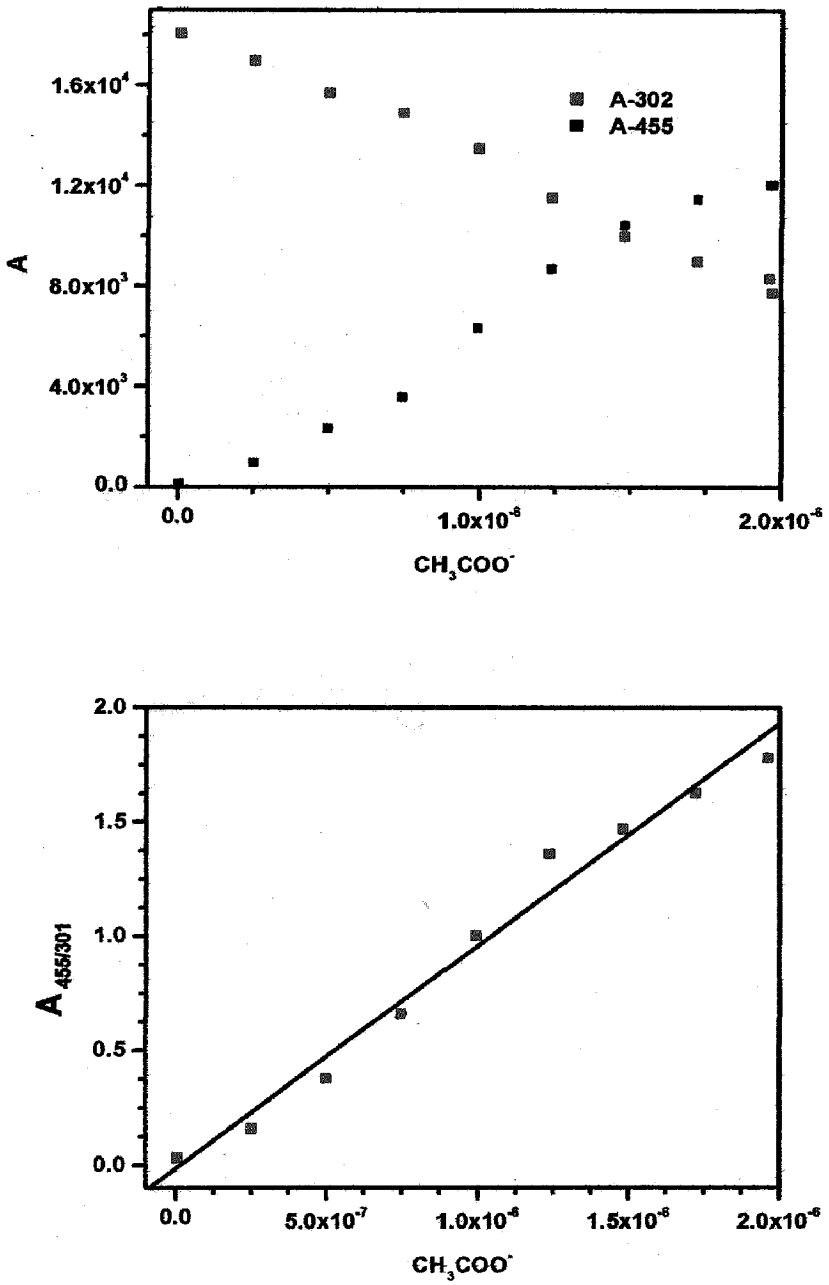

Figure 4.13 Plot of concentration of acetate vs. absorbance at 455 and 301 and 455/301 of **3a.**

In Figure 4.13 we can see that the peak around 301 nm generated due to π-π^* electronic transition that decreases and the band generated around 455 by the binding between anion and the **3a** that increases after addition of more equivalent of the acetate.

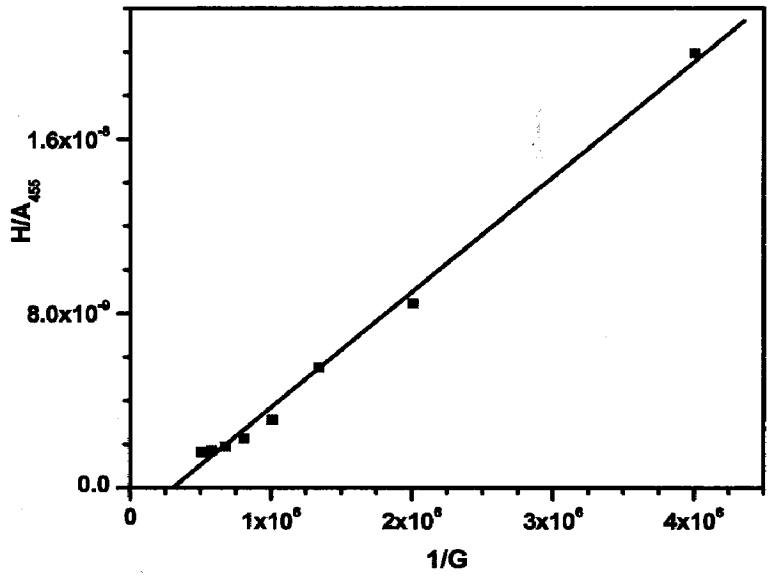

Figure 4.14 Plot of **3a** for binding constant calculation from Benesi-Hildebrand method with acetate.

Here in Figure 4.14 the host is **3a** and the guest is acetate and from this method we have also calculated the value of K_b of dye **3a** with the acetate ($1.66\times10^5\ M^{-1}$).

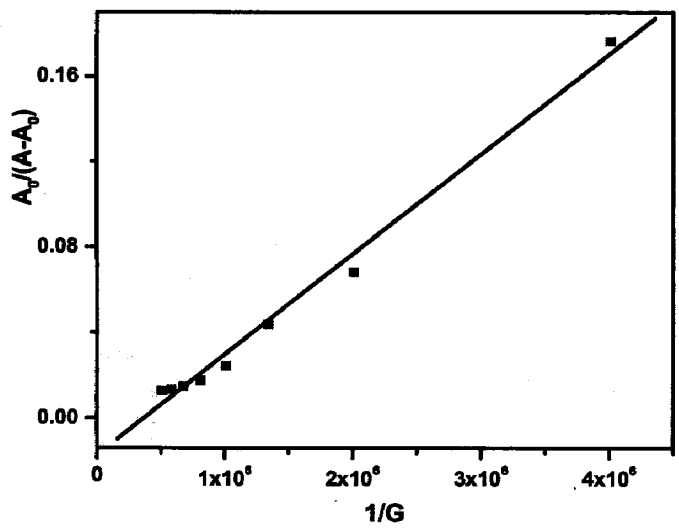

Figure 4.15 Plot of **3a** for Binding constant calculation from Alternate method with acetate.

According to the Alternate method in Figure 4.15 we have calculated the value of K of dye **3a** with acetate ($3.04\times10^4\ M^{-1}$).

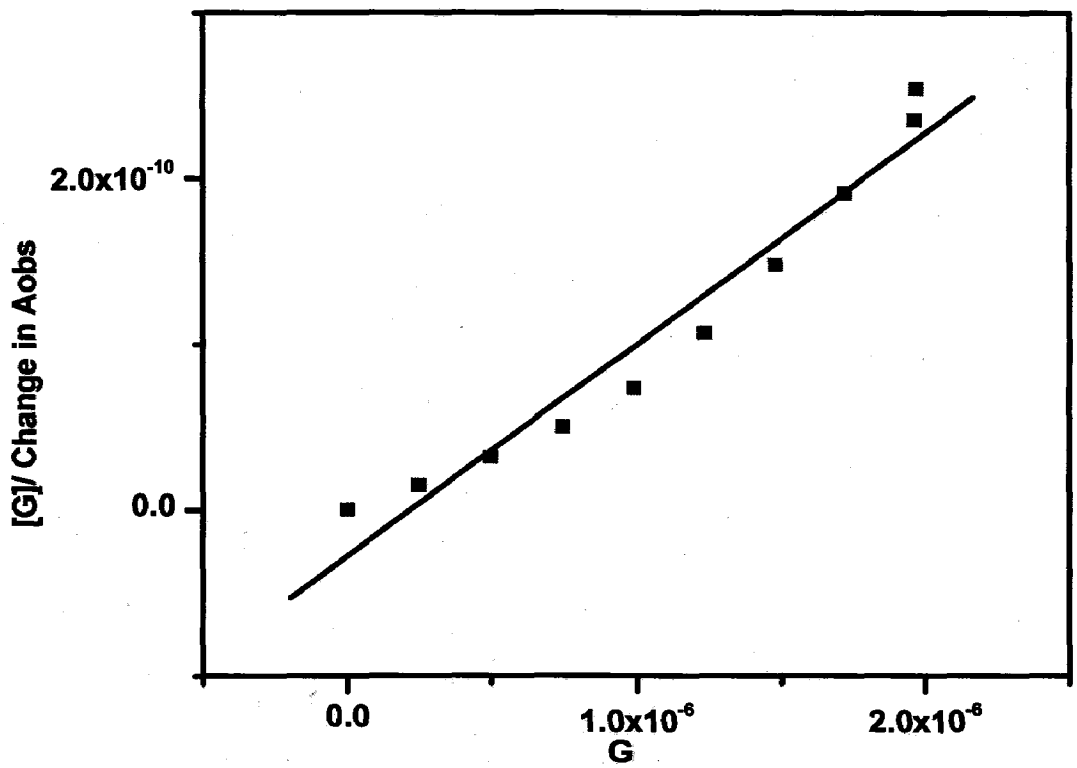

Figure 4.16 Plot of **3a** for Binding constant calculation from Scott method with acetate.

We can see in the Figure 4.16 the graph of Scott method and calculated the value of K_a from this method for dye 3a with acetate ($2.30\times10^5\ M^{-1}$).

We have calculated the binding constant by different three methods so, for the final value of K (binding constant) we has compared the all three values. From the binding constant calculation got the idea about the quenching property of the dye.

4.7 ^{1}H NMR titration of 3a

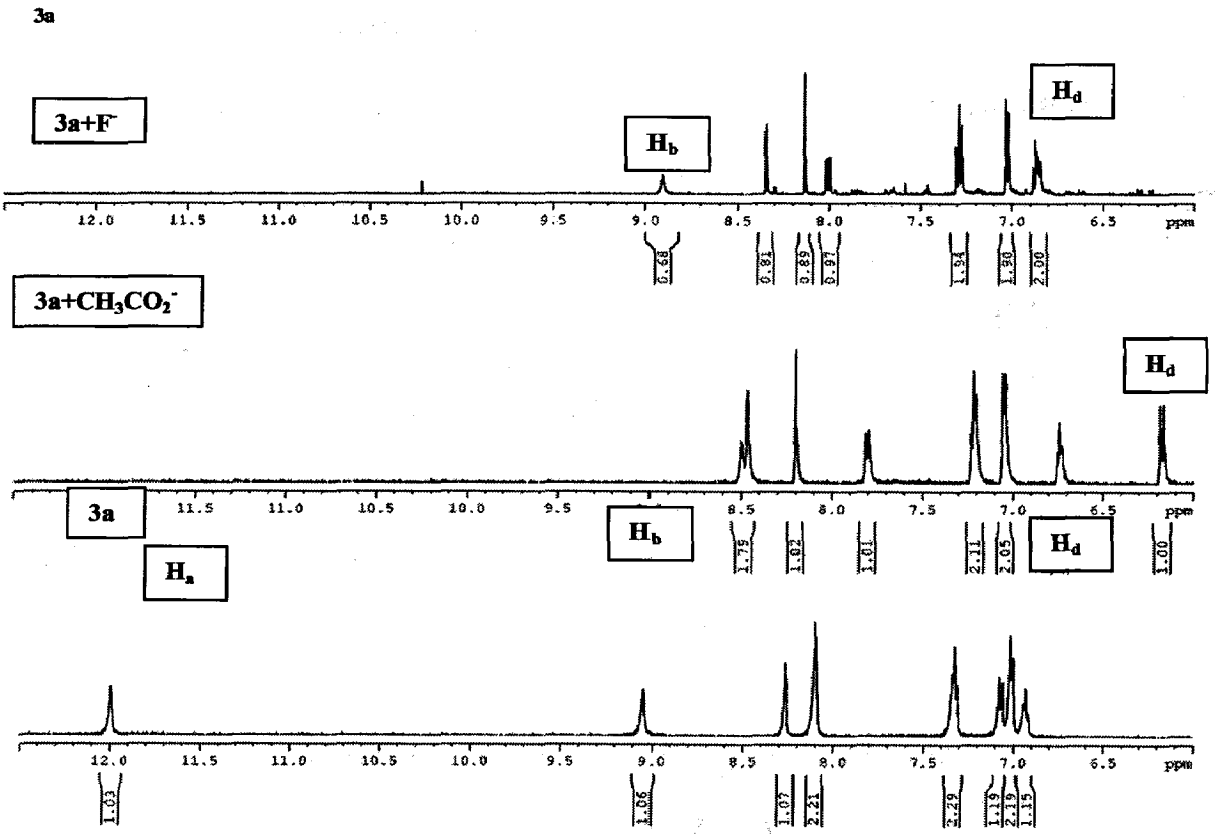

Figure 4.17 ^{1}H NMR titration spectra of dye **3a** with fluoride and acetate.

To further look into the nature of host–guest interactions, ^{1}H NMR titration experiments were conducted in acetonitrile (CD_3CN).^{1}HNMR fluoride titration spectra of the sensor 3a is shown in Figure 4.17 Upon addition of 10 equivalent of fluoride and acetate ions, the peaks at 12 ppm and 9 ppm which were assigned to a –OH and phenol –NH respectively, were disappeared in case of acetate and in case of fluoride the peak around 12 ppm disappeared but the peak

because of –NH was there in the spectra and the other signals who's generated because of the other hydrogen's sifted towards up filed . This indicated the formation of a hydrogen-bonding complex was at this stage. The signals of –NH and –OH were disappeared and the other protons, especially H_b and H_d, moved towards upfield, which indicated the bonding between dye and the anions. All the results observed indicate that during the ^1H NMR titrations the excess fluoride and acetate results the deprotonation of the sensor **(3a)** take place.

Table 4.2 Absorption spectral data for the host **3b** in the presence of different salts

Salts	λ, nm $\epsilon_{max}(M^{-1} cm^{-1} \times 10^3)$
None	293 (11.4), 378 (21.3)
Iodide	293 (11.2), 378 (21.2)
Bromide	293 (10.7), 378 (21.2)
Chloride	293 (10.8), 378 (21.1)
Hydrogen sulphate	293 (10.9), 378 (20.9)
Hexachlorophosphate	293 (10.9), 378 (20.8)
Perchlorate	293 (11.1), 378 (20.9)
Fluoride	299 (3.8), 410 (20.9), 472 (16.3)
Acetate	299 (3.4), 408 (20.7), 472 (18.1)

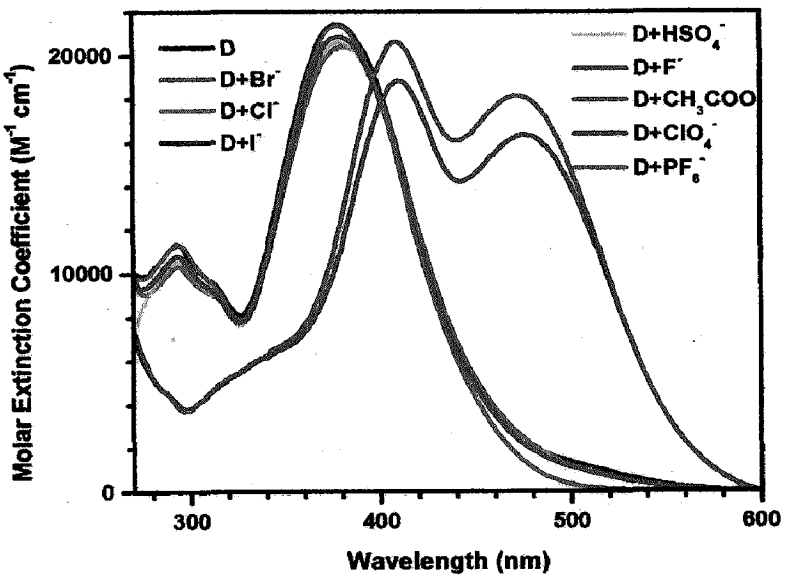

Figure 4.18 UV–Vis absorption spectral changes observed for **3b** in acetonitrile upon addition of 10 equivalent of tetrabutylammonium anion salt.

The absorption spectra of dye **3b** in the solution of acetonitrile with different anions bromide, chloride, flouride, hydrogen phosphate, iodide, chlorate, phosphate, acetate has recorded. There was not any essential change in the absorption spectra of dye with the anions bromide, chloride, hydrogen phosphate, iodide, chlorate and phosphate, two peaks same as the spectra of **3b** observed around at 293 and 378 nm because of the π-π^* electron transition. Large bathochromic shifts were observed in absorption spectra Figure 4.18 of **3b** with both anions fluoride and acetate. It is indicating the reorganization property of **3b** towards fluoride and acetate. There were three band observed in case of fluoride, acetate anions ,two band in the absorption spectra at 410 and 408 nm because of the π-π^* electron transition (the peak around 378 has shifted on around 410 nm after addition of the fluoride, acetate) and the other is a strong absorption in the visible region around 472 nm, which can be assigned to an intermolecular charge transfer (ICT) between the –OH donating unit and the electron withdrawing group (-NO_2), by the derotonation from –OH donating unit present in the dye after the addition of the anions (fluoride, acetate).

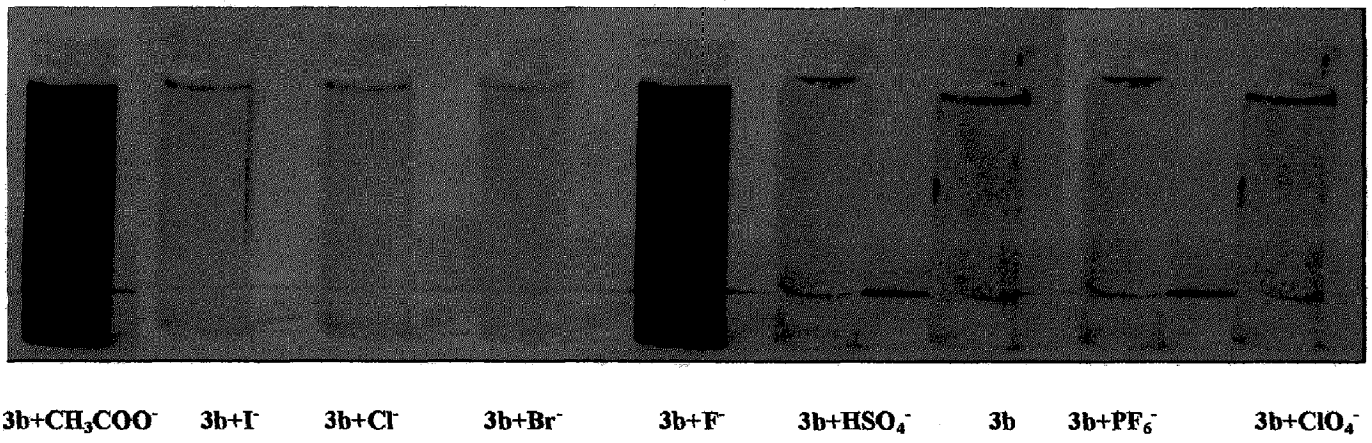

Figure 4.19 Color changes shown by the receptor **3b** in acetonitrile, on addition of 10 equivalents of different anions.

Upon the addition of the anions in Figure 4.19 (fluoride, acetate) the yellow color of **3b** turned into dark red this was because of the binding between **3b** and these two anions by the deprotonation from the donor unit of the dye. So we can say this is a colorimetric type of anion sensor. In case of other anion there were no color change has observed.

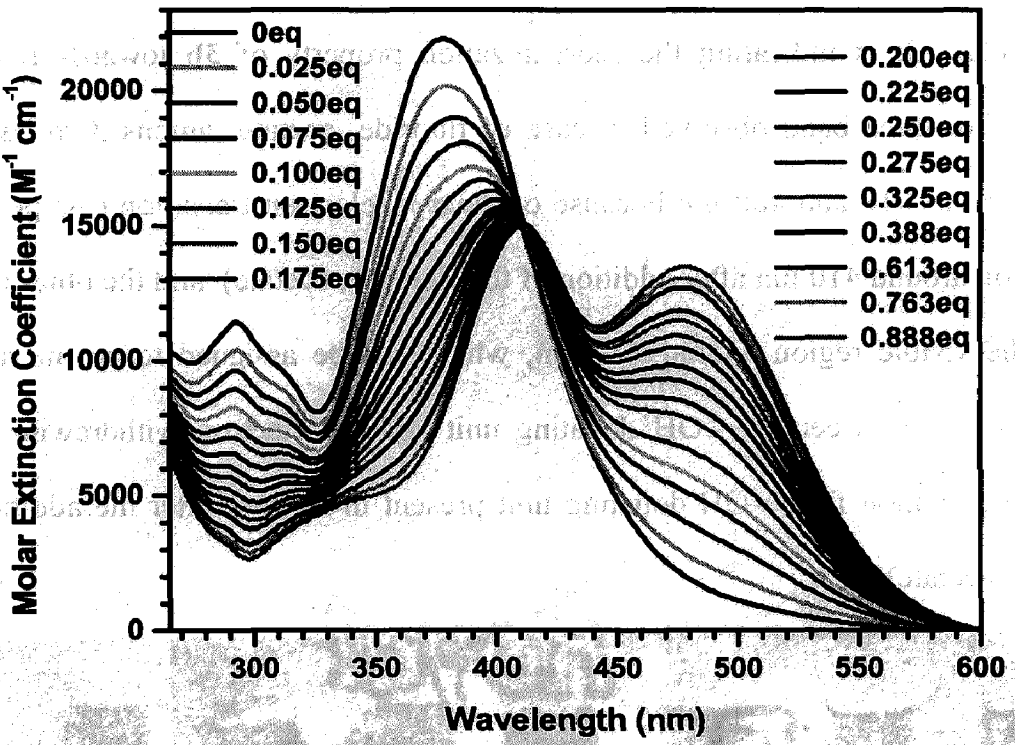

Figure 4.20 UV-Vis titration spectral changes of receptor dye **3b** upon addition of tetrabutylammonium fluoride.

After the addition of the fluoride up to 0.888 equivalent in **3b** in Figure 4.20 the new absorption band at 486 increases with the increment in the concentration of fluoride because interamolecular charge transfer transition takes place, because of the deprotonation of dye after addition of acetate and peak around 299 nm generated because of the π-π^* electronic transition, decreased after addition of these fluoride and the peak around 378 nm has shifted around at 410

nm. The selectivity of an anion sensor is related to the structure of the hydrogen bond complex and the basicity of the anions. Among anions, fluoride and acetate is the most electronegative atom and, as such usually forms the strongest H-bond interaction with an -NH or -OH groups. In particular reported receptor in this work are selective for both fluoride and acetate.

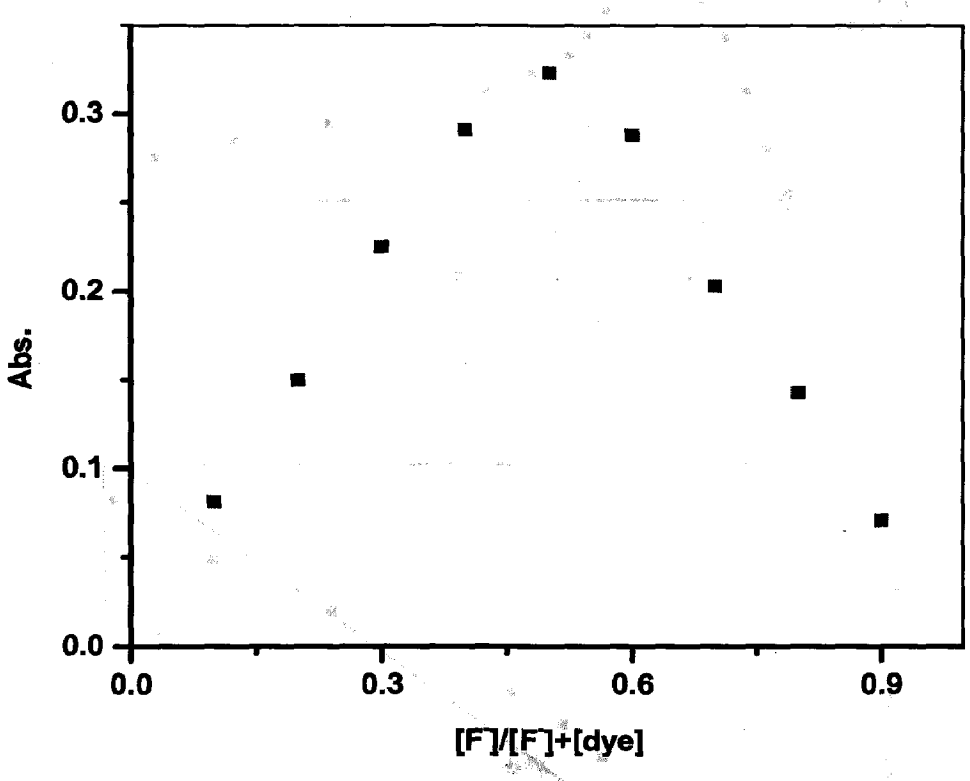

Figure 4.21 Job's plot between **3b** and fluoride, the plot indicates 1:1 binding stoichiometry between **3b** and fluoride.

From the Job' s plot Figure 4.21 analysis we got the idea about the 1:1 binding between **3b** and fluoride , one new band generated at around 472 nm. When we started the addition of fluoride in the solution of dye the band at 472 nm increased but after some time start decreasing.

binding constant calculation, we can see the 1:1 interaction of dyes and anions and the complex formation.

4.10 References

1. Jeon, S.; Park, D. H.; Lee, H. K.; Park, J. Y.; Kang, S. O.; Nam, K. C. *Bull. Korean Chem. Soc.* **2003**, *24*, 101465.
2. Shao, J. *J. Incl Phenom Macrocycl Chem.* **2011**, *70*, 91.
3. Kim, S. K., Lee, D. H., Hong, J., Yoon, J. Acc. Chem. Res. **2009**, *42*, 23.
4. Martínez-Máñez, R.; Sanceno, N. F. *Chem. Rev.* **2003**, *103*, 4419.
5. Xu, Z.; Kim, S. K.; Yoon, J. *Chem. Soc. Rev.* **2010**, *39*, 1457.
6. Dydio, P., Zieliński, T., Jurczak , J. *Org. Lett.* **2010**, *12*, 1076.
7. Hudson, Z. M., Zhao, S., Wang, R., Wang, S.; *Chem. Eur. J.* **2009**, *15*, 6131.
8. Park, C., Hong, J. *Tetrahedron Lett.* **2010**, *51*, 1960.

Chapter 5

Imidazole based anion sensors: Spectral analysis

5.1 Introduction

Here, we have reported imidazole **(4a-4b)** based anion sensor. These two anion sensor contain two binding site –OH, –NH attached with the electron withdrawing ($–NO_2$) group, which increase the acidity of the receptor unit and the easy deprotonation take place through the binding site, imidazole unit is also helped to increase the acidity of the receptor unit. As an acid proton donor, the proton of –NH of imidazole and –OH of phenol are to acidic to form a complex with fluoride and acetate. The affinity of –NH with anions in general is dramatically more powerful the –OH.

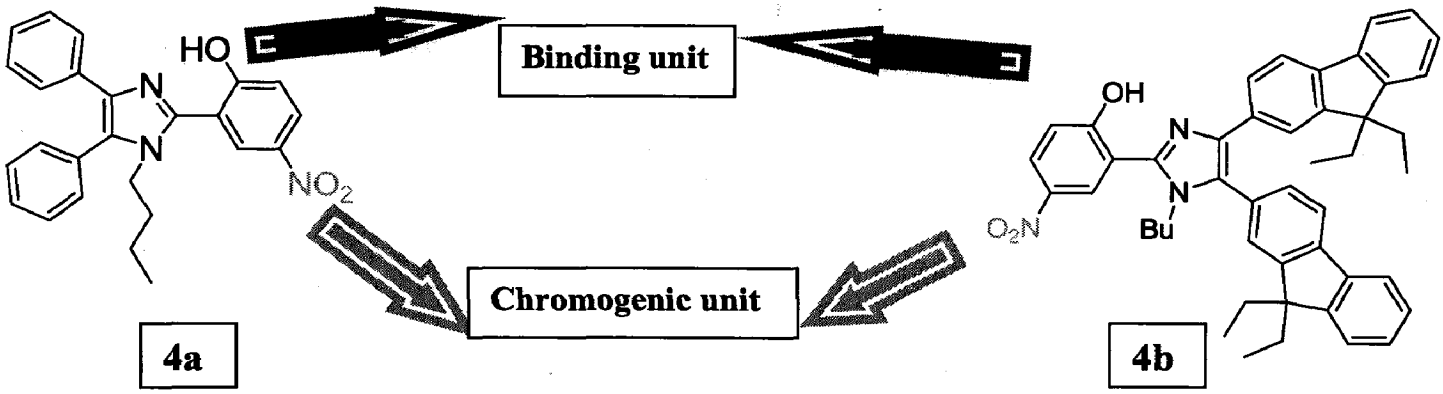

Figure 5.1 Receptor dyes **(4a-4b)** for fluoride.

5.2 Synthesis and characterization

The synthetic route leading to the formation of the two new imidazole based anion sensor dyes is displayed in Figure 5.2.The synthesis began with salicylaldehyde which generated the **2-**

hydroxy-5-nitrobenzaldehyde in moderate yield (41%) and in the presence of 1,3-diphenylpropane-1,2-dione it produced the 2-(1-butyl-4,5-diphenyl-1*H*-imidazole-2-yl)-4-nitrophenol **(4a)** with the moderate yield (41%).The **2**-hydroxy-5-nitrobenzaldehyde with the reaction 1-3-bis(9,9-diethyl-9*H*-fluoren-2-yl)propane-1,2-dione produce 2-(1-butyl-4,5-bis(9,9-diethyl-9*H*-fluoren-2-yl)-4-nitrophenol **(4b)** with a moderate yield (52%)

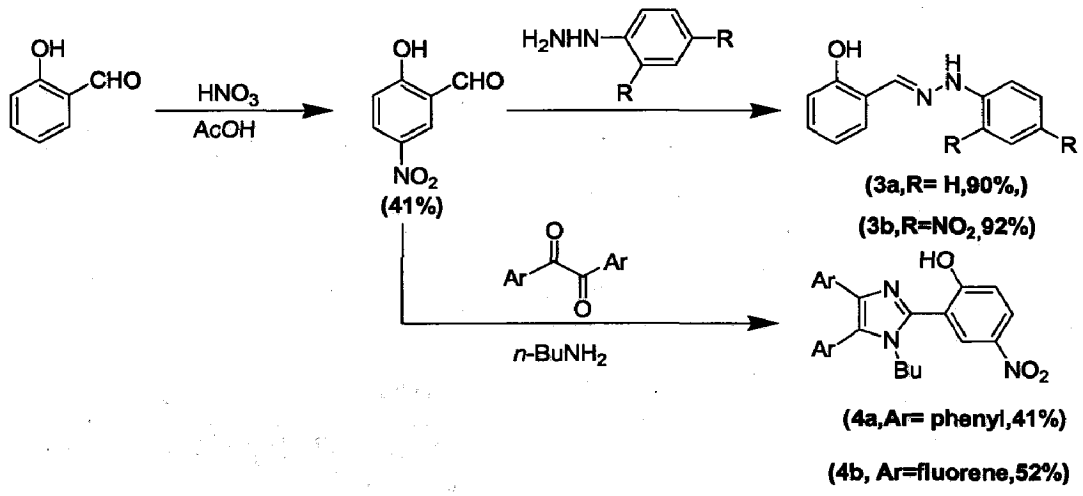

Figure 5.2 Synthetic scheme of receptors **3a, 3b & 4a, 4b.**

The entire targeted compounds were characterized by NMR & IR spectroscopy. The dyes were yellow **(4a)** and orange **(4b)** and freely soluble in acetonitrile, dimethyl sulphoxide or toluene and chloroform. The analytically pure samples were used for further spectroscopic investigations.

Table 5.1 Absorption spectral data for the host **4a** in the presence of different salts.

Salts	**λ, nm ϵ_{max}(M^{-1} cm^{-1} × 10^3)**
None	293 (11.4), 378 (21.3)
Iodide	293 (10.6), 378 (21.2)
Bromide	293 (10.7), 378 (21.2)
Chloride	293 (10.8), 378 (21.1)
Hydrogen sulphate	293 (10.9), 378 (20.9)
Hexachlorophosphate	293 (10.1), 378 (21.1)
Per chlorte	293 (11.1), 378 (21.2)
Fluoride	299 (3.8), 410 (20.9), 472 (16.3)
Acetate	299 (3.4), 408 (20.7), 472 (18.1)

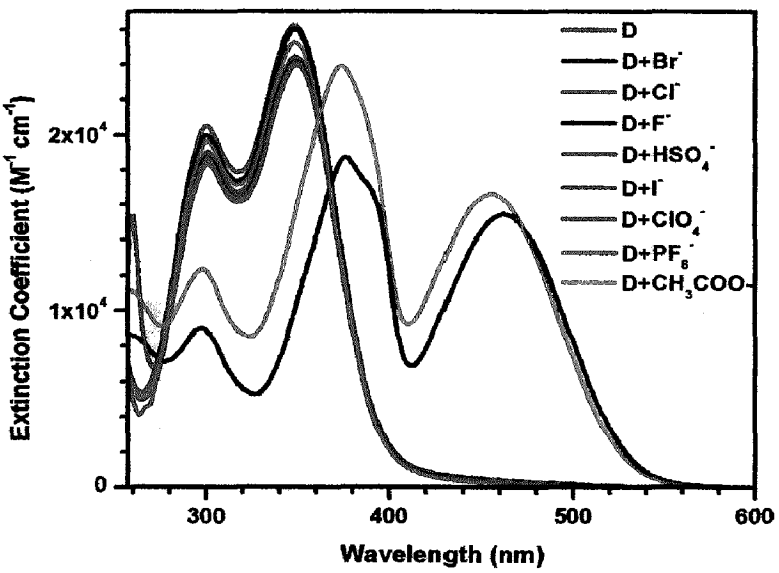

Figure 5.3 UV–Vis absorption spectral changes observed for **4a** in acetonitrile upon addition of 10 equivalents of tetrabutylammonium anion salts.

The absorption spectra of dye **4a** in the solution of acetonitrile with different anions bromide, chloride, fluoride, hydrogen sulphate, iodide, per chlorate, phosphate, acetate has recorded. There were not any essential change in the absorption spectra of dye with the anions bromide, chloride, hydrogen sulphate, iodide, chlorate, and phosphate two peaks same as the spectra of **4a** observed around at 293 and 378 nm because of the π-π^* electron transition. Large bathochromic shifts were observed in absorption spectra Figure 5.3 of **4a** with both anions fluoride and acetate. It is indicating the reorganization property of 4a towards fluoride and acetate. There were three band observed in case of fluoride, acetate anions ,two band in the absorption spectra at 293 nm because of the π-π^* electron transition (the peak around 378 has shifted on around 410 nm after addition of the fluoride, acetate) and the other is a strong absorption in the visible region around 472 nm, which can be assigned to an intermolecular

charge transfer (ICT) between the –OH donating unit and the electron withdrawing group (-NO_2), by the deprotonation from –OH donating unit present in the dye after the addition of the anions (fluoride, acetate) [1].

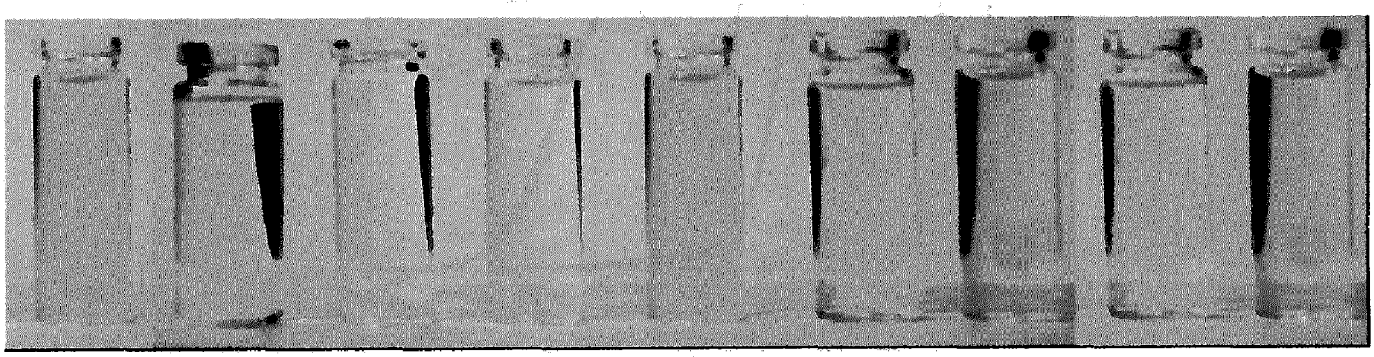

4a+CH_3COO^- **4a**+I^- **4a**+Cl^- **4a**+Br^- **4a**+F^- **4a**+HSO_4^- **4a** **4a**+PF_6^- **4a**+ClO_4^-

Figure 5.4 Color changes shown by the receptor **4a** in acetonitrile, on addition of 10 equivalents of different salts.

Upon the addition of the anions in Figure 5.4 (fluoride, acetate) the color almost transparent of **4a** turned into dark yellow this was because of the binding between **4a** and these two anions by the deprotonation from the donor unit of the dye. So we can say this is a colorimetric type of anion sensor. In case of other anion there were no color change has observed [2].

After the addition of the protic solvent the color disappeared because which proton has deprotonated then the protic solvent filled the deficiency of the proton which can clearly visible to necked eye.

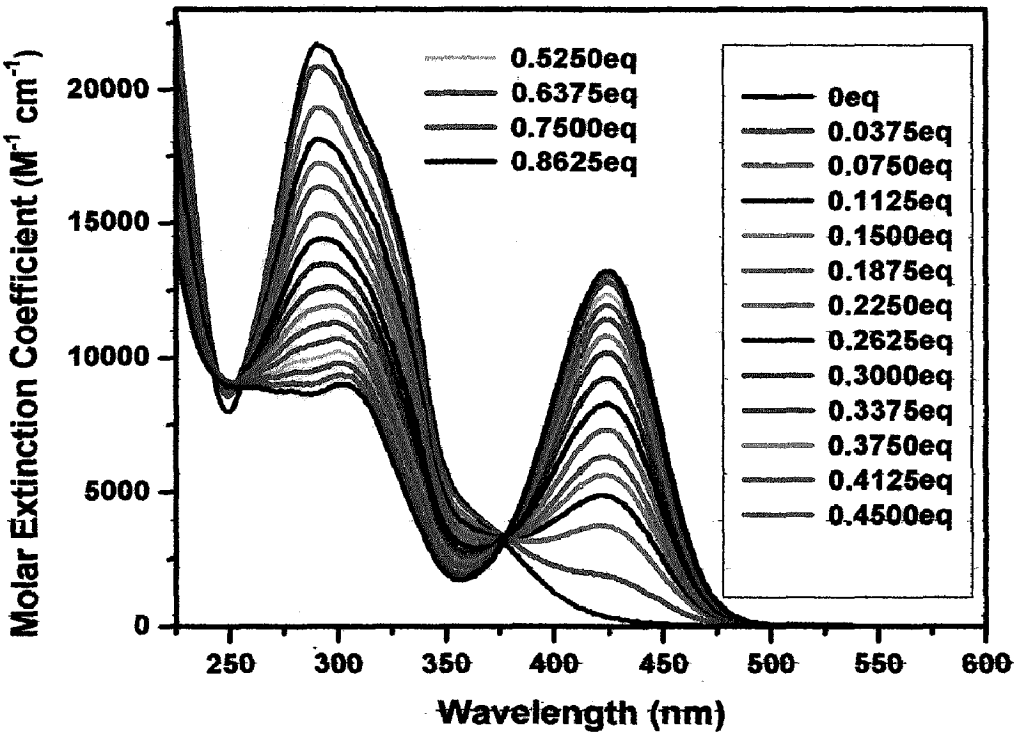

Figure 5.5 UV-Vis titration spectral changes observed for receptor dye **4a** upon addition of tetrabutylammonium fluoride.

After the addition of the fluoride up to 0.8625 equivalent in **4a** in Figure 5.5 the new absorption band at 422 nm increases with the increment in the concentration of fluoride because intramolecular charge transfer transition took place, because of the deprotonation of dye after addition of fluoride and another peak around 293 generated because of the π-π^* electronic transition, decreased after addition of these fluoride and the peak around 378 nm has shifted around at 410 nm. After addition of the fluoride in the dye a complex formed. The selectivity of an anion sensor is related to the structure of the hydrogen bond complex and the basicity of the anions. Among anions, fluoride is the most electronegative atom and, as such usually forms the

strongest H-bond interaction with an -NH or -OH groups. In particular reported receptor in this work are selective for both fluoride and acetate [1].

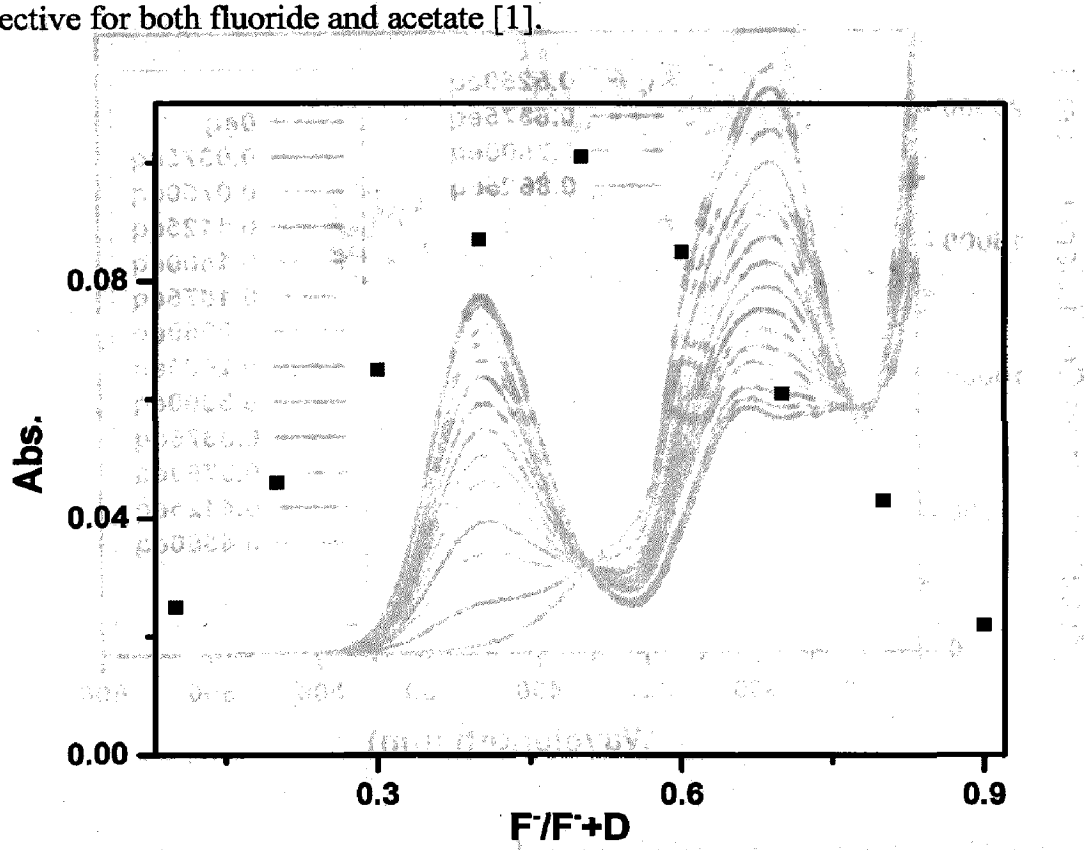

Figure 5.6 Job's plot between **4a** and fluoride, the plot indicates 1:1 binding stoichiometry between **4a** and fluoride.

From the Job' s plot Figure 5.6 analysis we got the idea about the 1:1 binding between **4a** and fluoride ,new band generated in absorption spectra at around 422 nm. When we started the addition of fluoride in the solution of dye the band at 422 nm increased but after some time start decreasing. From the jobs plot basically we got the idea of the binding property of the dye and anion [3, 4].

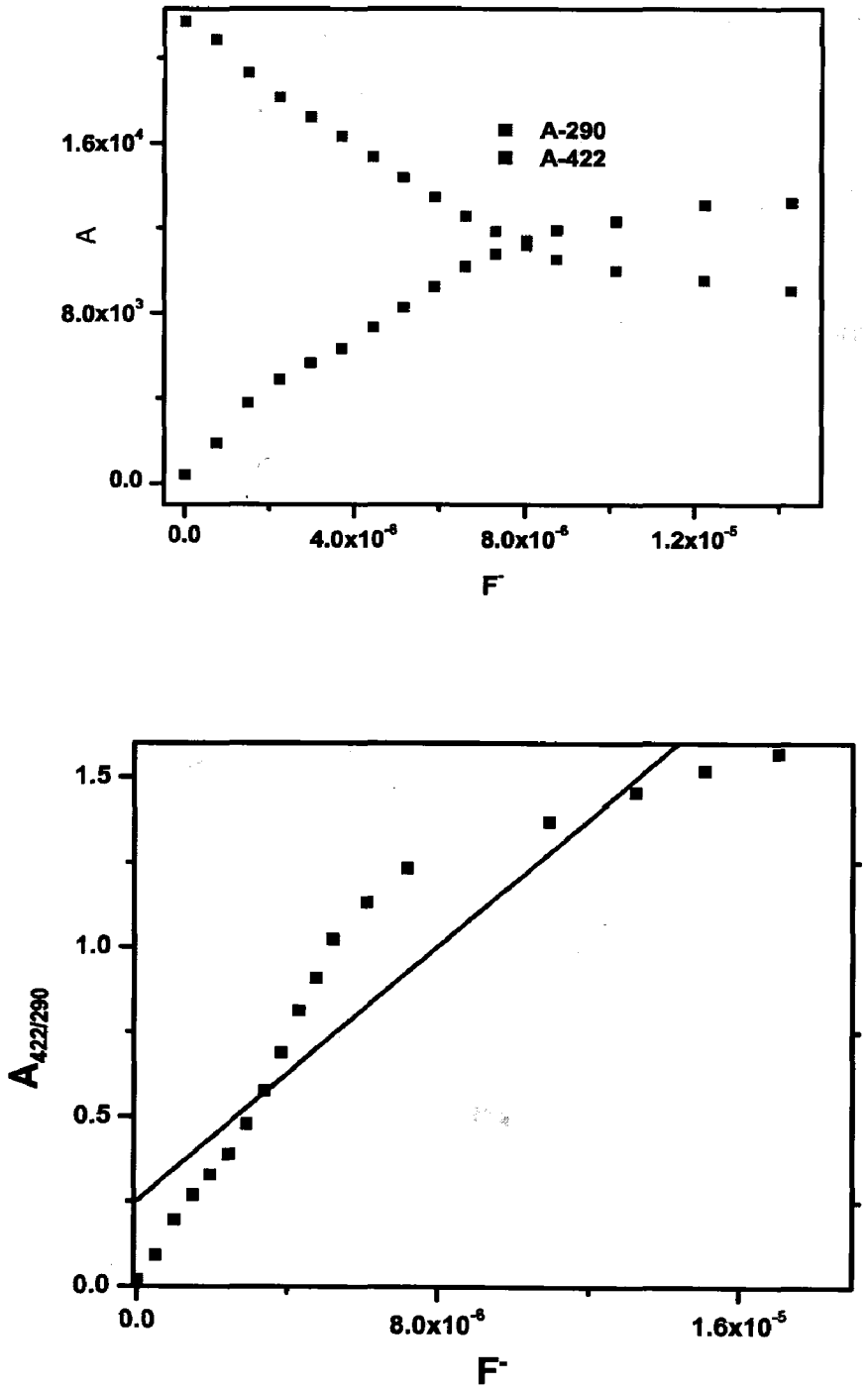

Figure 5.7 Plot of concentration of fluoride vs. absorbance at 422 and 290 and 422/290 of **4a.**

In Figure 5.7 we can see that the peak around 290 nm generated due to π-π^* electronic transition that decreases and the band generated around 422 by the binding between anion and the **4a** that increases after addition of more equivalent of the fluoride [5, 6].

5.3 Binding constant calculation

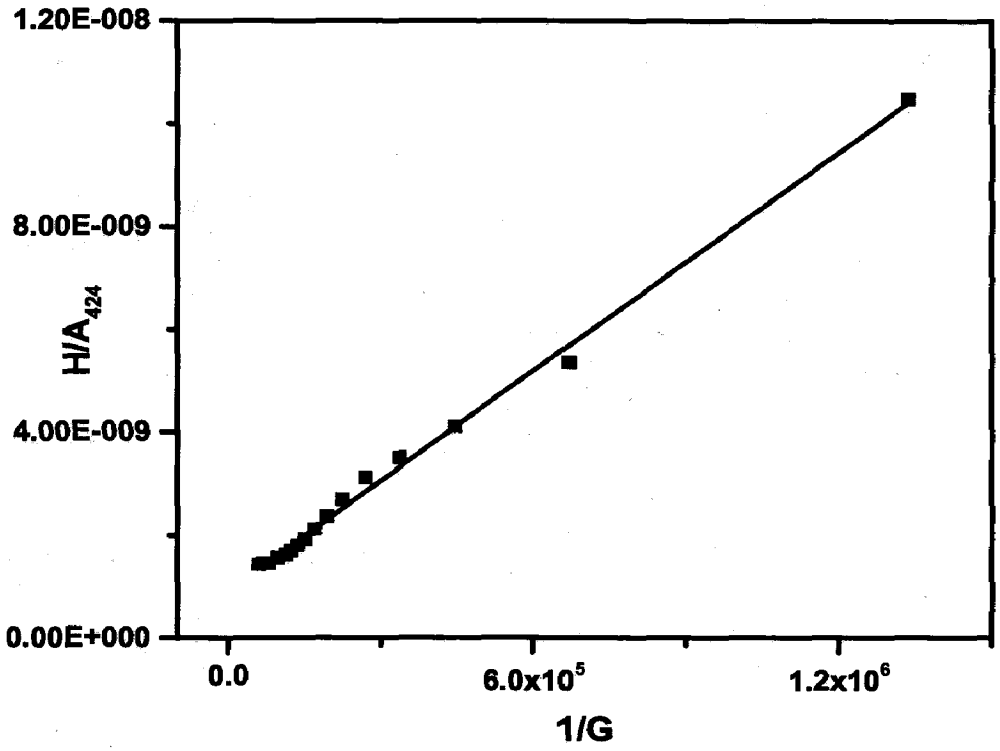

Figure 5.8 Plot of Benesi Hildebrand method for calculation of binding constant of **4a** with fluoride.

Here the host is **4a** and the guest is fluoride from Figure 5.8 we got the value of K_b by using Benesi-Hildbrand method in case of fluoride with the dye **4a** (1.31×10^5 M^{-1}). H is the host (dye) and G is the guest (anion).So when we started the addition of the anion to the host the absorption band around 424 increases this is the indication of the interaction between host and anion [7].

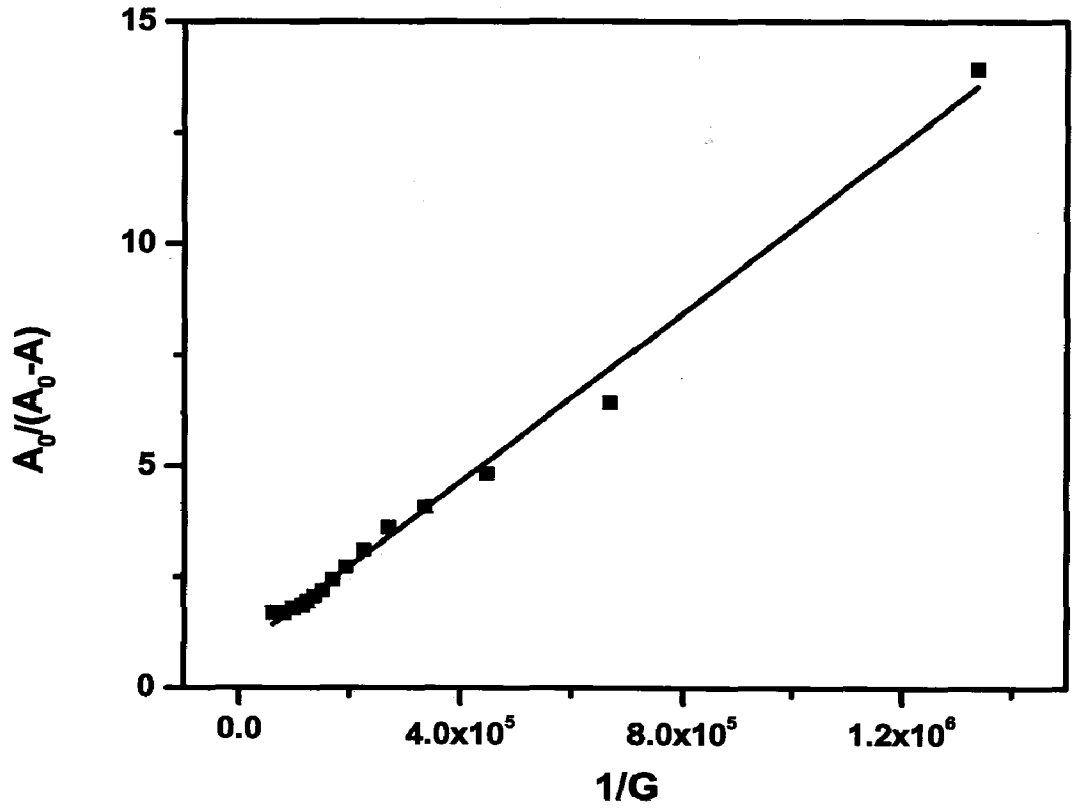

Figure 5.9 Plot of alternate method for calculation of binding constant of **4a** with fluoride.

From this method Figure 5.9, we have calculated the value of K (8.90×10^4 M^{-1}). H is the host (dye) and G is the guest (anion). So when we started the addition of the anion in the host the absorption band around 424 increases this is the indication of the interaction between host and anion.

We have calculated the binding constant by different three methods so, for the final value of K (binding constant) we has compared the all three values. From the binding constant calculation got the idea about the quenching property of the dye [8].

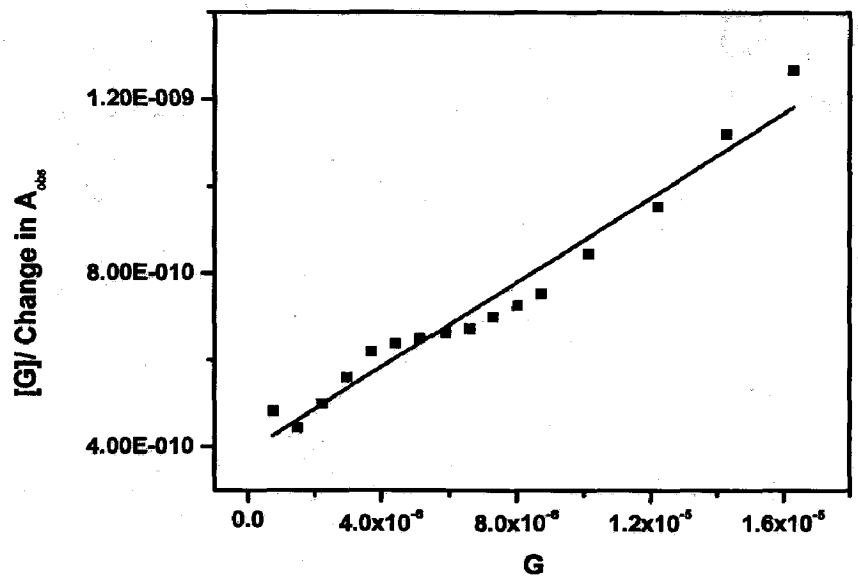

Figure 5.10 Plot of Scott method for calculation of binding constant of **4a** with fluoride.

From this method we have also calculated the value of K_a that is around ($1.25\times10^5\ M^{-1}$).

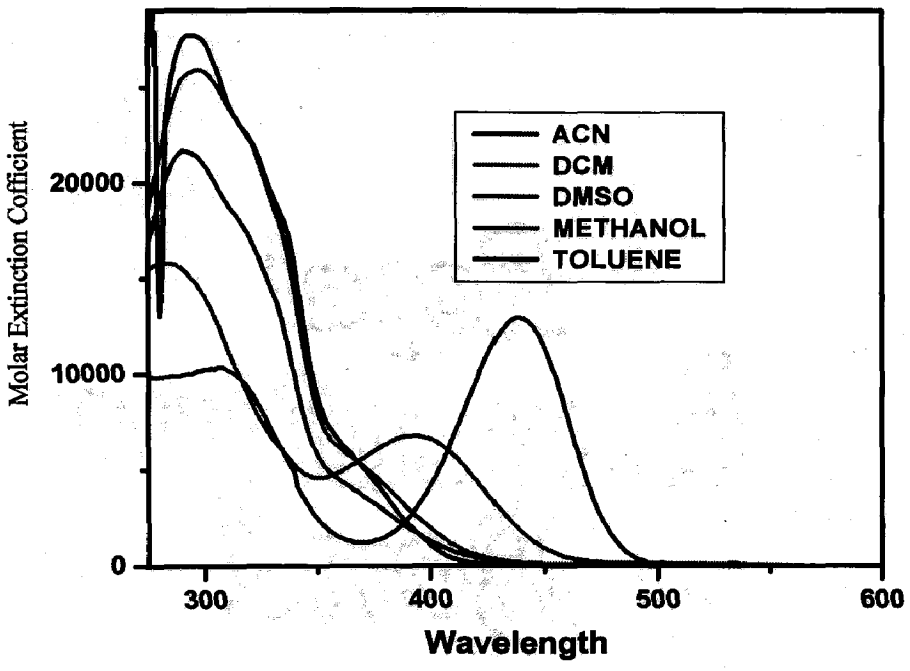

Figure 5.11 Solvatochromism exhibited by the receptor dye **4a.**

We have also done the solvatochromism study from the Figure 5.11 it observed that by moving from less polar to high polar solvent because the hydrogen bond capacity also increases with polarity. A hypsochromic shift took place by increasing the solvent polarity.

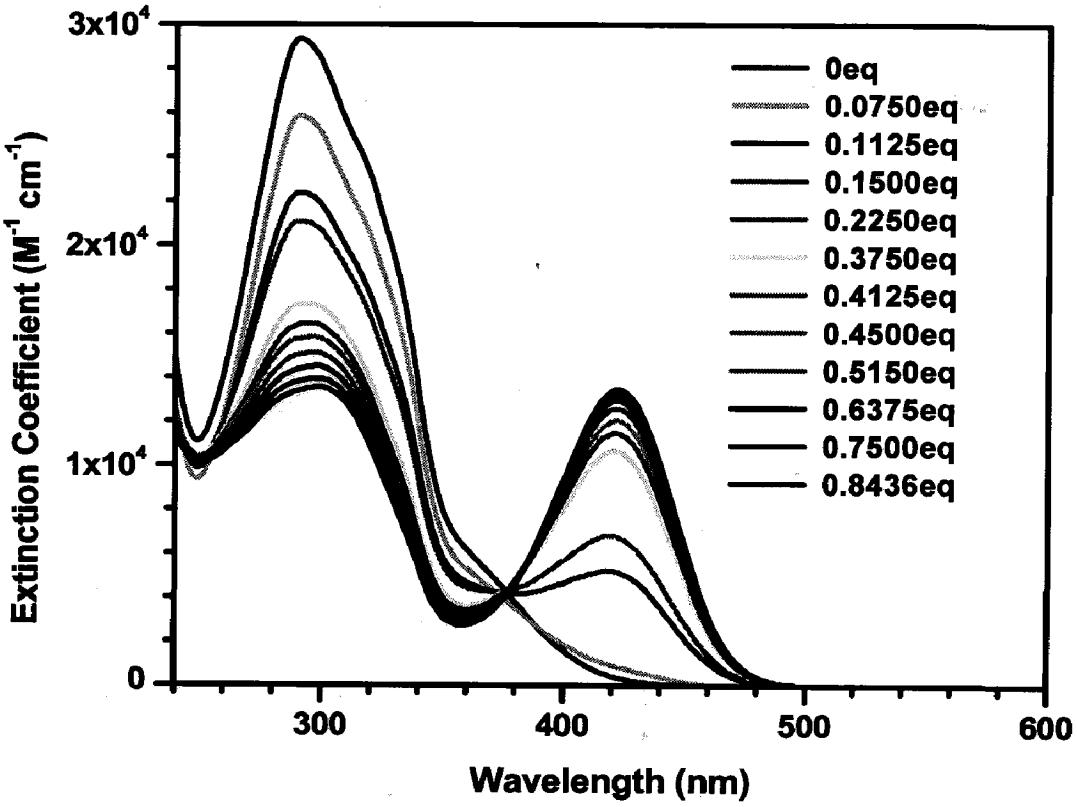

Figure 5.12 UV-Vis titration spectral changes observed for receptor dye **4a** upon addition of tetrabutylammonium acetate.

After the addition of the fluoride up to 0.8436 equivalents in **4a** in Figure 5.12 the new absorption band at 421 nm increases with the increment in the concentration of fluoride because intramolecular charge transfer transition takes place, because of the deprotonation of dye after addition of acetate and peak around 293 generated because of the π-π^* electronic transition, decreased after addition of these acetate and the peak around 378 nm has shifted around at 408 nm.

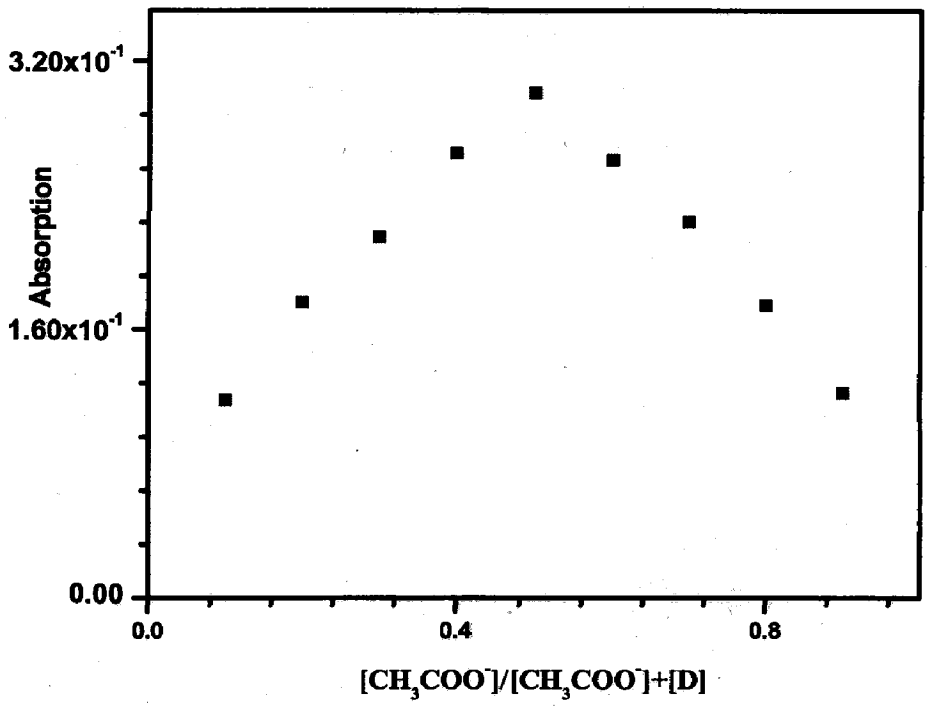

Figure 5.13 Job's plot between **4a** and acetate, the plot indicates 1:1 binding stoichiometry between **4a** and acetate.

From the job' s plot Figure 5.13 analysis we got the idea about the 1:1 binding between **4a** and acetate, new band generated in absorption spectra at around 421 nm. When we started the addition of fluoride in the solution of dye the band at 421 nm increased but after some time start decreasing.

From the jobs plot analysis we got the idea about the binding property between the dye and the acetate. After 1:1 addition of the dye and anion the band around 421 did not increase and further addition of the acetate the band decreases which we have studied from the jobs plot.

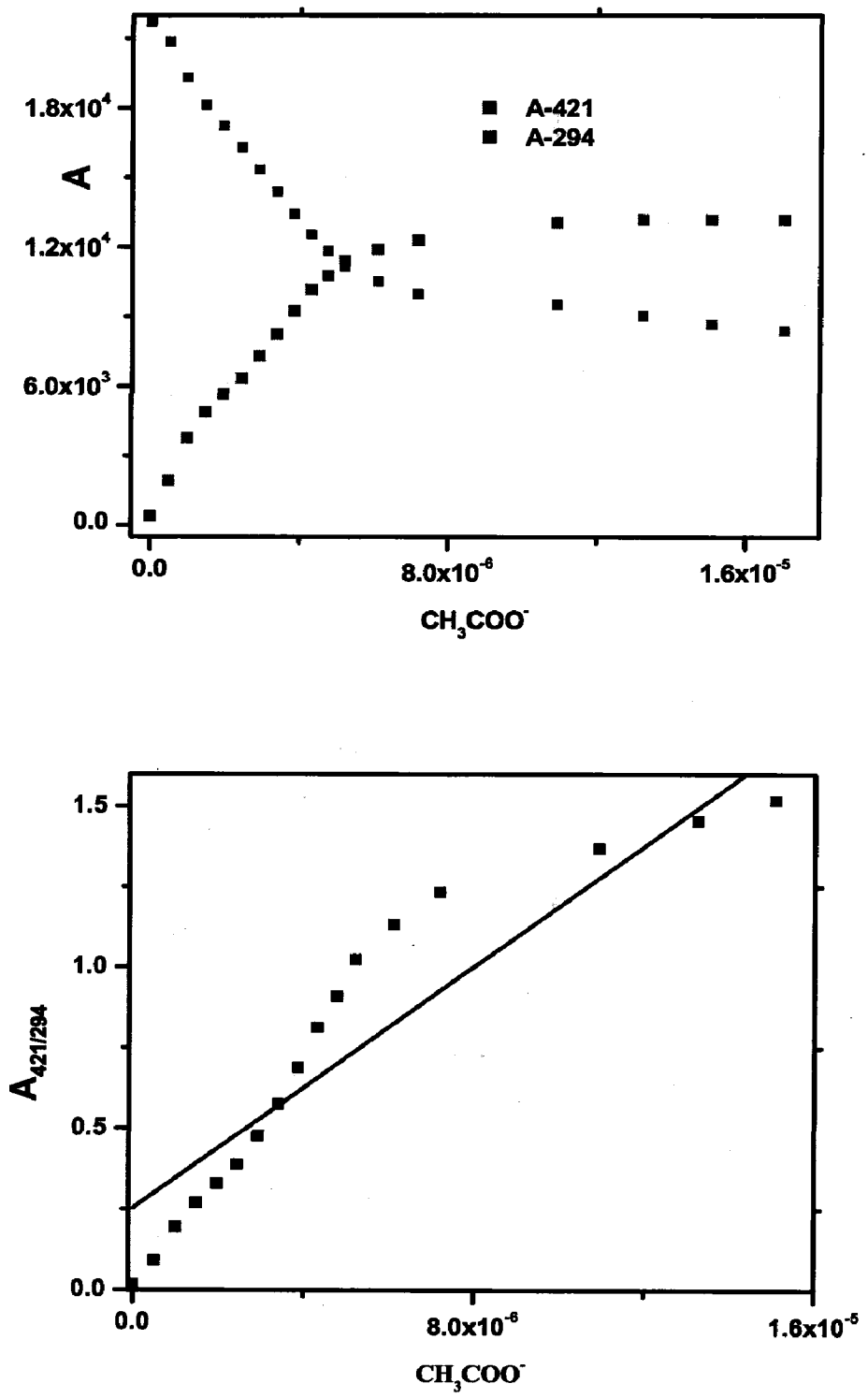

Figure 5.14 Plot of concentration of acetate vs. absorbance at 294 and 421 and 421/294 of **4a.**

In Figure 5.14 we can see that the peak around 294 nm generated due to π-π^* electronic transition that decreases and the band generated around 421 by the binding between anion and the **4a** that increases after addition of more equivalent of the acetate.

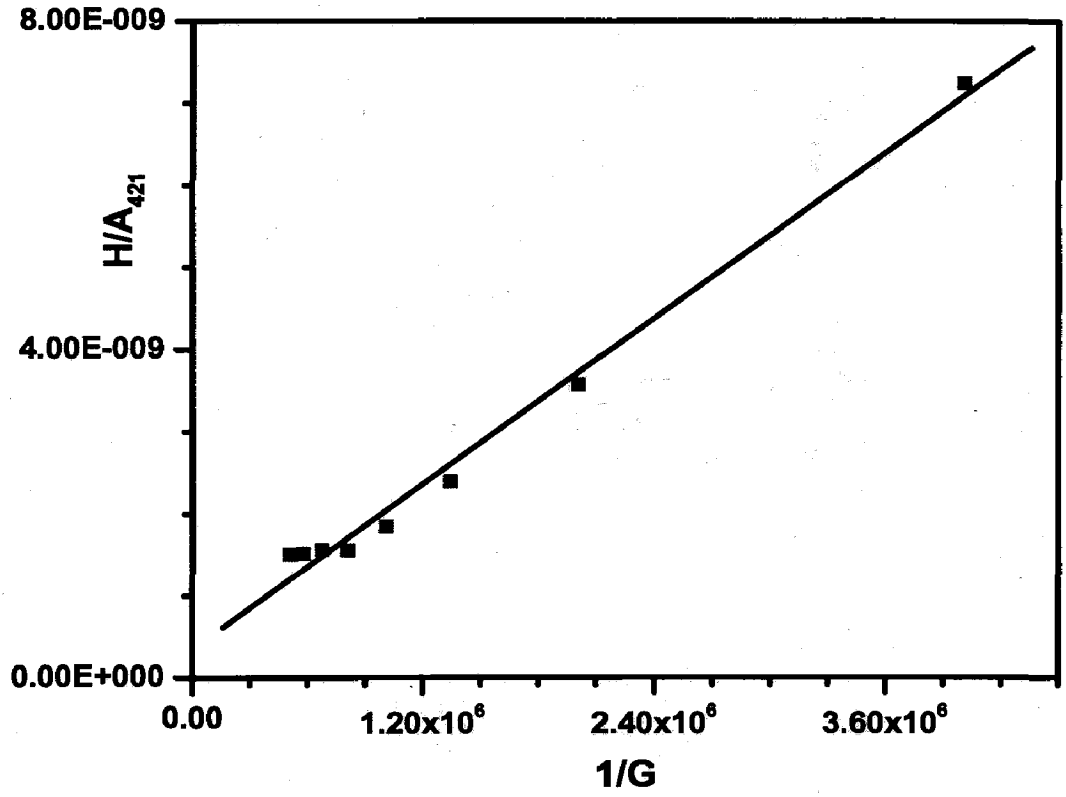

Figure 5.15 Plot of Benesi-Hildbrand method for calculation of binding constant of **4a** with acetate.

Figure 5.15 we got the value of K_b by using Benesi-Hildbrand method in case of acetate with the dye **4a** ($1.33\times10^5\ M^{-1}$).

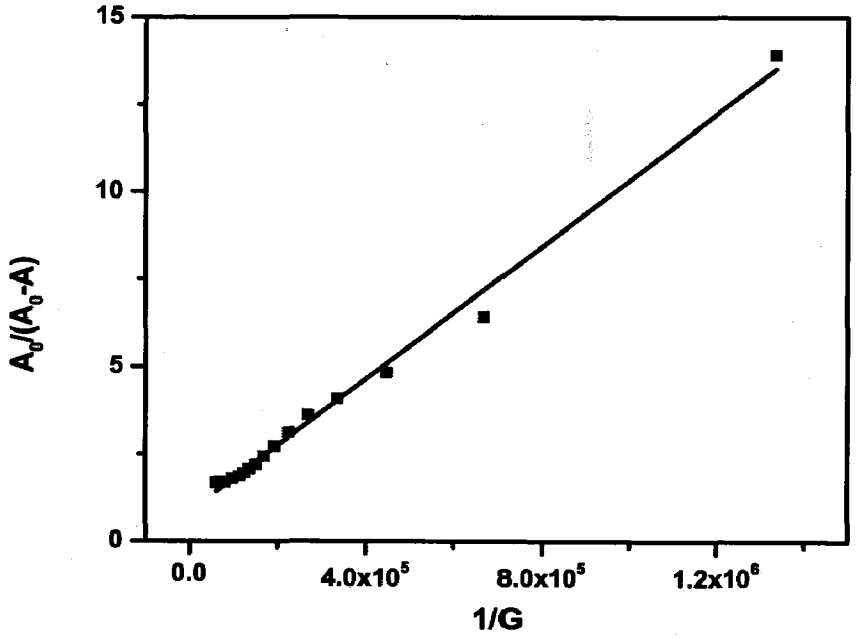

Figure 5.16 Plot of alternate method for calculation of binding constant of **4a** with acetate.

From this method Figure 5.16 we have calculated the value of K ($1.01\times10^5\ M^{-1}$).

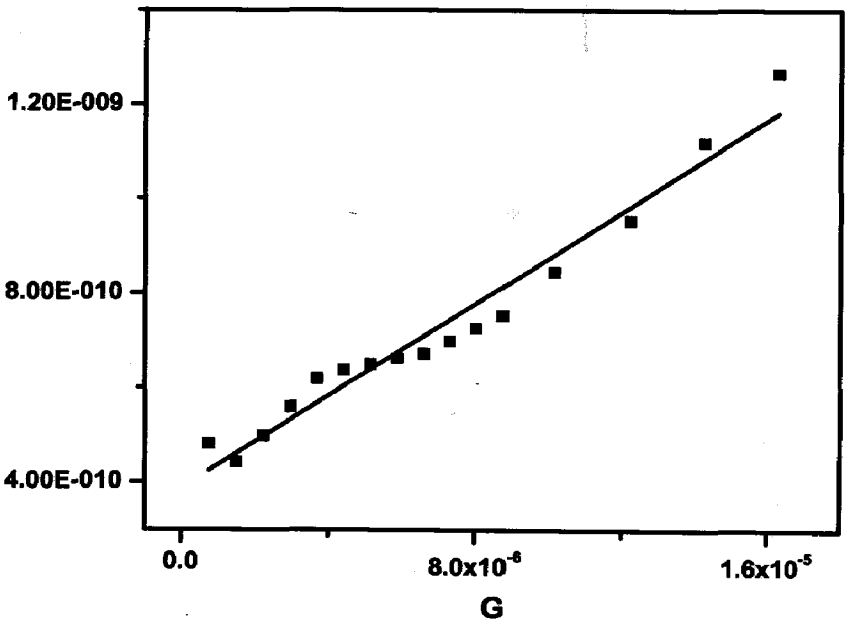

Figure 5.17 Plot of Scott method for calculation of binding constant of **4a** with acetate.

From this method we have also calculated the value of K_a that is around ($1.21\times10^5\ M^{-1}$).

5.4 ^{1}H NMR titration of4a

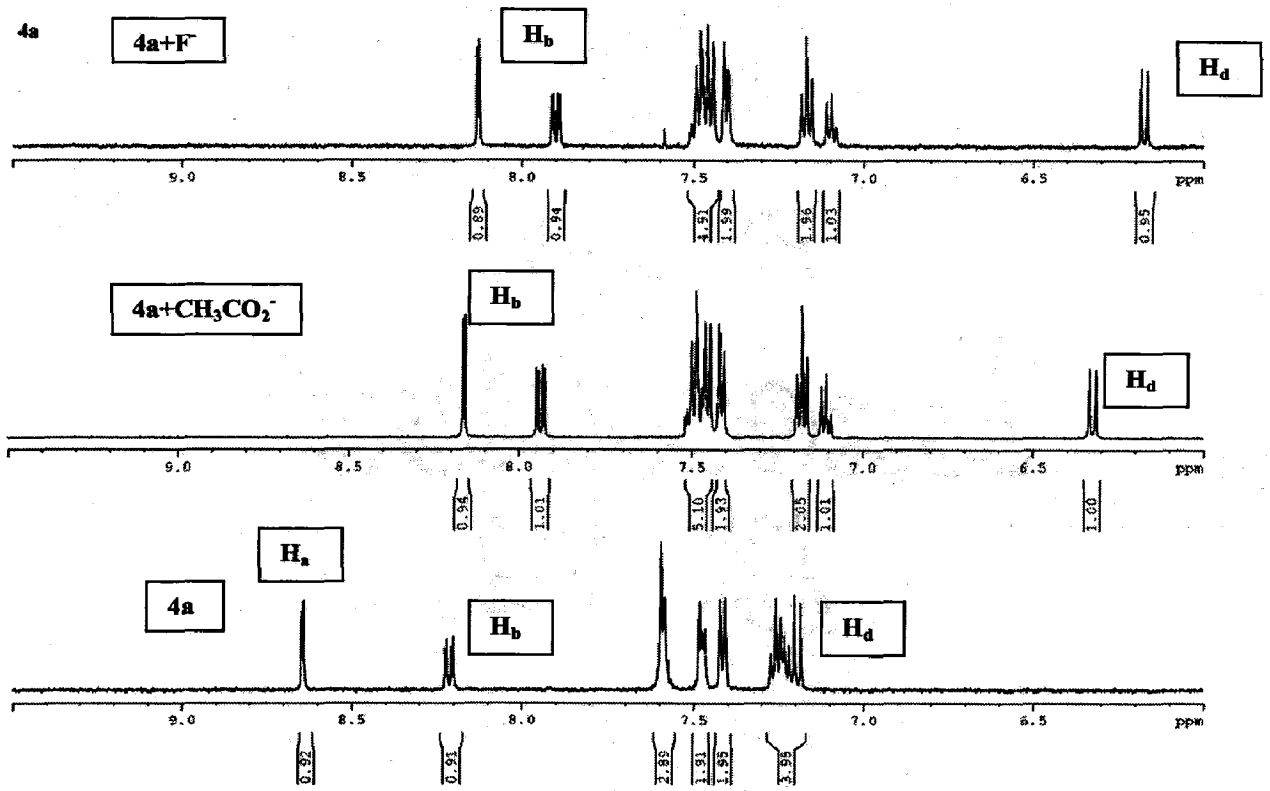

Figure 5.18 ^{1}H NMR titration spectra of dye **4a** with fluoride and acetate.

To further look into the nature of host–guest interactions, ^{1}H NMR titration experiments were conducted in acetonitrile (CD_3CN).^{1}HNMR fluoride titration spectra of the sensor **3a** is shown in Figure 5.18 Upon addition of 10 equivalent of fluoride and acetate ions, the peaks at 8.8 ppm which were assigned to a –OH respectively, were disappeared in case of acetate and in case of fluoride. This indicated the formation of a hydrogen-bonding complex was at this stage. The signal of –OH were disappeared and the other protons, especially H_b and H_d, moved towards upfield, which indicated the bonding between dye and the anions. All the results observed

indicate that during the ^1H NMR titrations the excess fluoride and acetate results the deprotonation of the sensor **(4a)** take place.

Table 5.2 Absorption spectral data for the host **4b** in the presence of different salts.

Salts	λ, nm $\epsilon_{max}(M^{-1} cm^{-1} \times 10^3)$
None	325 (48.5)
Iodide	325 (39.3)
Bromide	325 (41.3)
Chloride	325 (39.2)
Hydrogen sulphate	325 (35.8)
Hexachlorophosphate	325 (41.2)
Per chlorate	325 (39.8)
Fluoride	331 (27.4), 428 (20.9)
Acetate	331 (27.3), 423 (18.1)

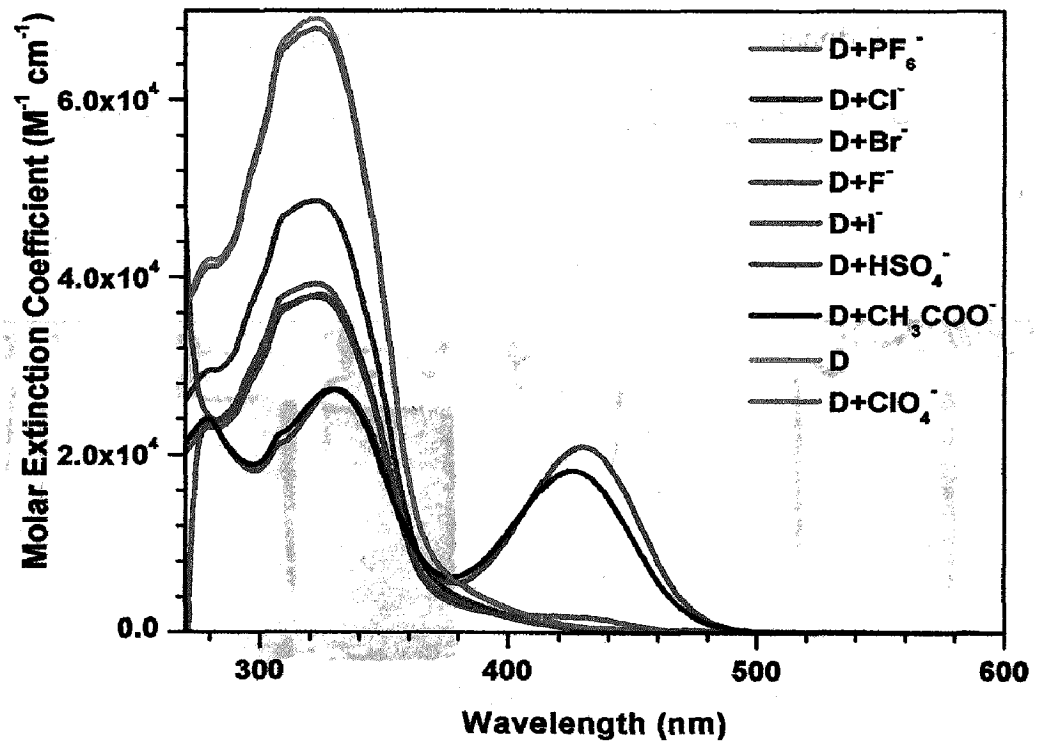

Figure 5.19 UV–Vis absorption spectral changes observed for **4b** in acetonitrile upon addition of 10 equivalents of tetrabutylammonium anion salts.

The absorption spectra of dye **4a** in the solution of acetonitrile with different anions bromide, chloride, fluoride, hydrogen sulphate, iodide, per chlorate, phosphate, and acetate has recorded. There was not any essential change in the absorption spectra of dye with the anions bromide, chloride, hydrogen sulphate, iodide, chlorate, and phosphate one peaks same as the spectra of **4b** observed around at 325 nm because of the π-π^* electron transition. Large bathochromic shifts were observed in absorption spectra Figure 5.19 of **4b** with both anions F^- and acetate. It is indicating the reorganization property of **4b** towards fluoride and acetate. There were three band observed in case of fluoride, acetate anions ,two band in the absorption spectra at 331 nm because of the π-π^* electron transition and the other is a strong absorption in the visible region around 428 or 423 nm, which can be assigned to an intermolecular charge transfer (ICT) between the –OH donating unit and the electron withdrawing group ($-NO_2$) , by the deprotonation from –OH donating unit present in the dye after the addition of the anions (fluoride, acetate).

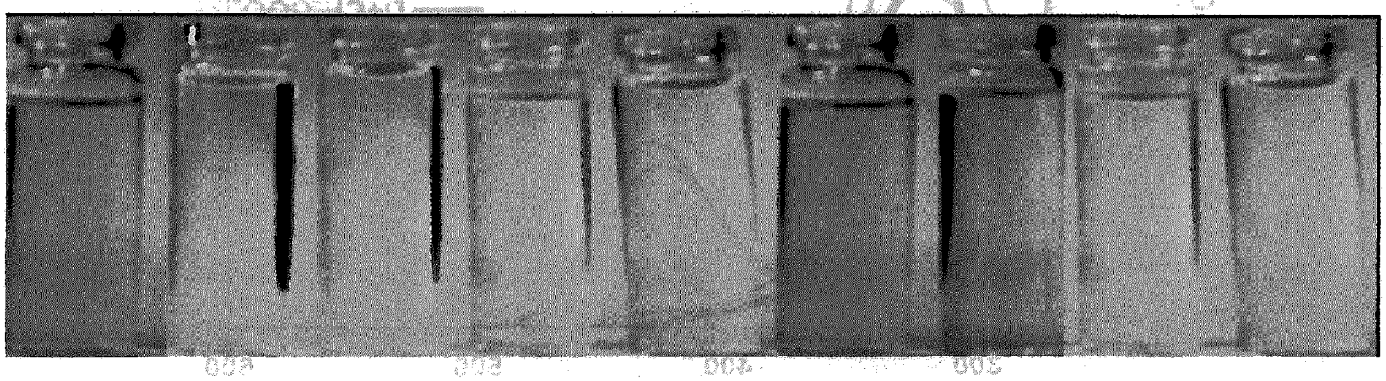

$4a+CH_3COO^-$ $4a+I^-$ $4a+Cl^-$ $4a+Br^-$ $4a+HSO_4^-$ $4a+F^-$ 4a $4a+PF_6^-$ $4a+ClO_4^-$

Figure 5.20 Color changes shown by the receptor **4b** in acetonitrile, on addition of 10 equivalents of different salts.

Upon the addition of the anions in Figure 5.20 (fluoride, acetate) the color almost transparent of **4b** turned into dark yellow this was because of the binding between **4b** and these two anions by the deprotonation from the donor unit of the dye. So we can say this is a colorimetric type of anion sensor. In case of other anion there were no color change has observed.

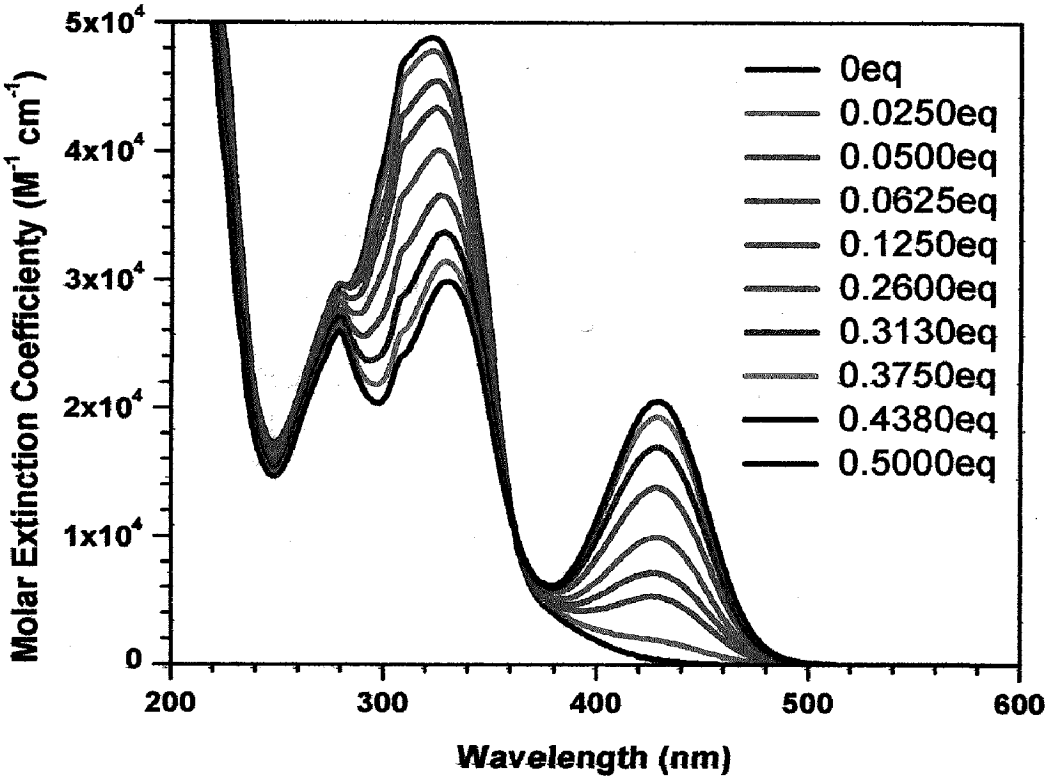

Figure 5.21 UV-Vis titration spectral changes observed for receptor dye **4b** upon addition of tetrabutylammonium fluoride.

After the addition of the fluoride up to 0.5000 equivalent in **4b** in Figure 5.21 the new absorption band at 428 nm increases with the increment in the concentration of fluoride because intramolecular charge transfer transition takes place, because of the deprotonation of dye after addition of fluoride and peak around 331 generated because of the π-π^* electronic transition, decreased after addition of these fluoride. After addition of the fluoride in the dye a complex formed. The selectivity of an anion sensor is related to the structure of the hydrogen bond

complex and the basicity of the anions. Among anions, fluoride is the most electronegative atom and, as such usually forms the strongest H-bond interaction with an -NH or -OH.

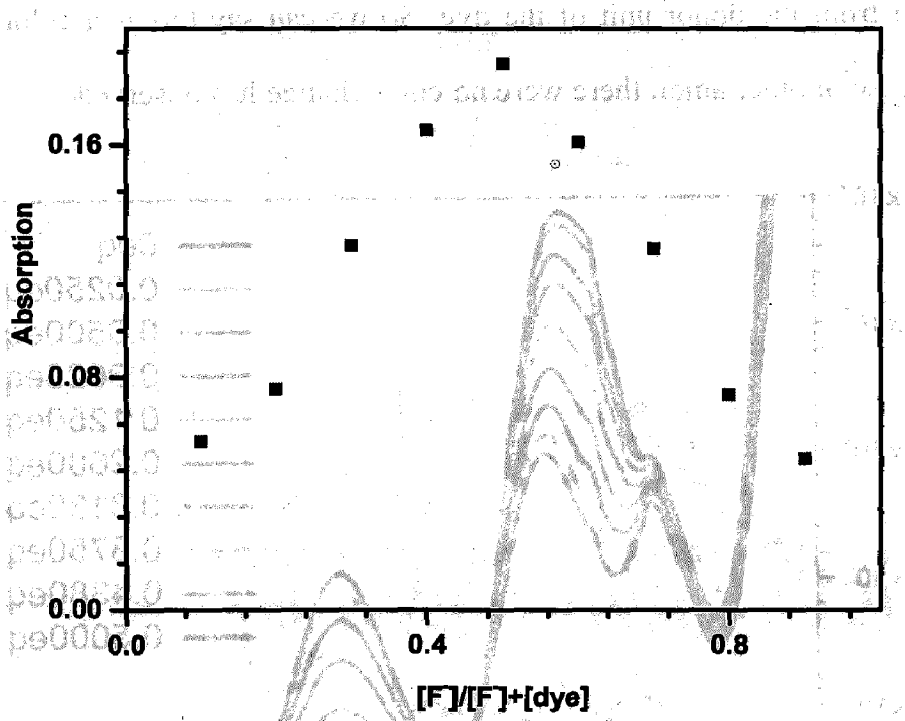

Figure 5.22 Job's plot between **4b** and fluoride, the plot indicates one to one binding stoichiometry between **4b** and fluoride.

From the Job' s plot Figure 5.22 analysis we got the idea about the 1:1 binding between **4b** and fluoride , band generated in absorption spectra at around 428 nm. When we started the addition of fluoride in the solution of dye the band at 428 nm increased but after some time start decreasing.

From the jobs plot analysis we got the idea about the binding property between the dye and the acetate. After 1:1 addition of the dye and anion the band around 428 did not increase and further addition of the acetate the band decreases which we have studied from the jobs plot.

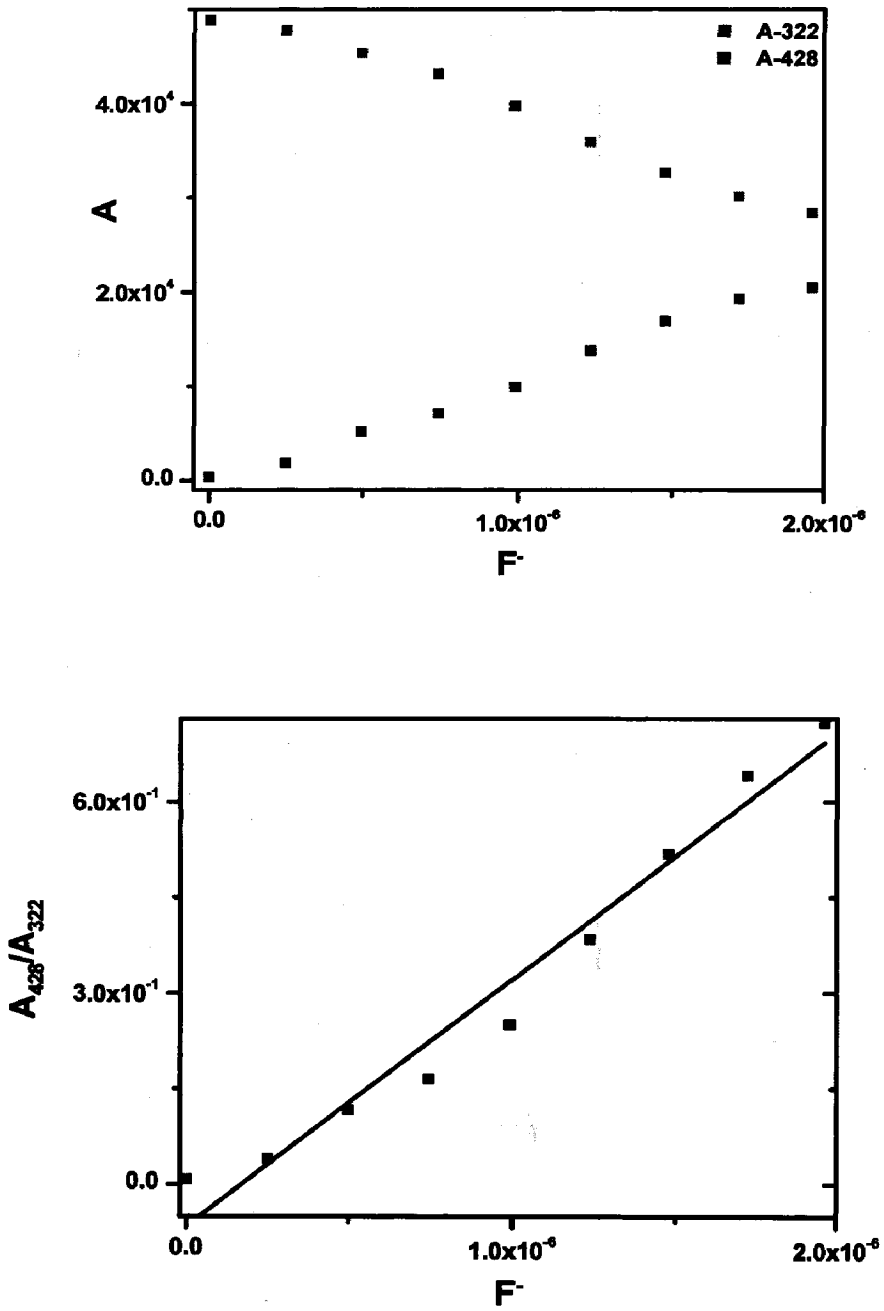

Figure 5.23 Plot of concentration of fluoride vs. absorbance at 428 and 322 and 428/322 of **4b.**

In Figure 5.23 we can see that the peak around 322 nm generated due to π-π^* electronic transition that decreases and the band generated around 428 by the binding between anion and the **4b** that increases after addition of more equivalent of the fluoride

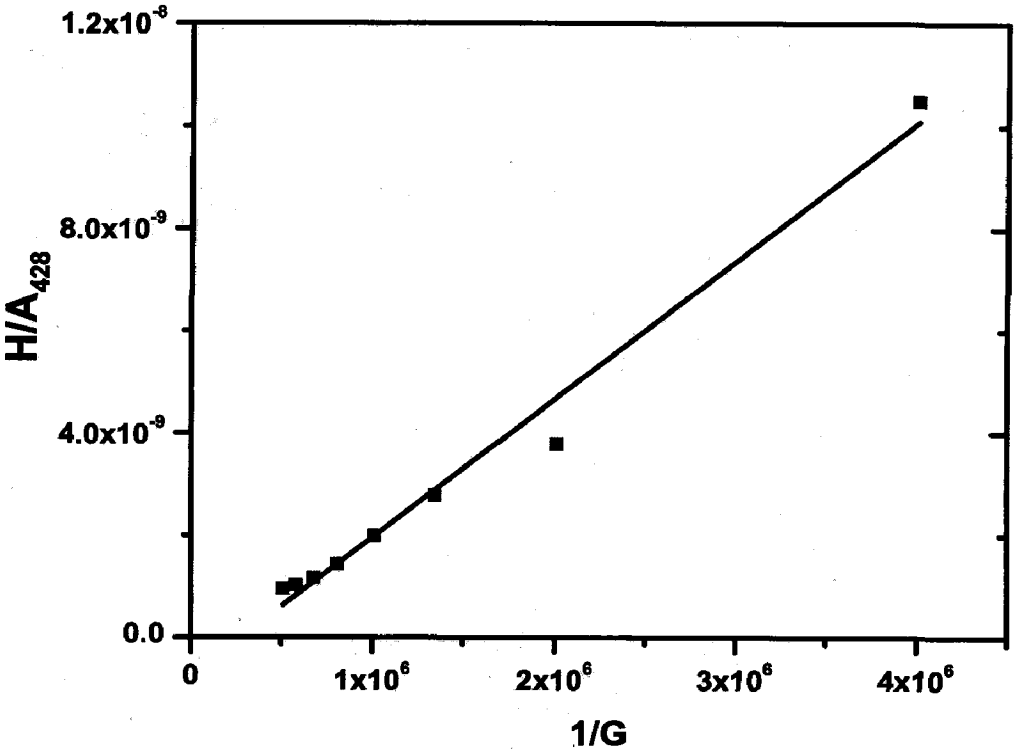

Figure 5.24 Benesi-Hildebrand plot for calculation of binding constant of **4b.**

Here the host is **4b** and the guest is fluoride from Figure 5.24 we got the value of K_b by using Benesi-Hildbrand method in case of acetate with the dye **4b** ($2.67\times10^5\ M^{-1}$).

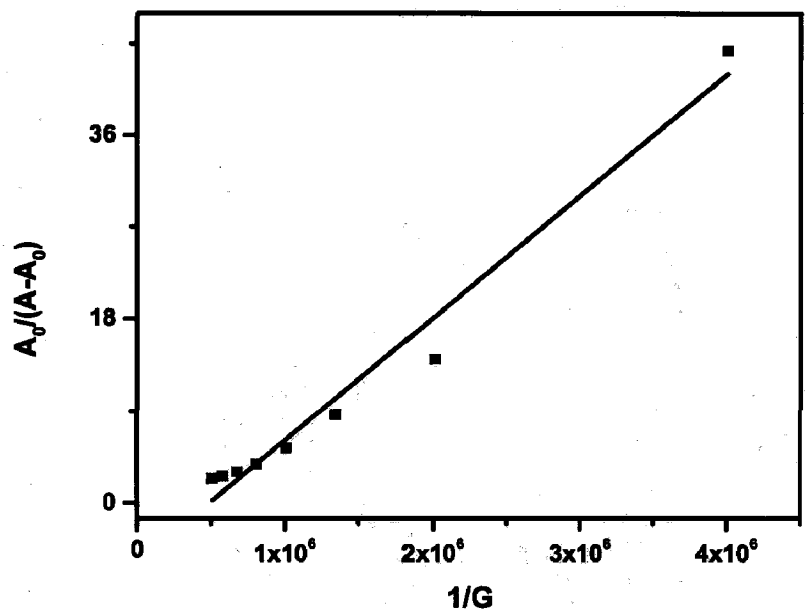

Figure 5.25 Plot of alternate method for calculation of binding constant of **4b** with fluoride.

From this method Figure 5.25 we have calculated the value of K ($3.89\times10^5\ M^{-1}$).

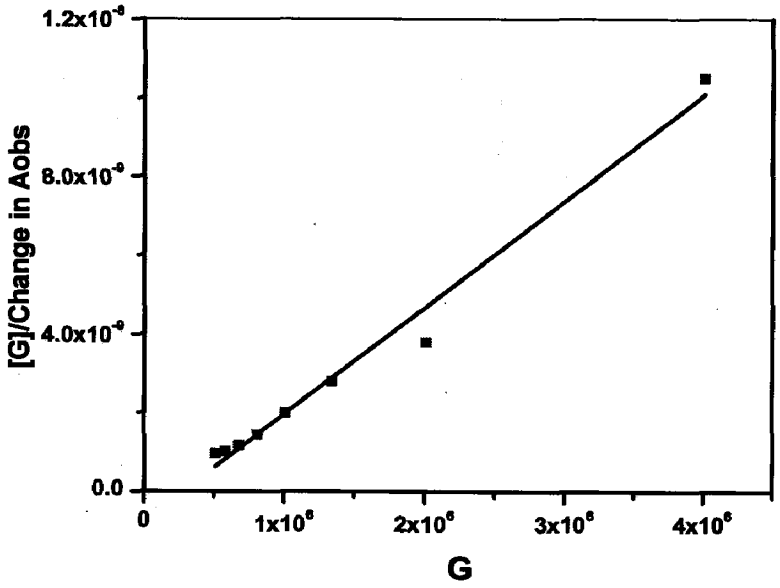

Figure 5.26 Plot of Scott method for calculation of binding constant of **4b** with fluoride.

From this method we have also calculated the value of K_a that is around ($3.29\times10^5\ M^{-1}$).

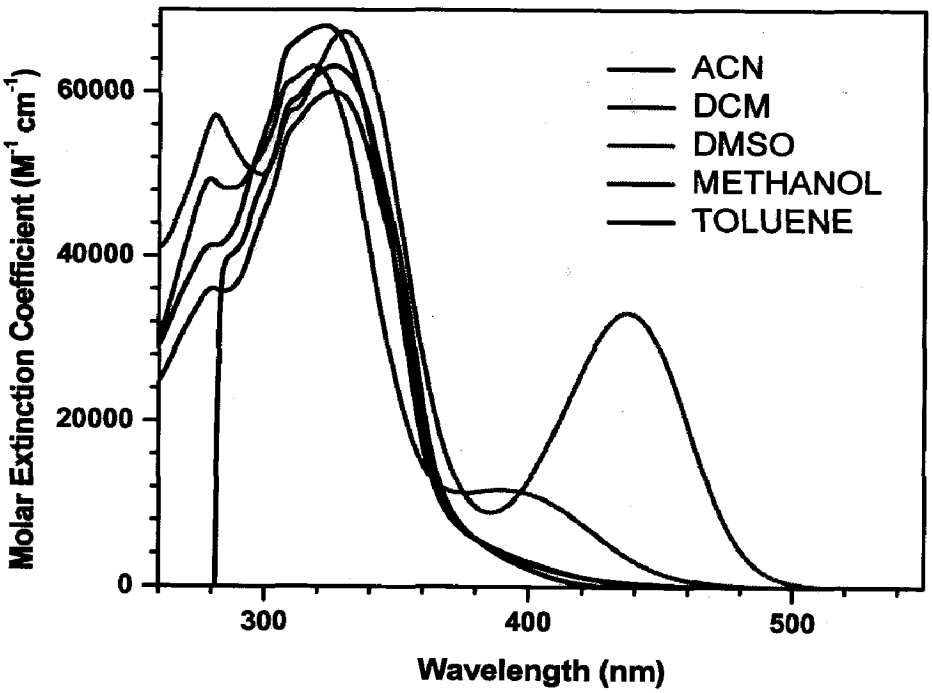

Figure 5.27 Solvatochromism exhibited by the receptor dye **4b.**

We have also done the solvatochromism study from the Figure 5.27 it observed that by moving from less polar to high polar solvent because the hydrogen bond capacity also increases with polarity. A hypsochromic shift took place by increasing the solvent polarity.

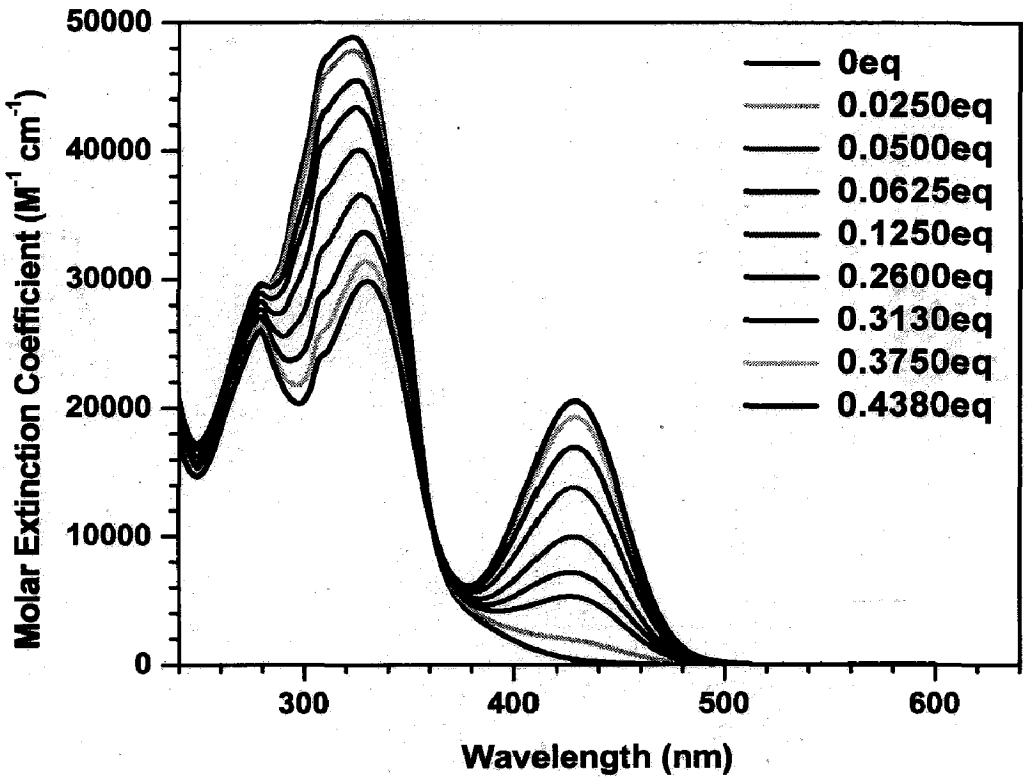

Figure 5.28 UV-Vis titration spectral changes observed for receptor dye **4b** upon addition of tetrabutylammonium acetate.

After the addition of the fluoride up to 0.4380 equivalent in **4b** in Figure 5.28 the new absorption band at 423 nm increases with the increment in the concentration of fluoride because intramolecular charge transfer transition because of the deprotonation of dye after addition of acetate and peak around 331 generated because of the π-π^* electronic transition, decreased after addition of these acetate.

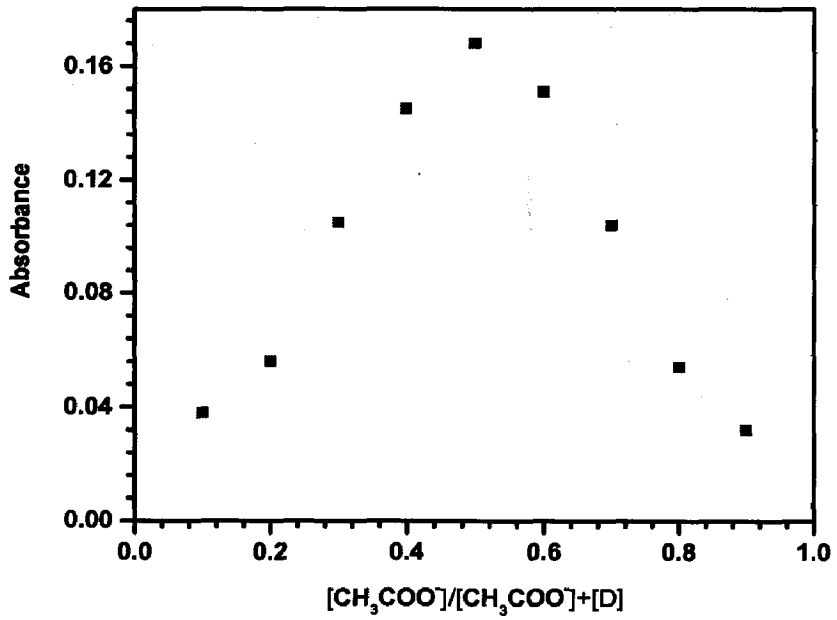

Figure 5.29 Job's plot between **4b** and acetate, the plot indicates 1:1 binding stoichiometry between **4b** and acetate.

From the job' s plot Figure 5.29 analysis we got the idea about the 1:1 binding between **4b** and acetate, new band generated in absorption spectra at around 423 nm. When we started the addition of acetate in the solution of dye the band at 428 nm increased but after some time start decreasing.

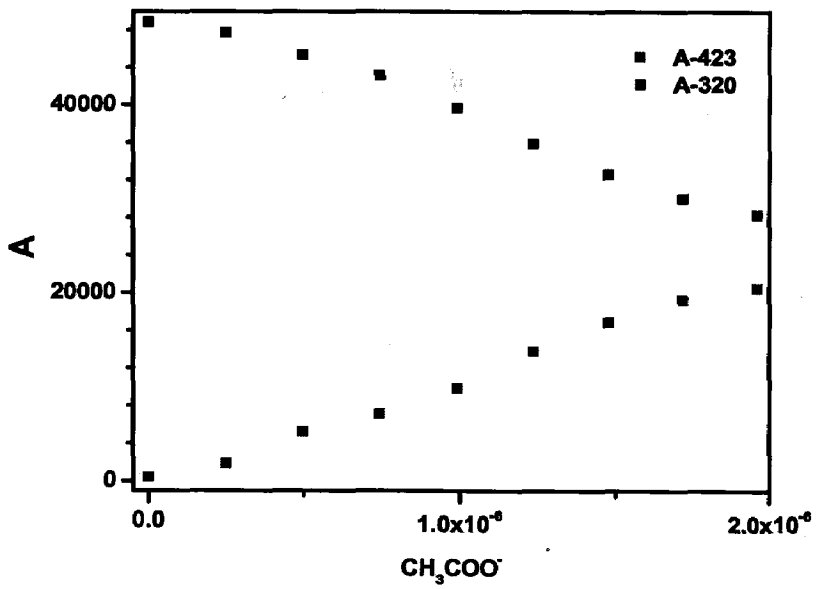

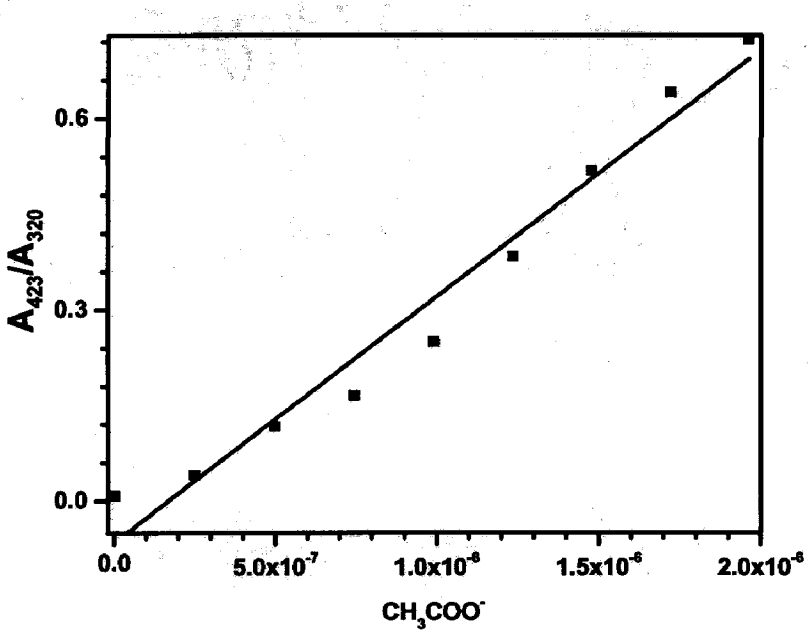

Figure 5.30 Plot of concentration of acetate vs. absorbance at 320 and 423 and 423/320 of **4b.**

In Figure 5.30 we can see that the peak around 331 nm generated due to π-π^* electronic transition that decreases and the band generated around 423 by the binding between anion and the **4b** that increases after addition of more equivalent of the acetate.

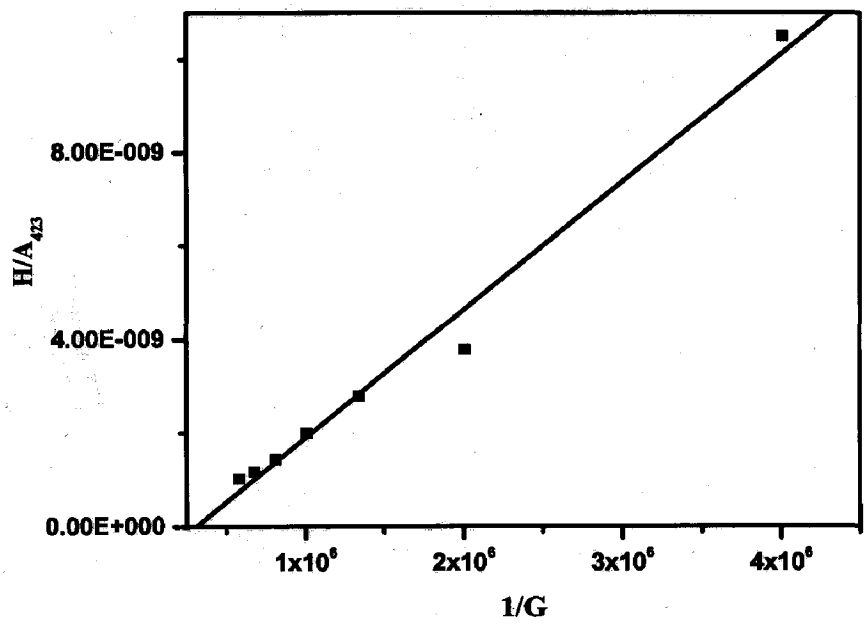

Figure 5.31 Plot of Benesi-Hildebrand method for calculation of binding constant of **4b** with acetate.

Here the host is **4b** and the guest is fluoride from Figure 5.31 we got the value of K_b by using Benesi-Hildbrand method in case of acetate with the dye **4b** ($2.09\times10^5\ M^{-1}$).

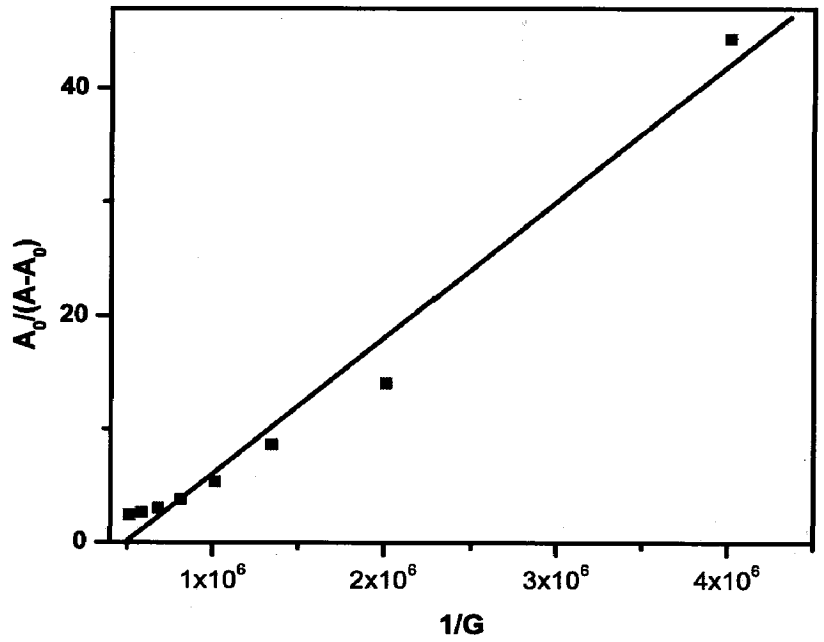

Figure 5.32 Plot of Alternate method for calculation of binding constant of **4b** with acetate.

From this method Figure 5.32 we have calculated the value of K ($2.99\times10^5\ M^{-1}$).

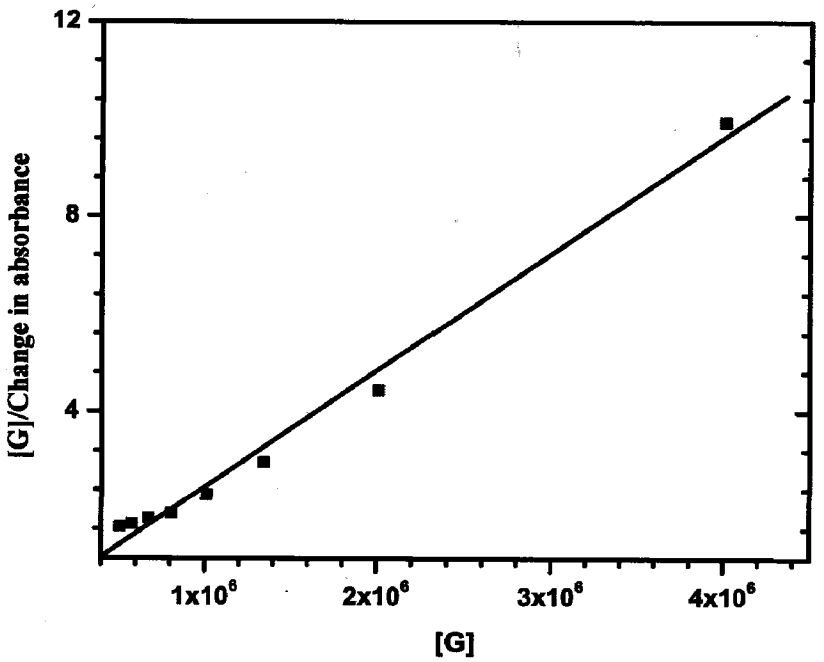

Figure 5.33 Plot of Scott method for calculation of binding constant of **4b** with acetate.

From this method we have also calculated the value of K_a that is around ($2.80\times10^5\ M^{-1}$)

Table 5.3 Data of binding constant calculation (K) for different dyes for fluoride and acetate

Compound	Benesi-Hildebrand method, K_b		Alternate Method, K		Scott Method, K	
	Fluoride	Acetate	Fluoride	Acetate	Fluoride	Acetate
3a	1.60×10^5	1.66×10^5	3.00×10^4	3.04×10^4	2.10×10^5	2.30×10^5
3b	3.53×10^5	3.98×10^5	1.72×10^5	1.92×10^5	1.59×10^5	1.87×10^5
4a	1.31×10^5	1.33×10^5	8.90×10^4	1.01×10^5	1.25×10^5	1.21×10^5
4b	2.76×10^5	2.09×10^5	3.89×10^5	2.99×10^5	3.29×10^5	2.80×10^5

From this table we can compare the binding constant for all dyes. So the value of binding constant for fluoride for receptors **3a** and **3b** from all the methods is closely same to the value of binding constant for acetate but in case of receptors **4a** and **4b** the value of binding constant in case of acetate is heigh as compare to fluoride because The two oxygen atoms of acetate effectively form four hydrogen bonds (two per oxygen atom) with each receptor in case of imidazole based dyes and interacting with -OH and –NH hydrogen of the dyes. The basicity of the acetate is may be high in case of imidazole based anion sensor for the interaction between dye and acetate.

5.5 ^{1}H NMR titration of 4b

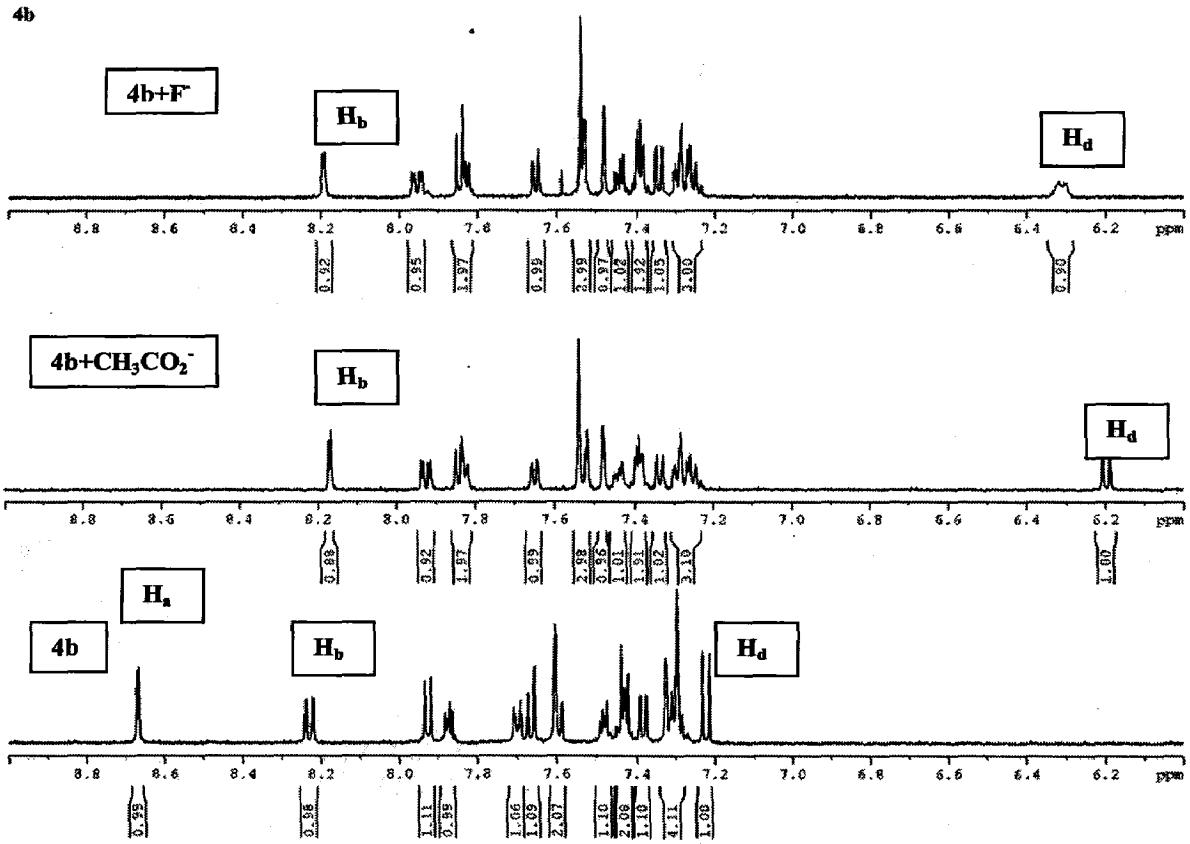

Figure 5.34 ^{1}H NMR titration spectra of dye 4a with fluoride and acetate.

To further look into the nature of host–guest interactions, ^{1}H NMR titration experiments were conducted in acetonitrile (CD_3CN).^{1}HNMR fluoride titration spectra of the sensor 3a is shown in Figure 5.34 Upon addition of 10 equiv. of fluoride and acetate ions, the peaks at 8.7 ppm which were assigned to a –OH respectively, were shifted towards upfield in case of acetate and in case of fluoride. This indicated the formation of a hydrogen-bonding complex was at this stage.–OH was shift towards upfield and the other protons also, especially H_b and H_d, moved towards upfield, which indicated the bonding between dye and the anions. All the results

observed indicate that during the ^1H NMR titrations the excess fluoride and acetate results the deprotonation of the sensor **(4b)** take place.

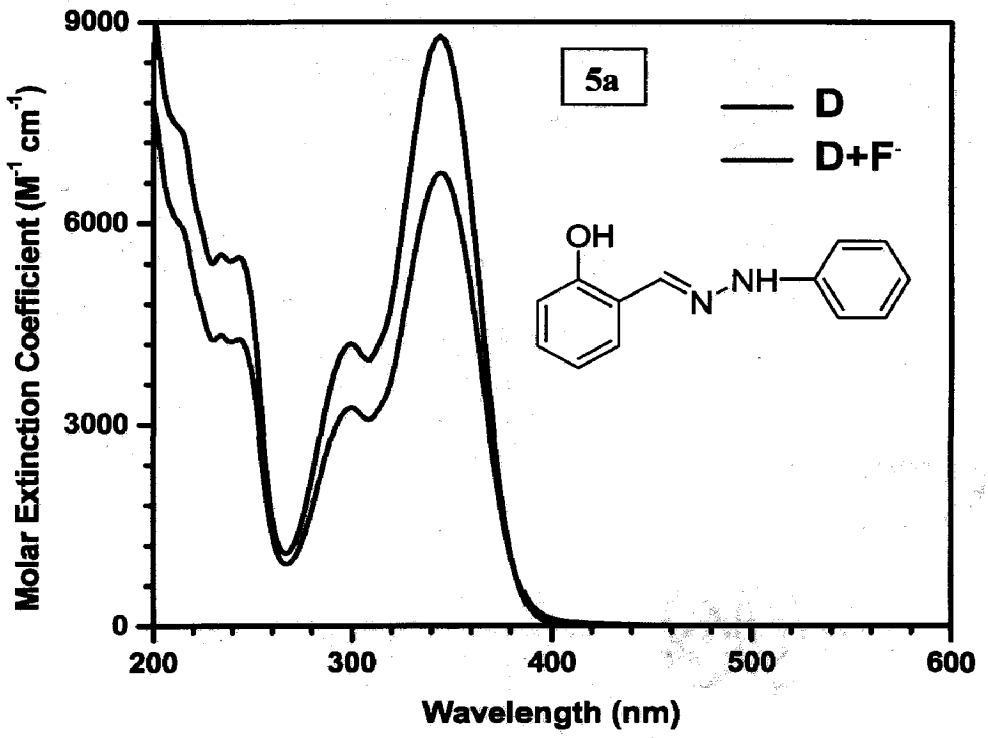

Figure 5.35 UV–Vis absorption spectral changes obserbed for **5a** (control molecule) in acetonitrile upon addition of 10 equivalents of tetrabutylammonium fluoride salt

We also selected a control molecule without introducing the electron withdrawing group and it confirmed by the absorption spectra that the presence of electron withdrawing group in the receptor unit play a very important role in the binding between the anion and the receptor unit, in the enhancement of the acidity towards the deprotonation.

5.6 Conclusions

We have successfully given the different spectral analysis of two imidazole based anion sensor. imidazole based anion sensor can quantitatively detect two anions fluoride and acetate by

generating a new peak in absorption spectra after addition of these two anions and with other anions there were not any significant change in the absorption spectra of dye. By ^{1}H NMR experiment, in the titration spectra of the dye after addition of the anions (fluoride and acetate), peaks because of –OH in the NMR spectra of dyes **4a** and **4b** disappeared and other peaks shifted towards upfield. So from all the spectral analysis it is clear that a strong interaction has taken place between dye and anion. From the Job's plot and other methods for binding constant calculation, we can see the 1:1 interaction of dyes and anions and the complex formation.

5.7 Reference

1. Jeon, S.; Park, D. H.; Lee, H. K.; Park, J. Y.; Kang, S. O.; Nam, K. C. *Bull. Korean Chem. Soc.* **2003**, *24*, 101465.
2. Shao, J. *J. Incl Phenom Macrocycl Chem.* **2011**, *70*, 91.
3. Kim, S. K., Lee, D. H., Hong, J., Yoon, J. Acc. Chem. Res. **2009**, *42*, 23.
4. Martínez-Máñez, R.; Sanceno, N. F. *Chem. Rev.* **2003**, *103*, 4419.
5. Xu, Z.; Kim, S. K.; Yoon, J. *Chem. Soc. Rev.* **2010**, *39*, 1457.
6. Dydio, P., Zieliński, T., Jurczak , J. *Org. Lett.* **2010**, *12*, 1076.
7. Hudson, Z. M., Zhao, S., Wang, R., Wang, S.; *Chem. Eur. J.* **2009**, *15*, 6131.
8. Park, C., Hong, J. *Tetrahedron Lett.* **2010**, *51*, 1960.

Chapter 6

Summary

In conclusion, we have successfully developed a simple, highly selective, and sensitive system (optical chemosensors) for quantitative detection of anions. This type of sensors also shows a sharp color change after addition of anions fluoride and acetate, so we also can call to this type of sensors colorimetric type anion sensors.

Here, we have reported hydrazones (**3a-3b**) and imidazole (**4a-4b**) based anion sensor. These four anion sensor contain two binding site –OH, –NH attached with the electron withdrawing ($–NO_2$) group, which increase the acidity of the receptor unit and the easy deprotonation take place through the binding site. We also report a control molecule without the introduction of the electron withdrawing group to see the affect in binding between the receptor and the anion.

In the absorption spectra of all the dyes in the solution of acetonitrile with different anions bromide, chloride, fluoride, hydrogen sulphate, iodide, per chlorate, hexafluorophosphate ' acetate has recorded . There were not any essential change in the absorption spectra of all the dyes with the anions bromide, chloride, hydrogen sulphate, iodide, perchlorate, hexafluorophosphate and in case of fluoride and acetate one new peak generated in the absorption spectra , which assigned to an intermolecular charge transfer (ICT) between the –OH donating unit and the electron withdrawing group ($-NO_2$) , by the derotonation from –OH donating unit present in the dye after the addition of the anions (fluoride, acetate).

Upon the addition of the anions in (fluoride, acetate) the color almost transparent of **3a** and **3b** turned into dark yellow and orange respectively and in case of **4a** and **4b** the color turned into

yellow. This was because of the binding between **3a** and these two anions by the deprotonation from the donor unit of the dye. So we can say this is a colorimetric type of anion sensor. In case of other anion there were no color change has observed.

To further look into the nature of host–guest interactions, ^{1}H NMR titration experiments were conducted in acetonitrile.^{1}HNMR titration spectra of the sensor **3a, 3b** or **4a** and **4b** in the presence of fluoride and acetate ions, the peakes because of –OH and –NH disappears or upfield shift was the indication of the interaction between dye and anion.

From the Job's plot analysis we got the idea about the 1:1 binding between dyes and fluoride and acetate, band generated after addition of the anion due to charge transfer, when we started the addition of fluoride and acetate in the solution of dye that band increased but after some time starts decreasing.

We also selected a control molecule without introducing the electron withdrawing group and it confirmed by the absorption spectra that the presence of electron withdrawing group in the receptor unit play a very important role in the binding between the anion and the receptor unit, in the enhancement of the acidity towards the deprotonation.

Supporting information

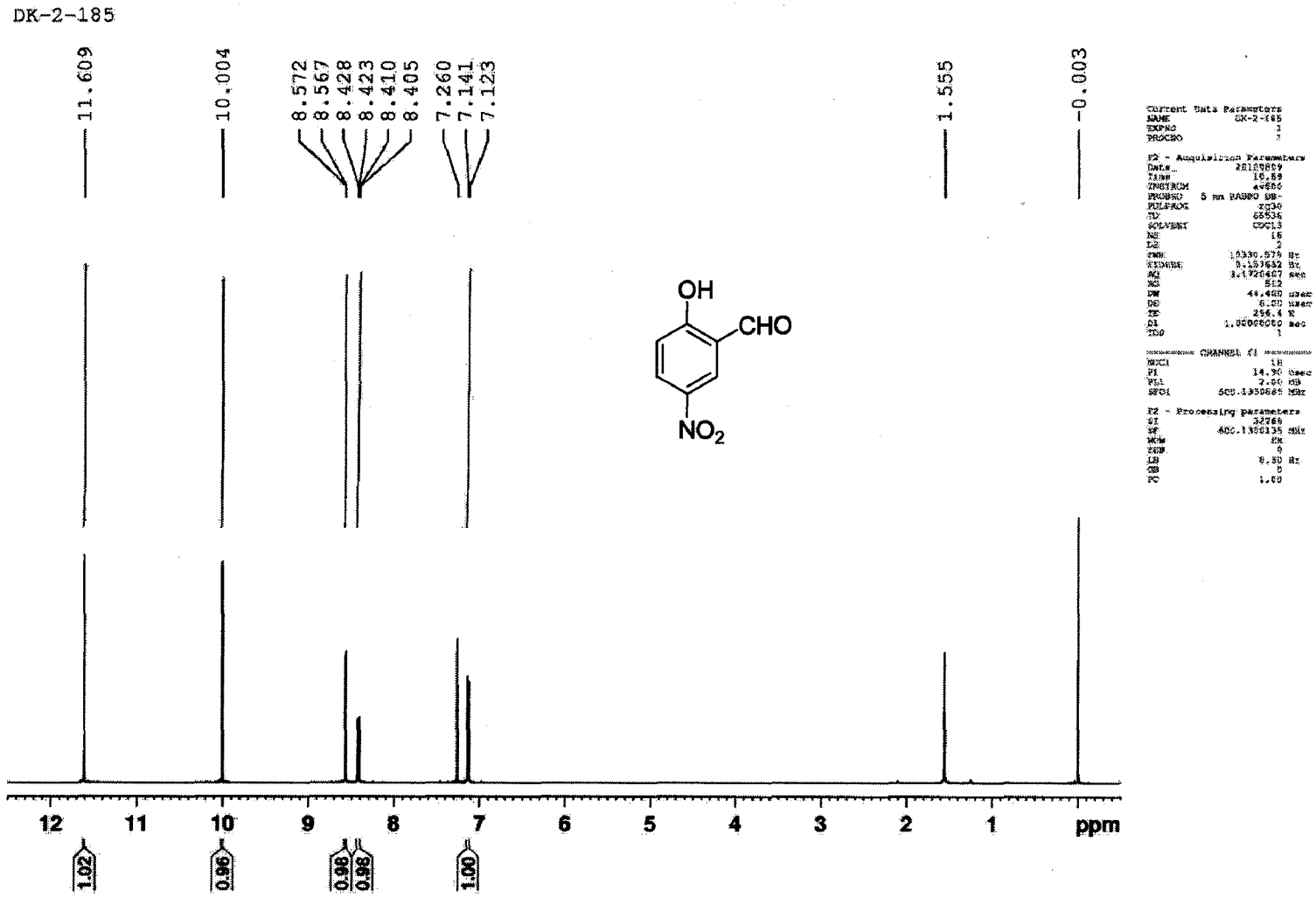

Figure S1. ^{1}H NMR Spectra of **2-hydroxy-5-nitrobenzaldehyde**

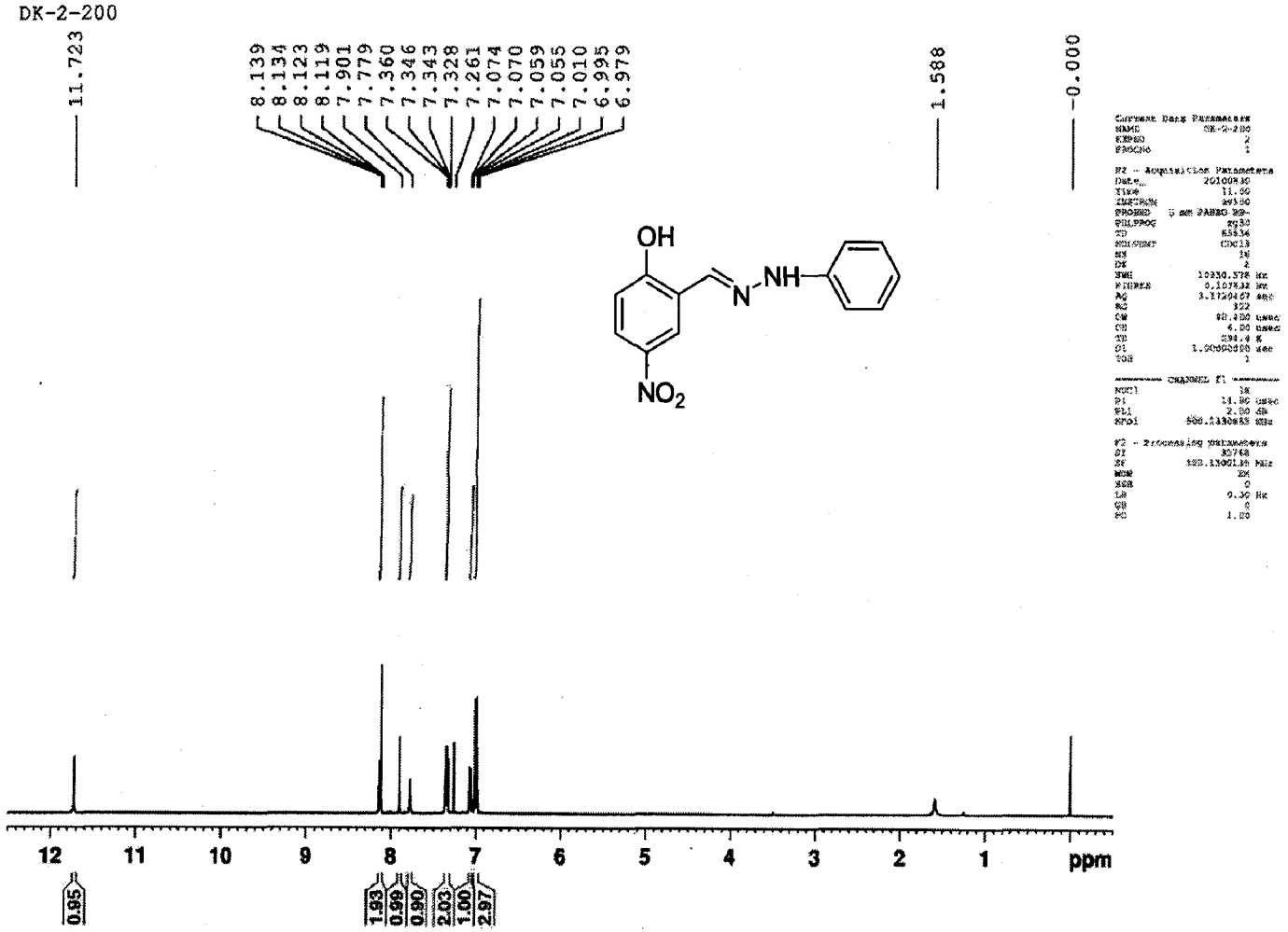

Figure S2. ^{1}H NMR Spectra of **3a**

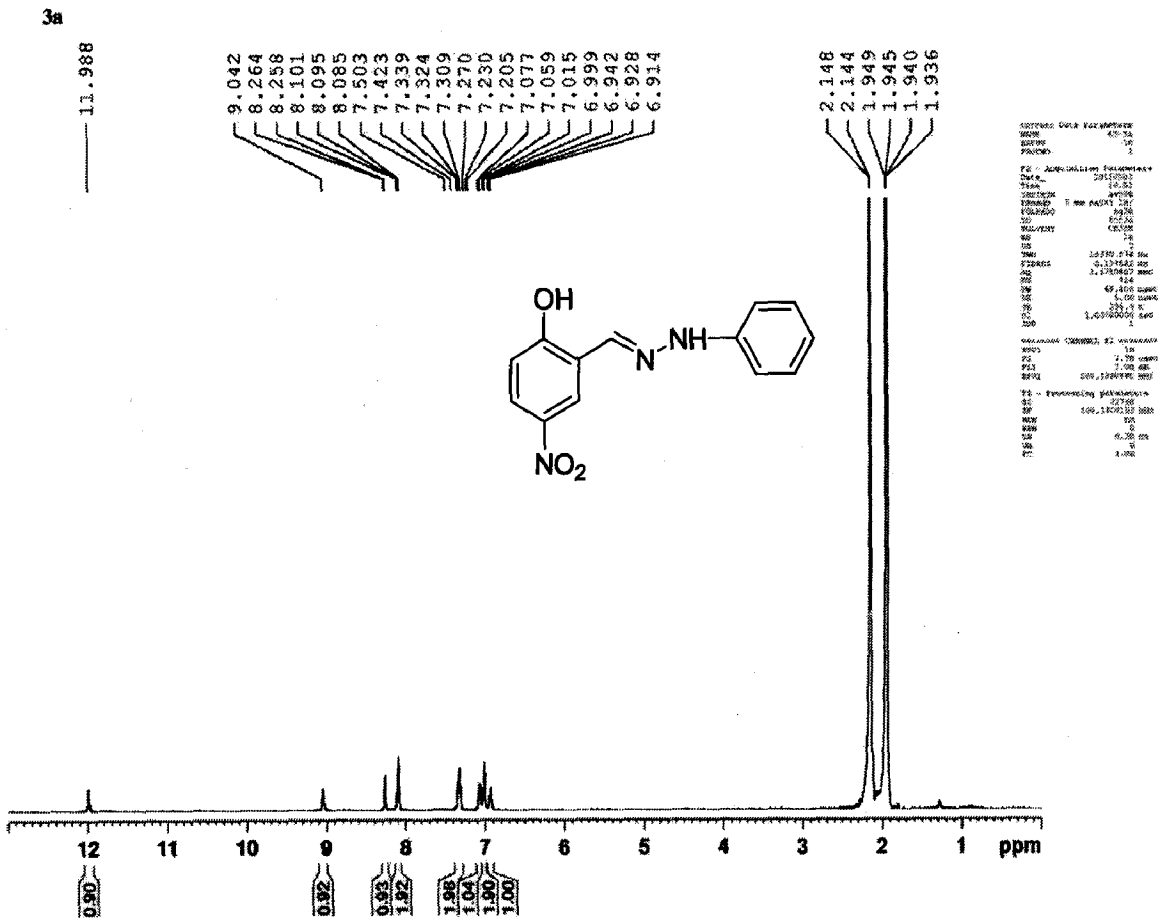

Figure S3. ^{1}H NMR Spectra of **3a** Expansion

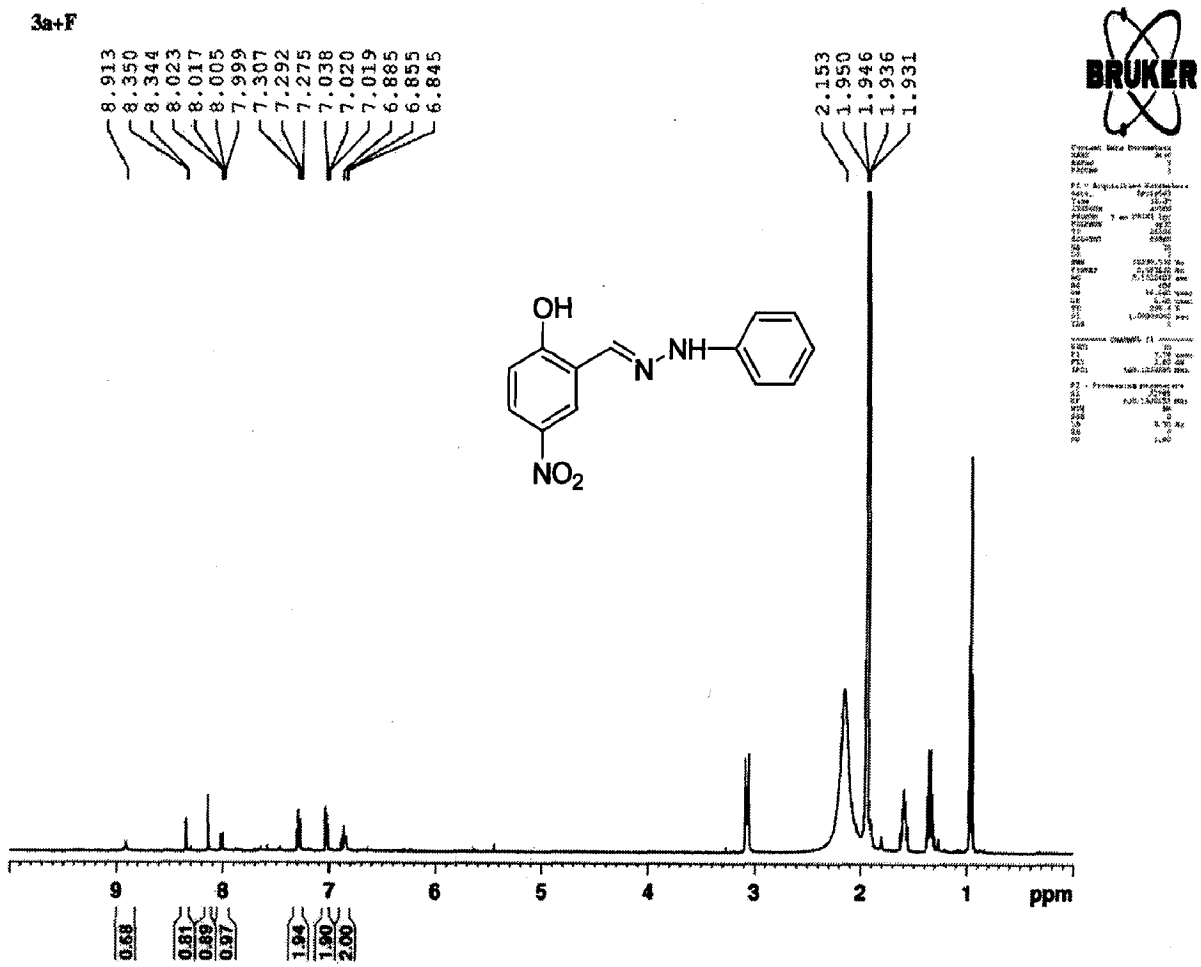

Figure S4. ^{1}H NMR Spectra of **3a+F** Expansion

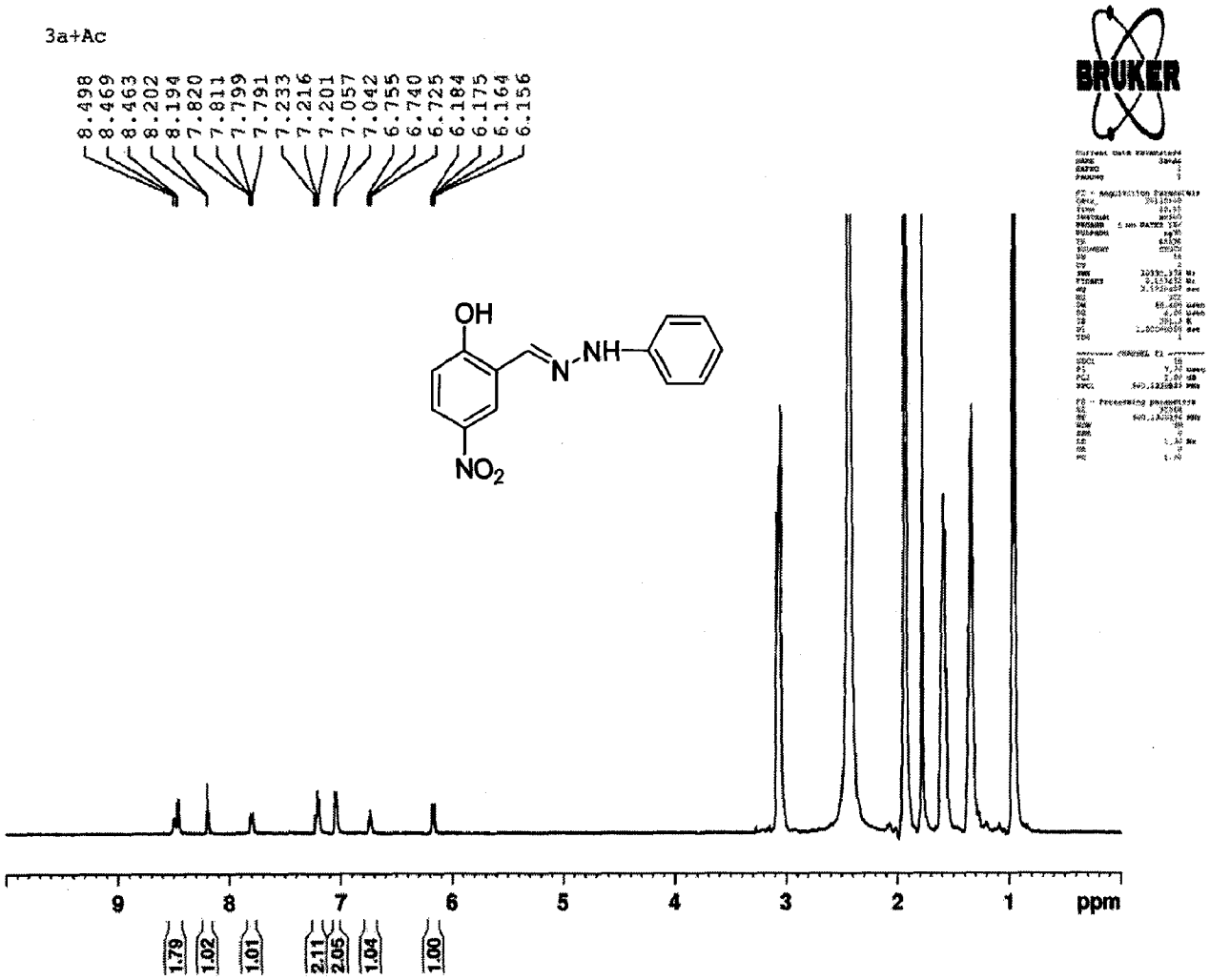

Figure S5. ^{1}H NMR Spectra of **3a**+CH_3COO^- Expansion

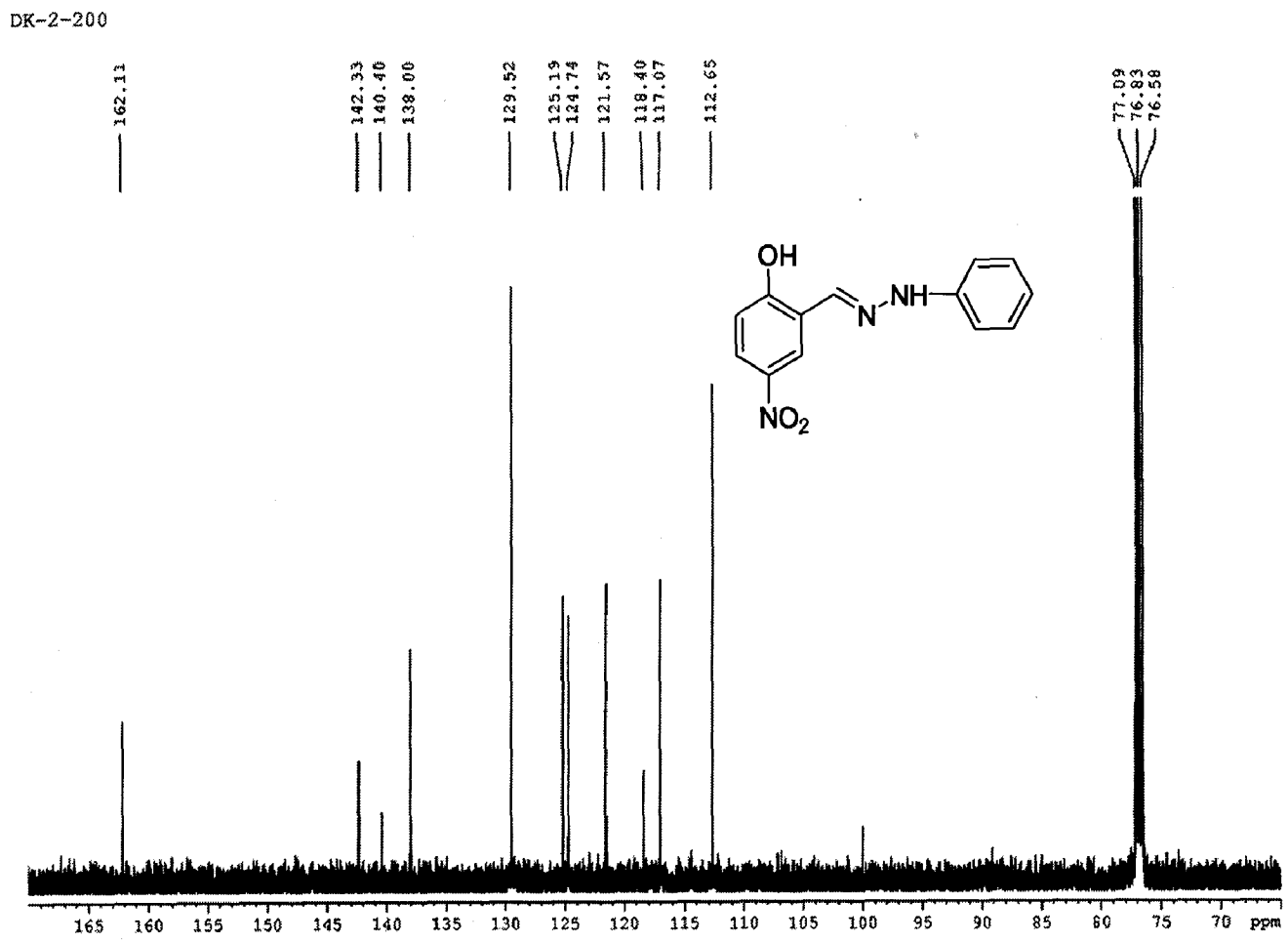

Figure S6. ^{13}C NMR Spectra of **3a**

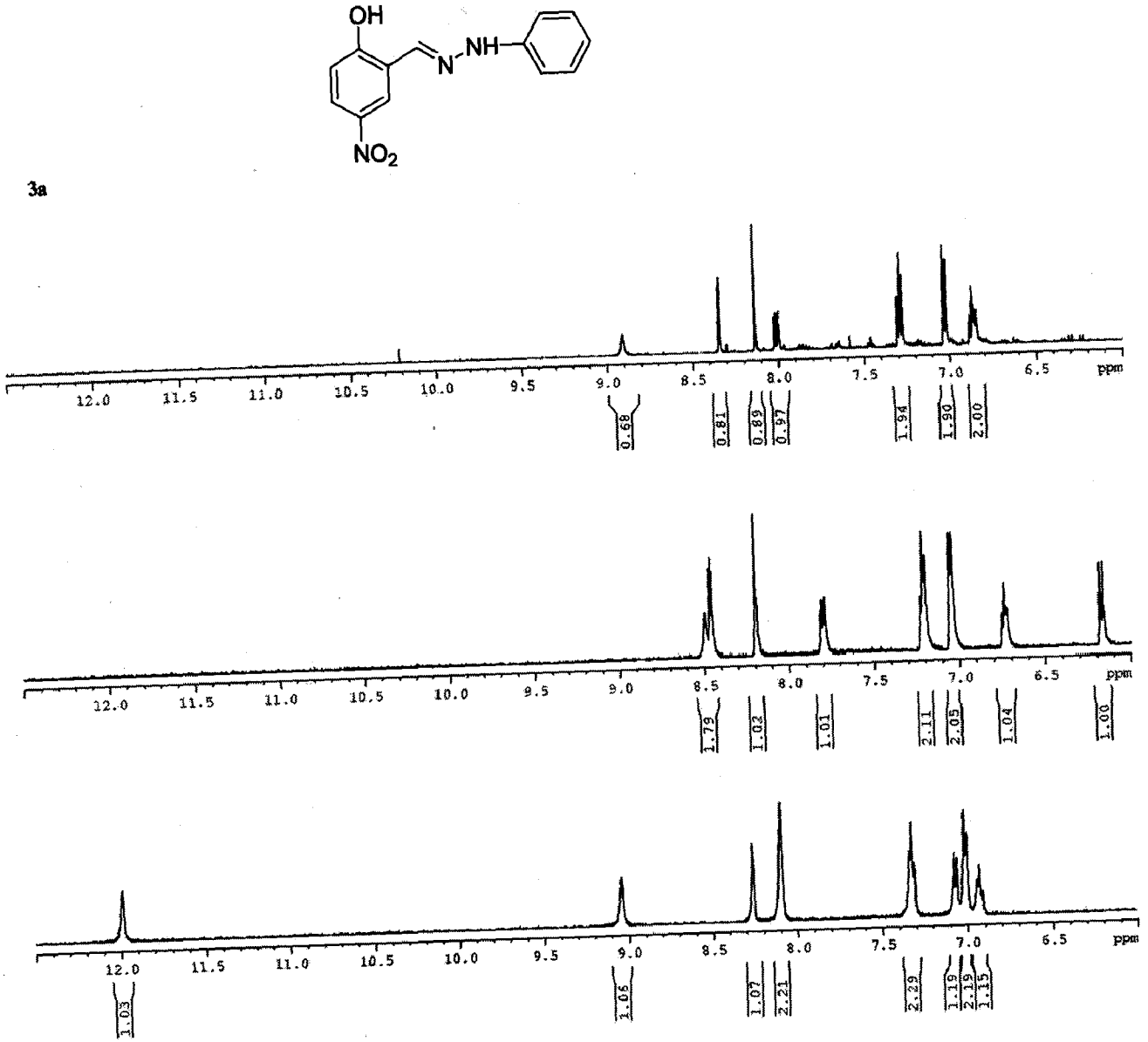

Figure S7. Comparison of ^{1}H NMR Spectra of **3a, 3a+CH_3COO^- and 3a+F^-**

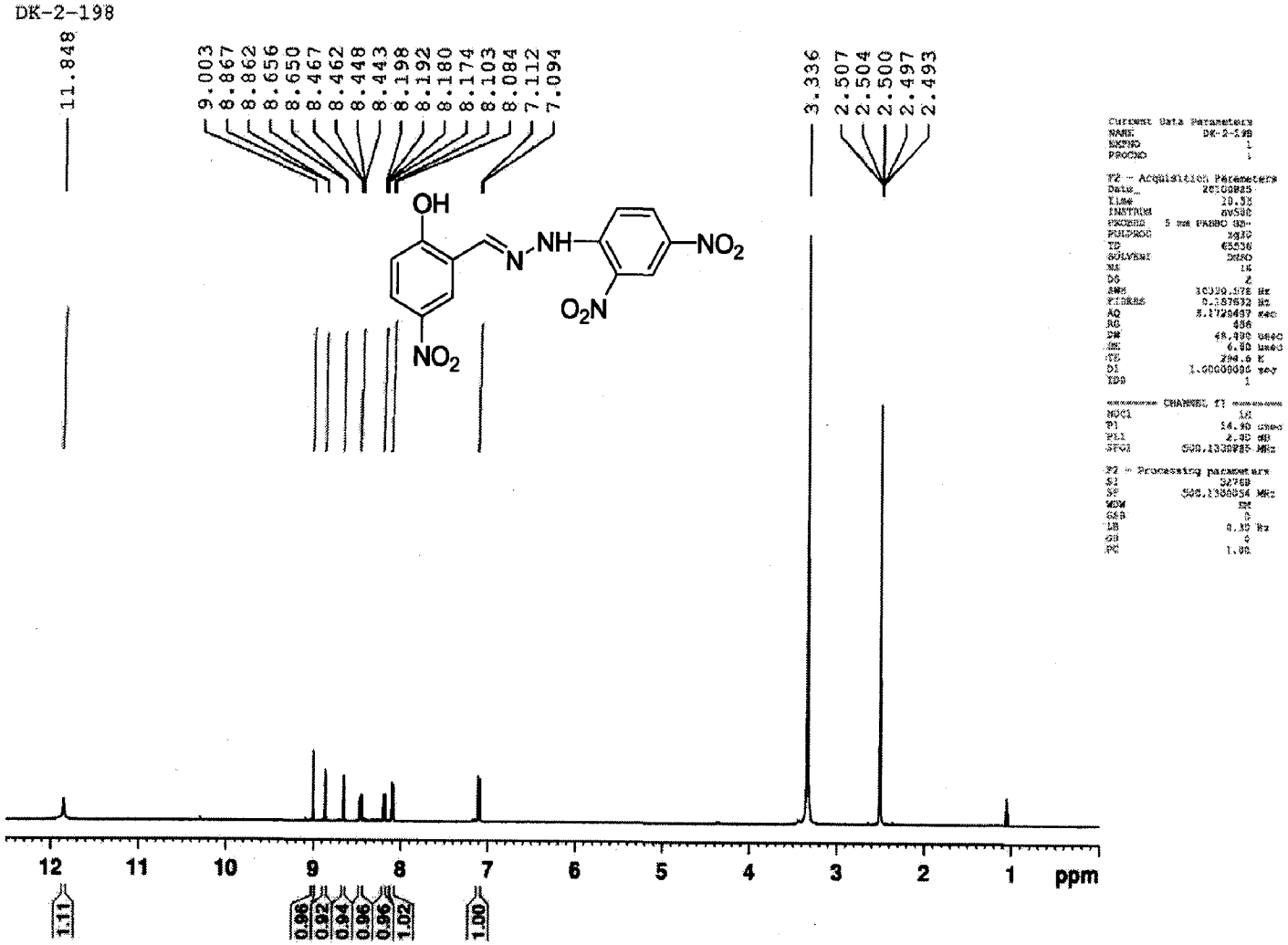

Figure S8. ^{1}H NMR Spectra of **3b**

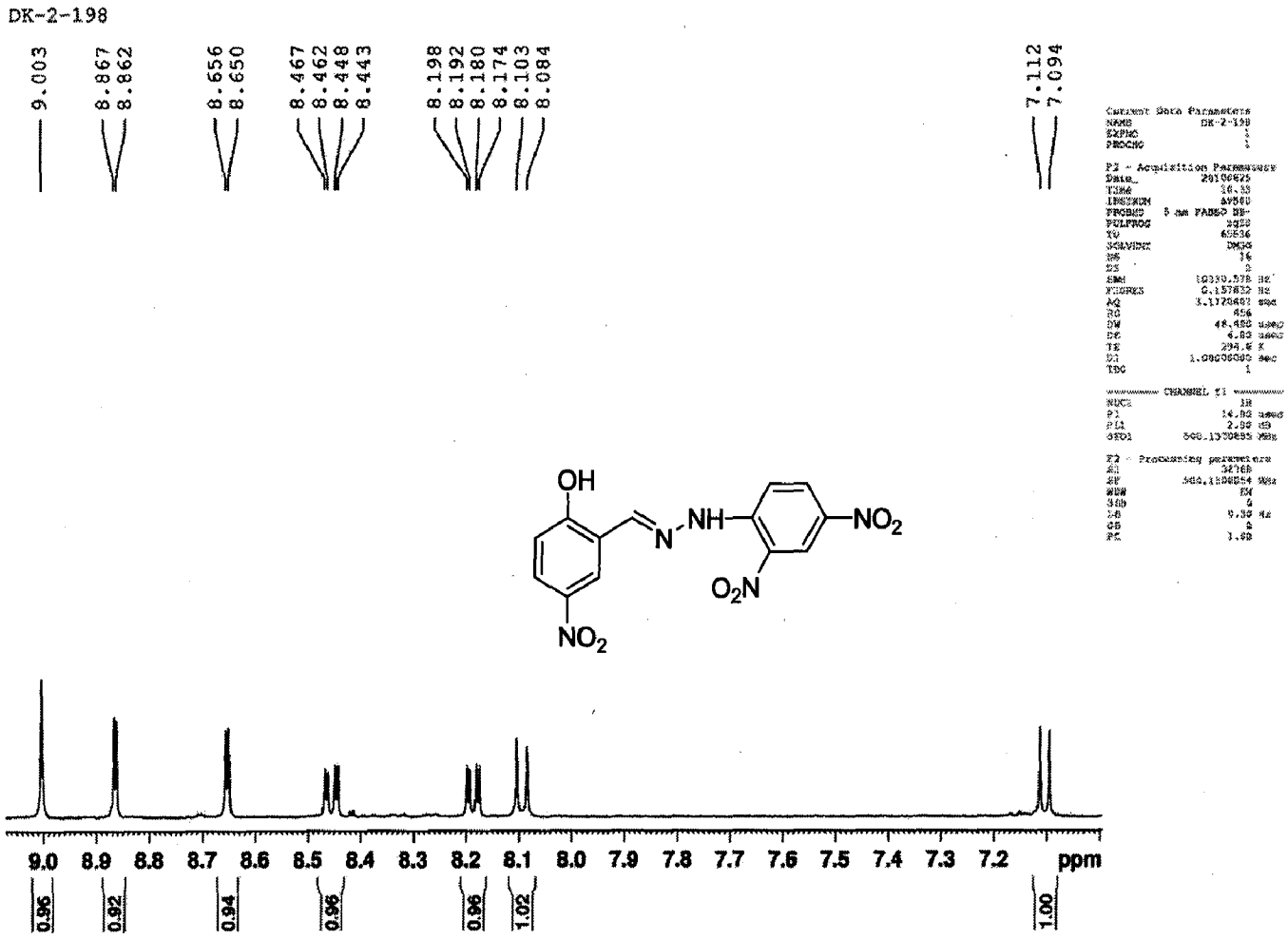

Figure S9. ^{1}H NMR Spectra of **3b** Expansion

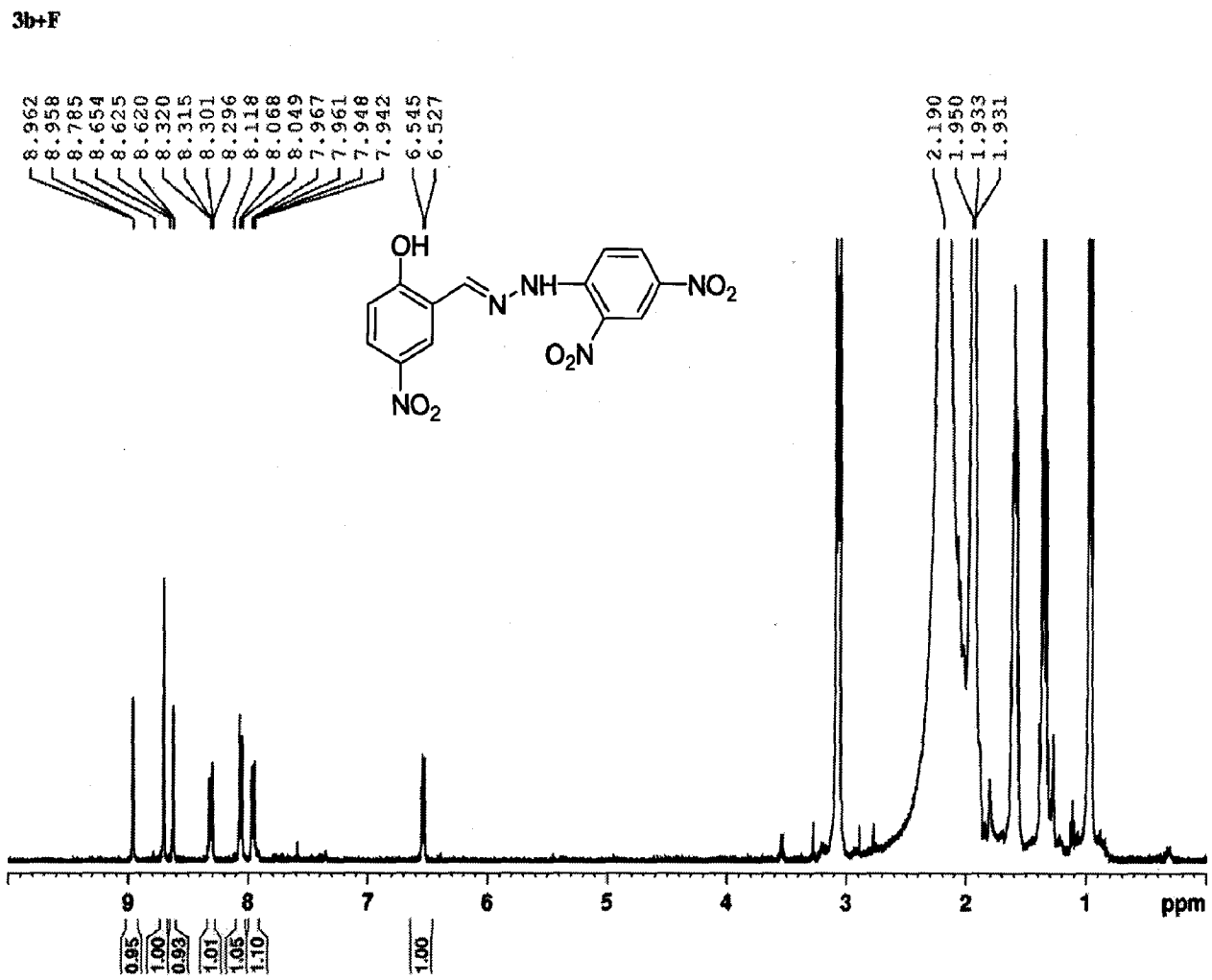

Figure S10. ^{1}H NMR Spectra of **3b+F**$^{-}$ Expansion

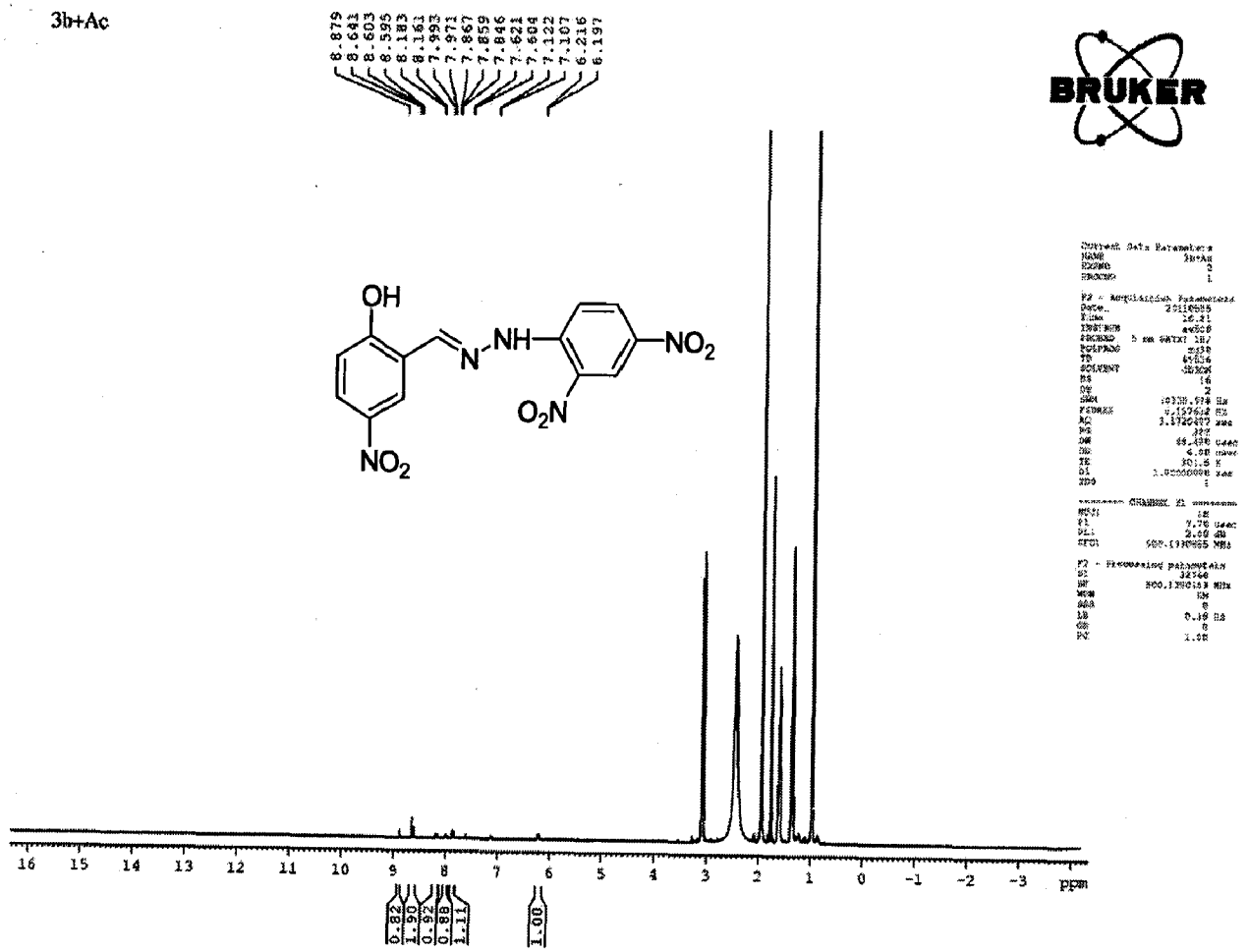

Figure S11. ^{1}H NMR Spectra of **3b+CH_3COO^-** Expansion

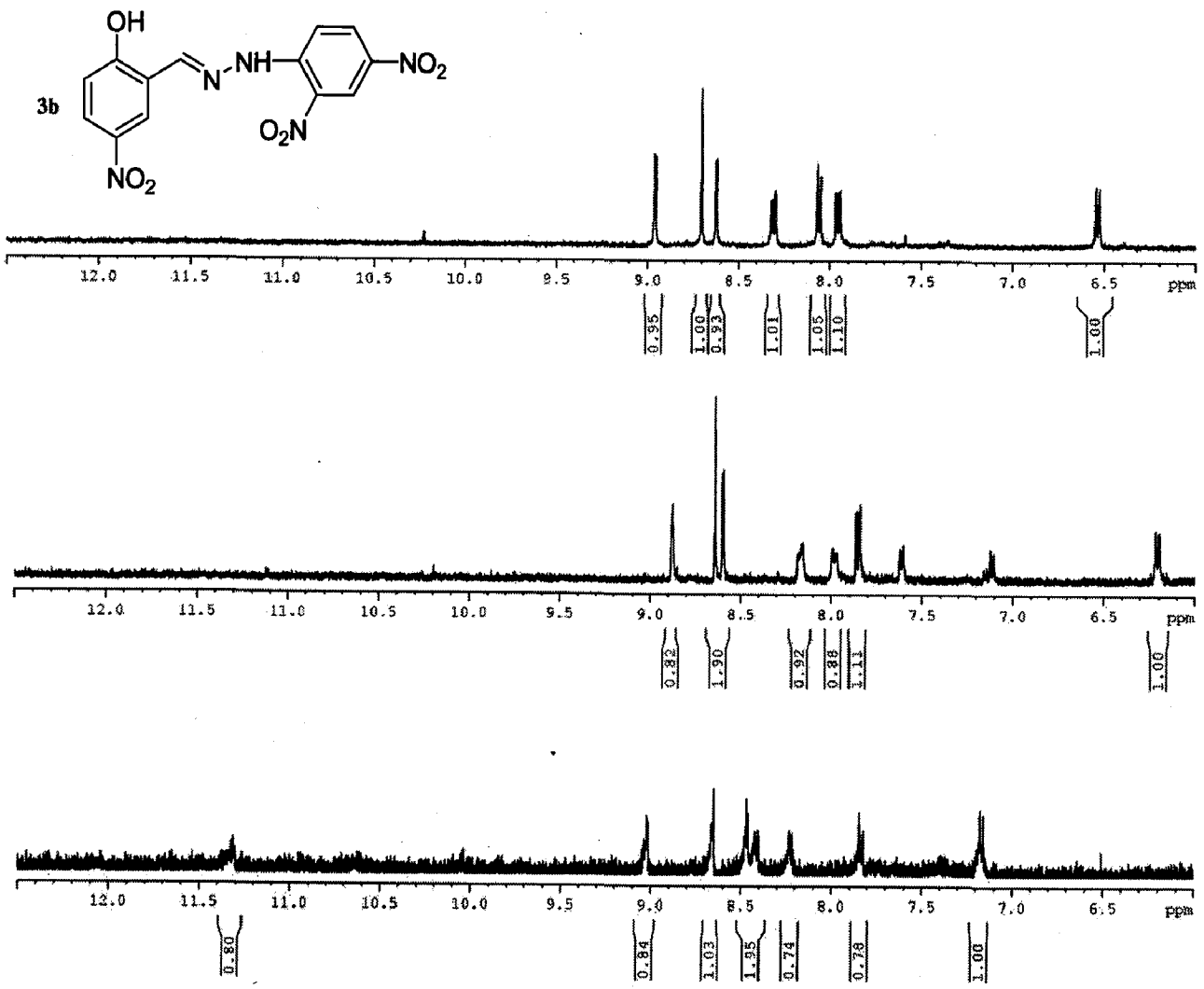

Figure S12. Comparison of ^{1}H NMR Spectra of **3b, 3b+CH_3COO^- and 3b+F^-**

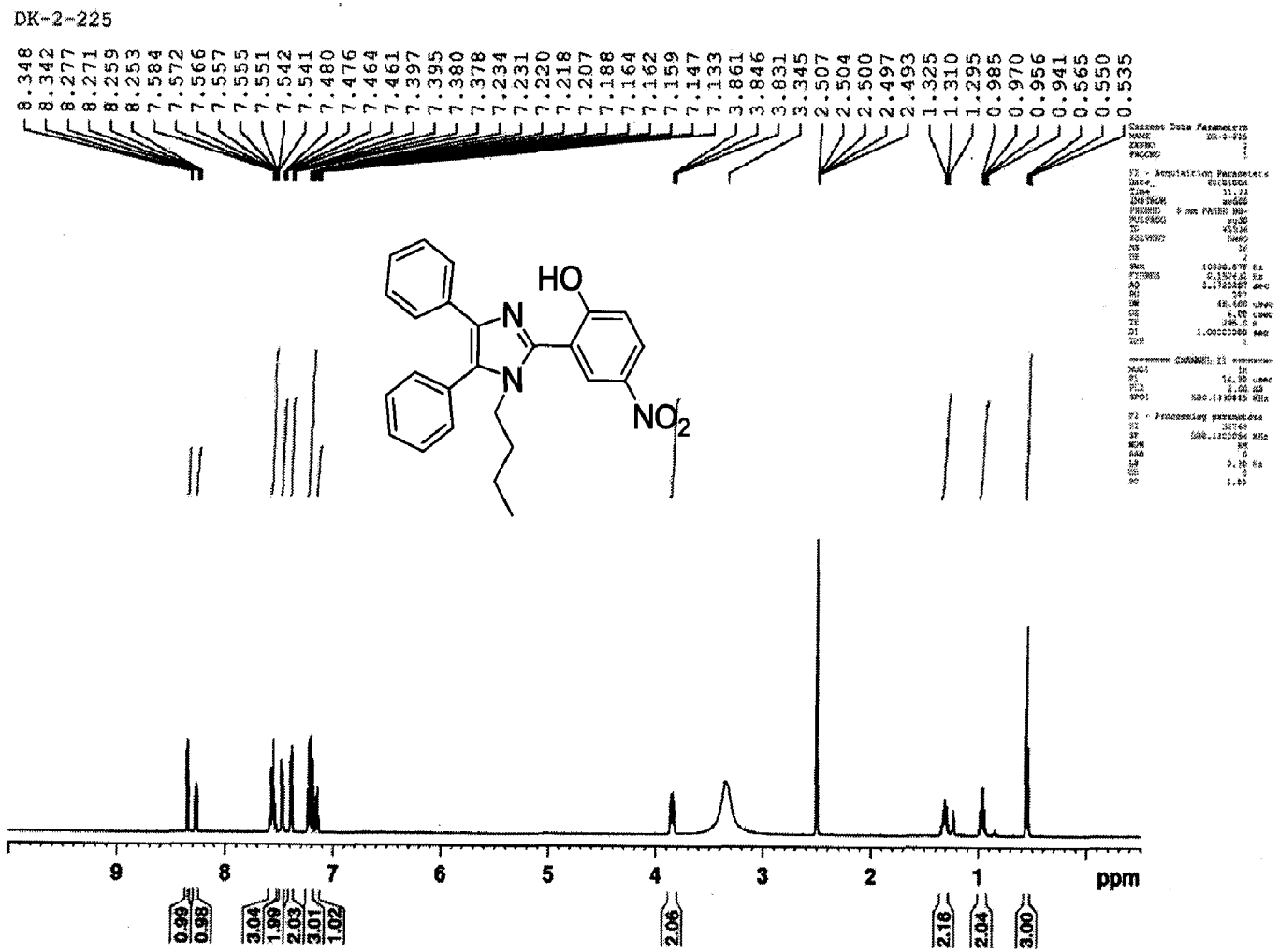

Figure S13. ^{1}H NMR Spectra of **4a**

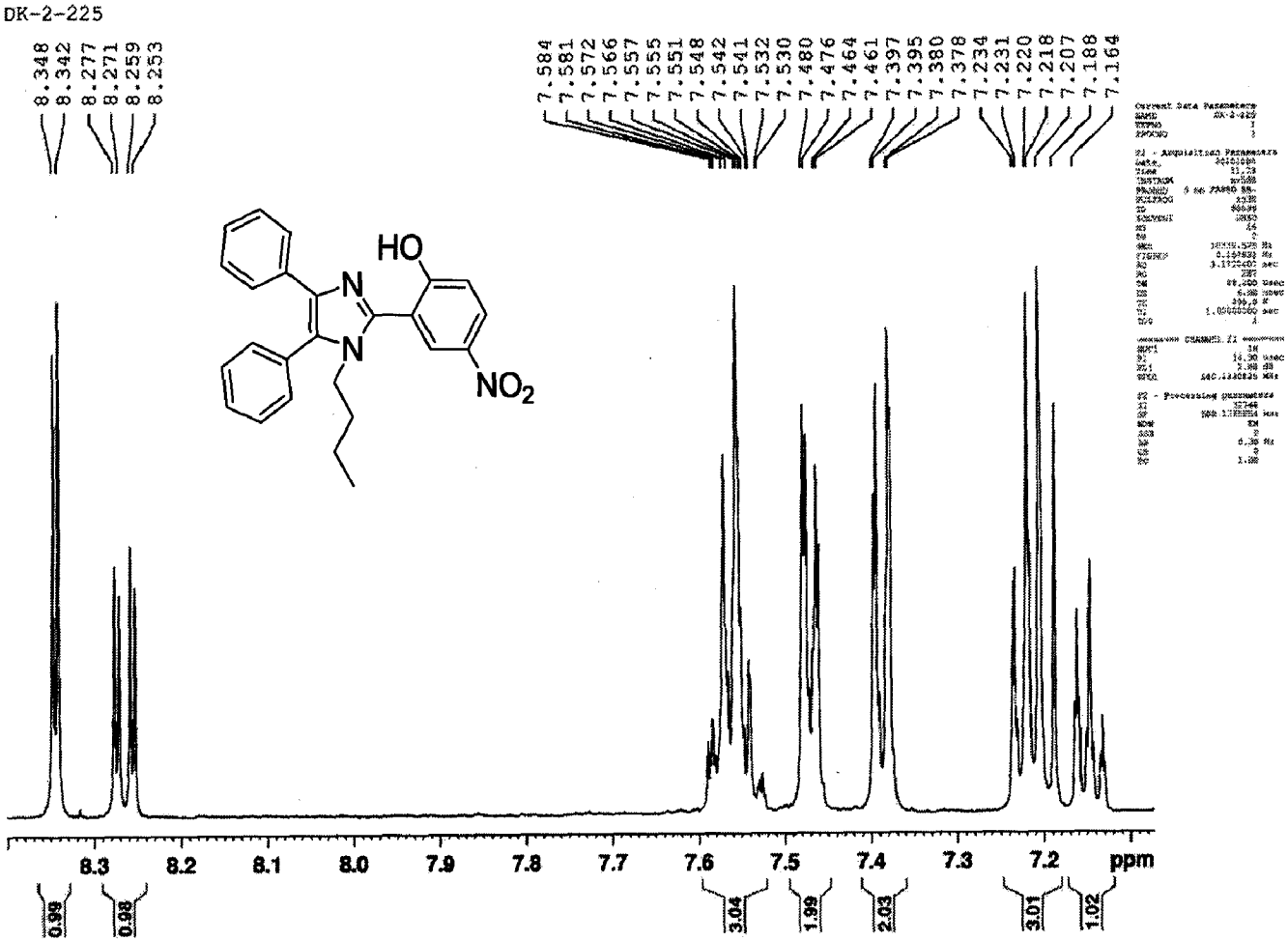

Figure S14. ^{1}H NMR Spectra of **4a** Expansion

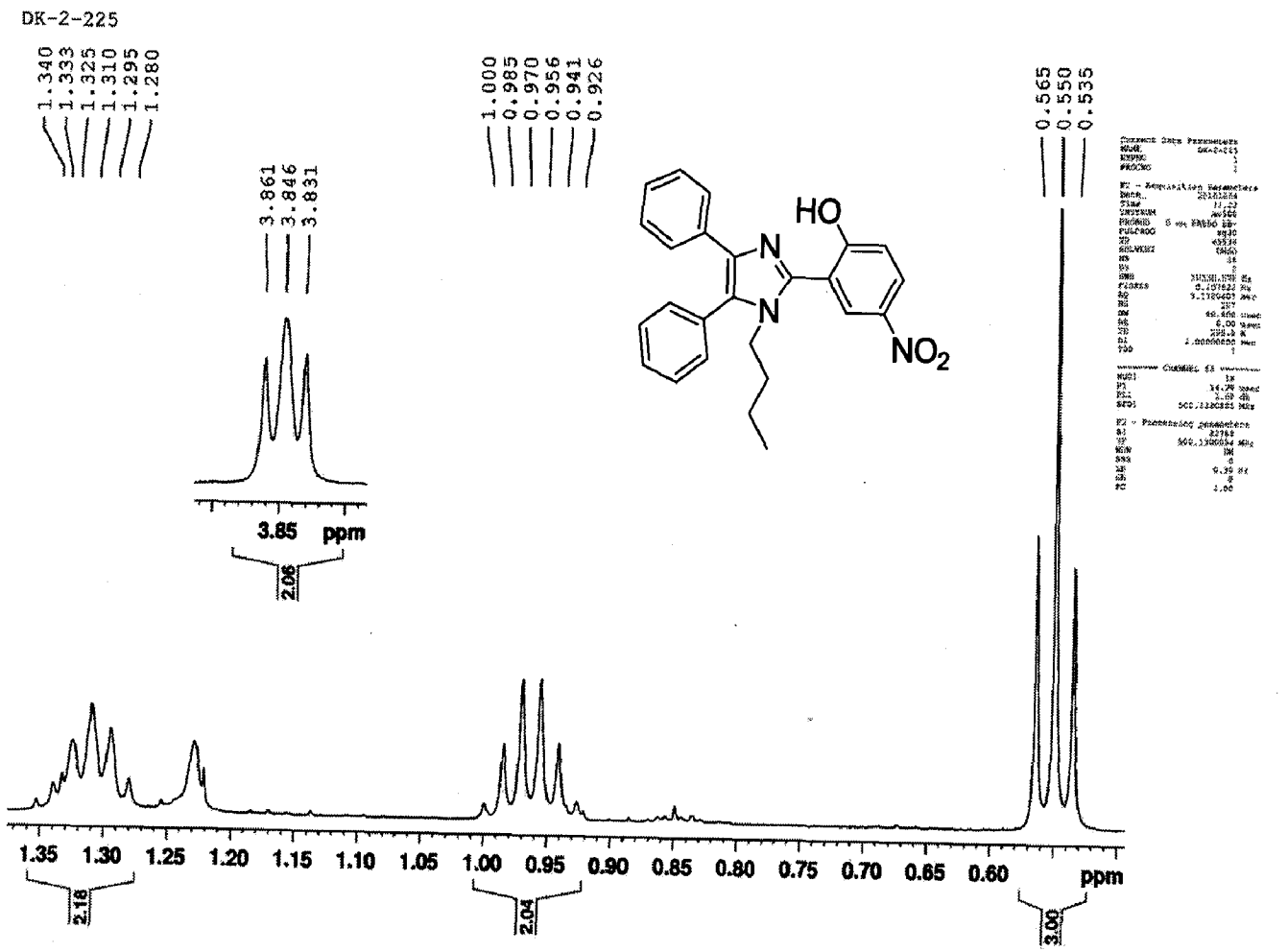

Figure S15. ^{1}H NMR Spectra of **4a** Expansion

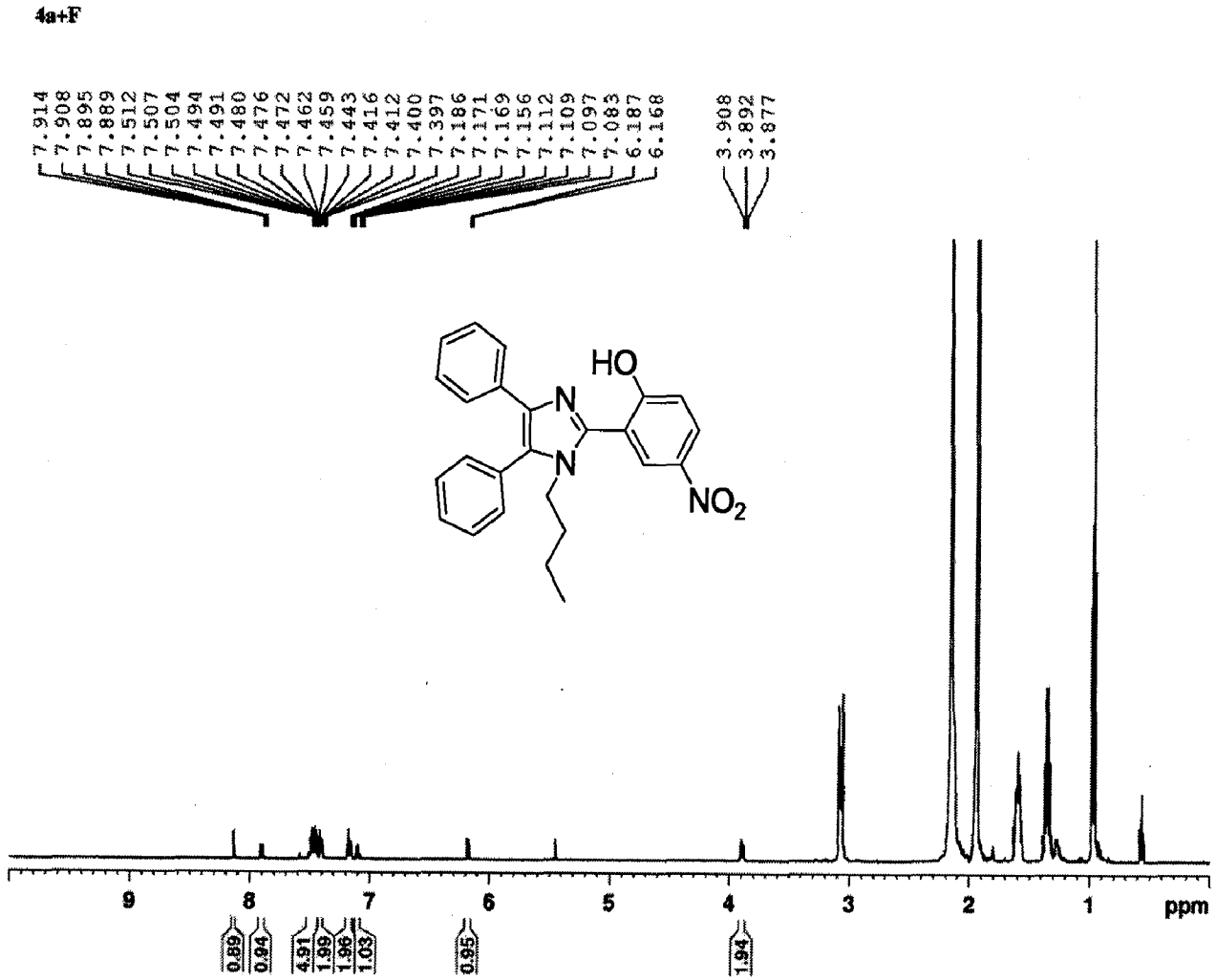

Figure S16. ^{1}H NMR Spectra of **4a**+ **F**$^{-}$ Expansion

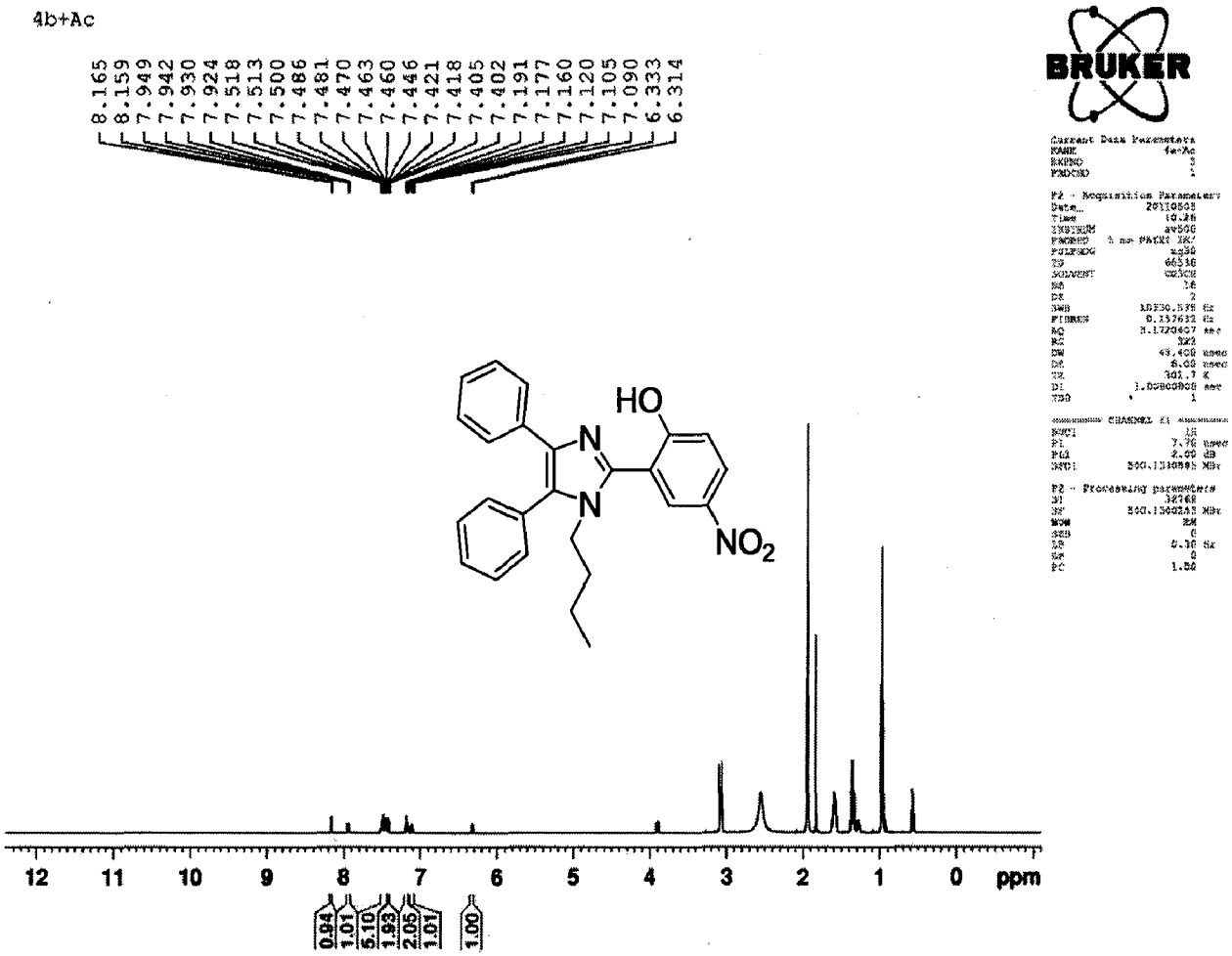

Figure S17. ^{1}H NMR Spectra of **4a**+CH_3COO^- Expansion

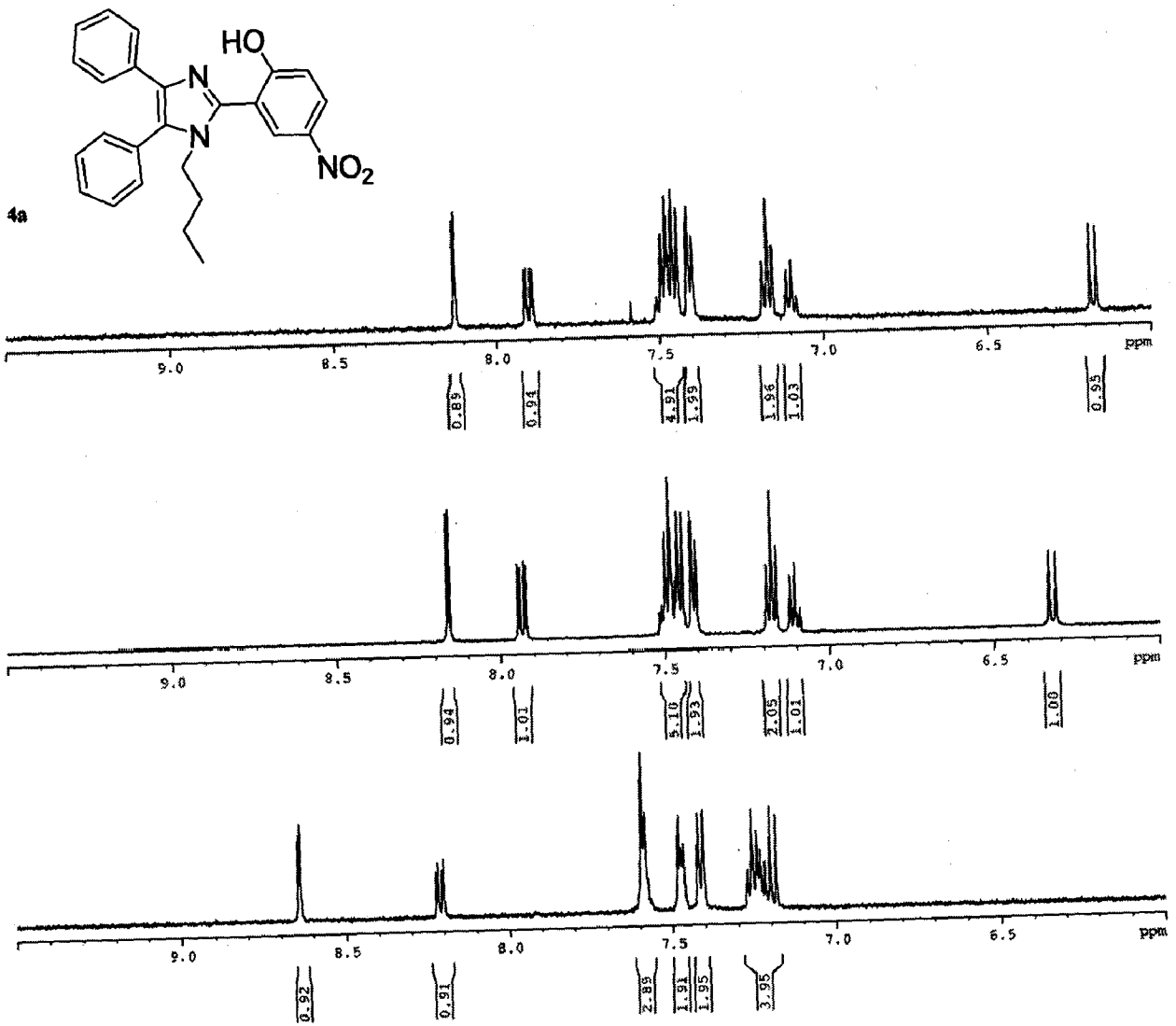

Figure S18. Comparison of ^{1}H NMR Spectra of **4a, 4a+CH_3COO^- and 4a+F^-**

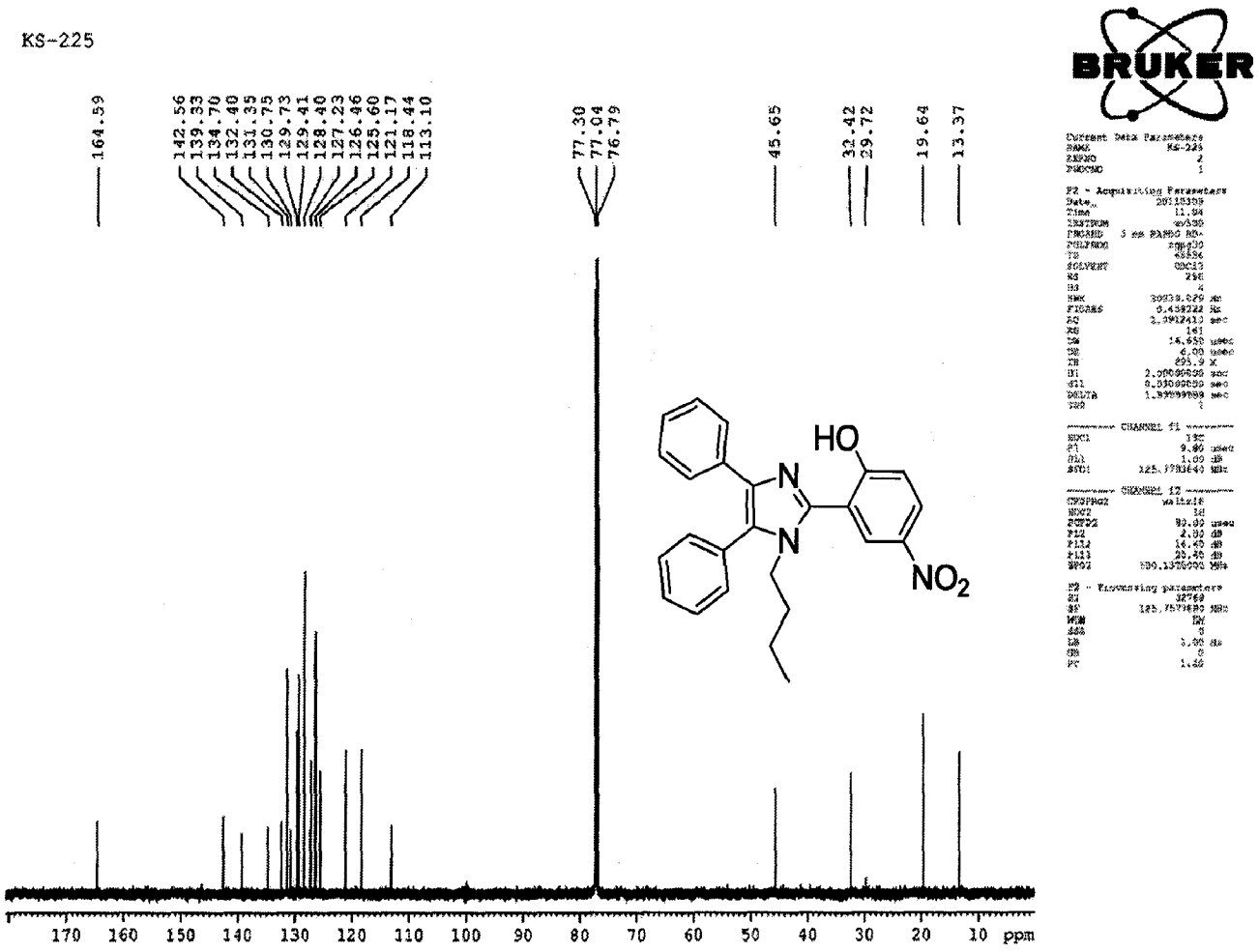

Figure S19. ^{13}C NMR Spectra of **4a**

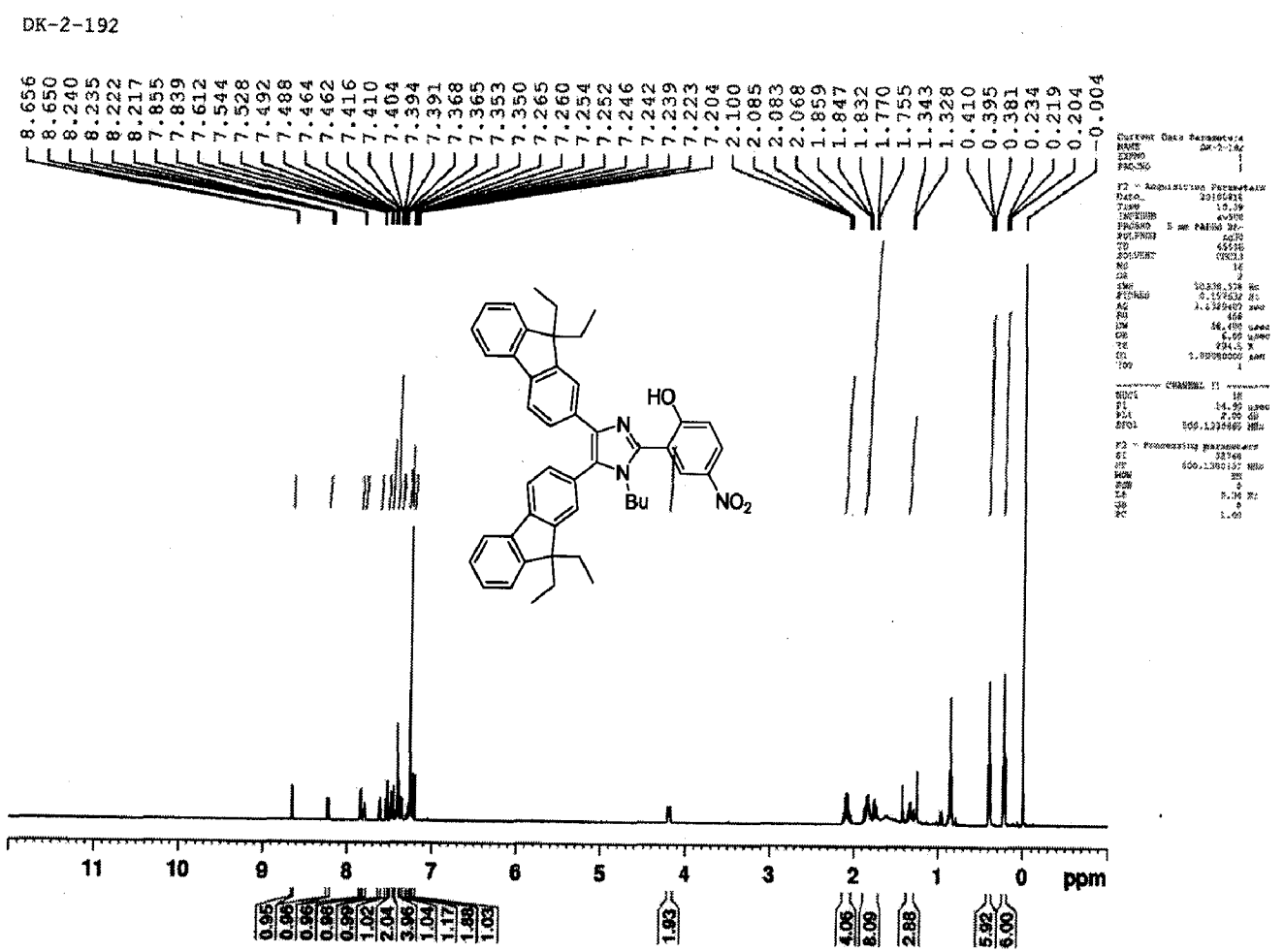

Figure S20. ^{1}H NMR Spectra of **4b**

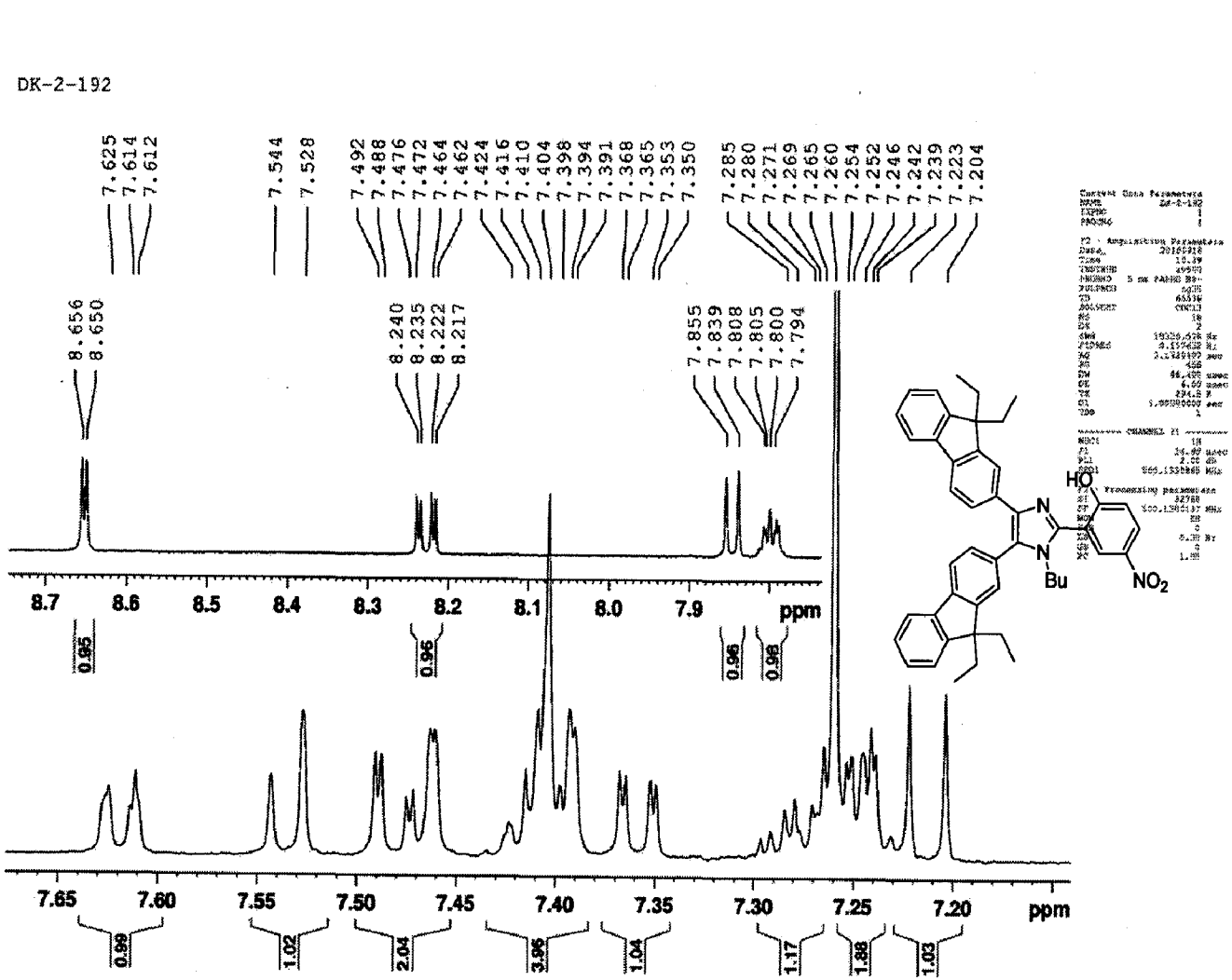

Figure S21. ^{1}H NMR Spectra of **4b**

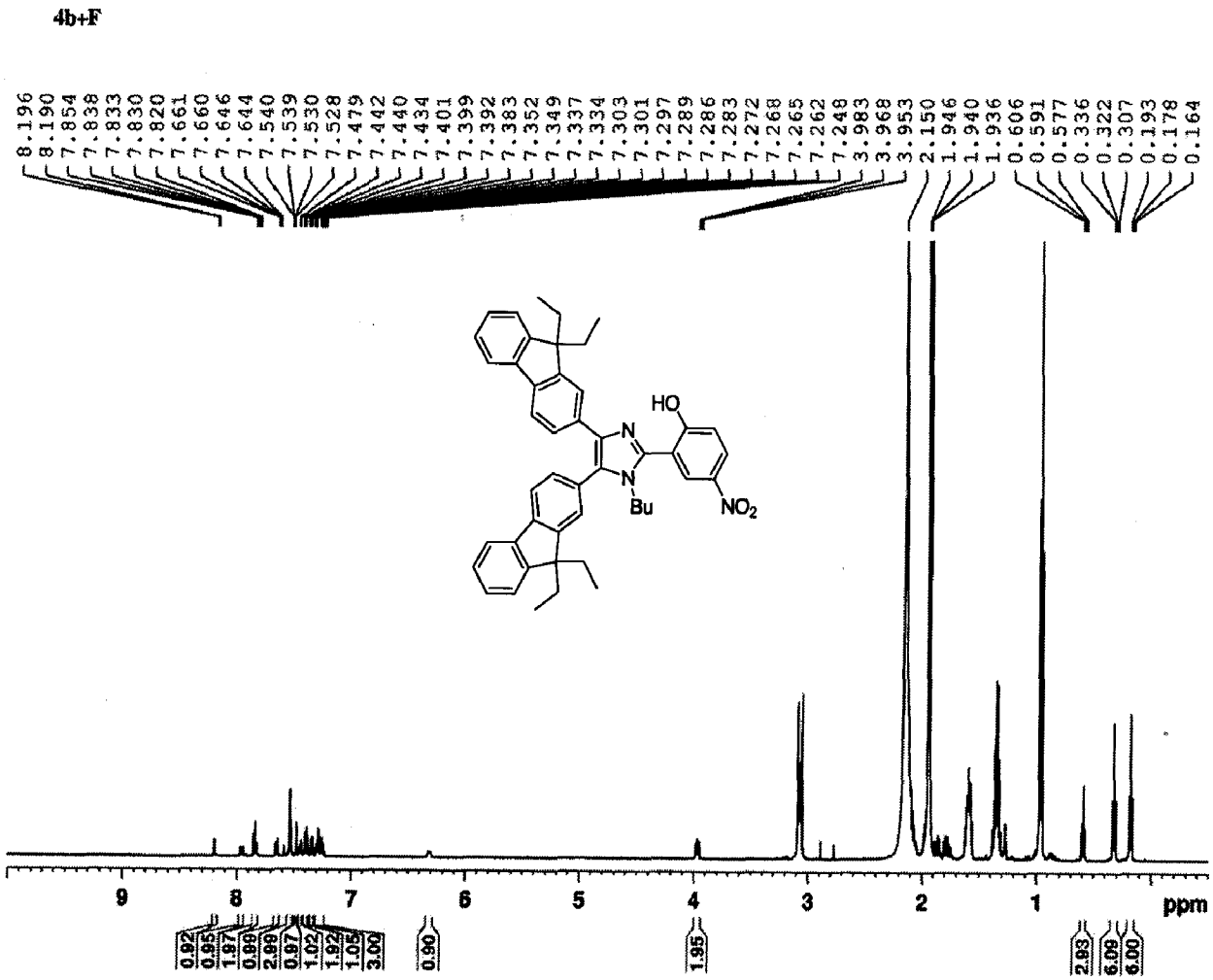

Figure S22. ^{1}H NMR Spectra of **4b+F** Expansion

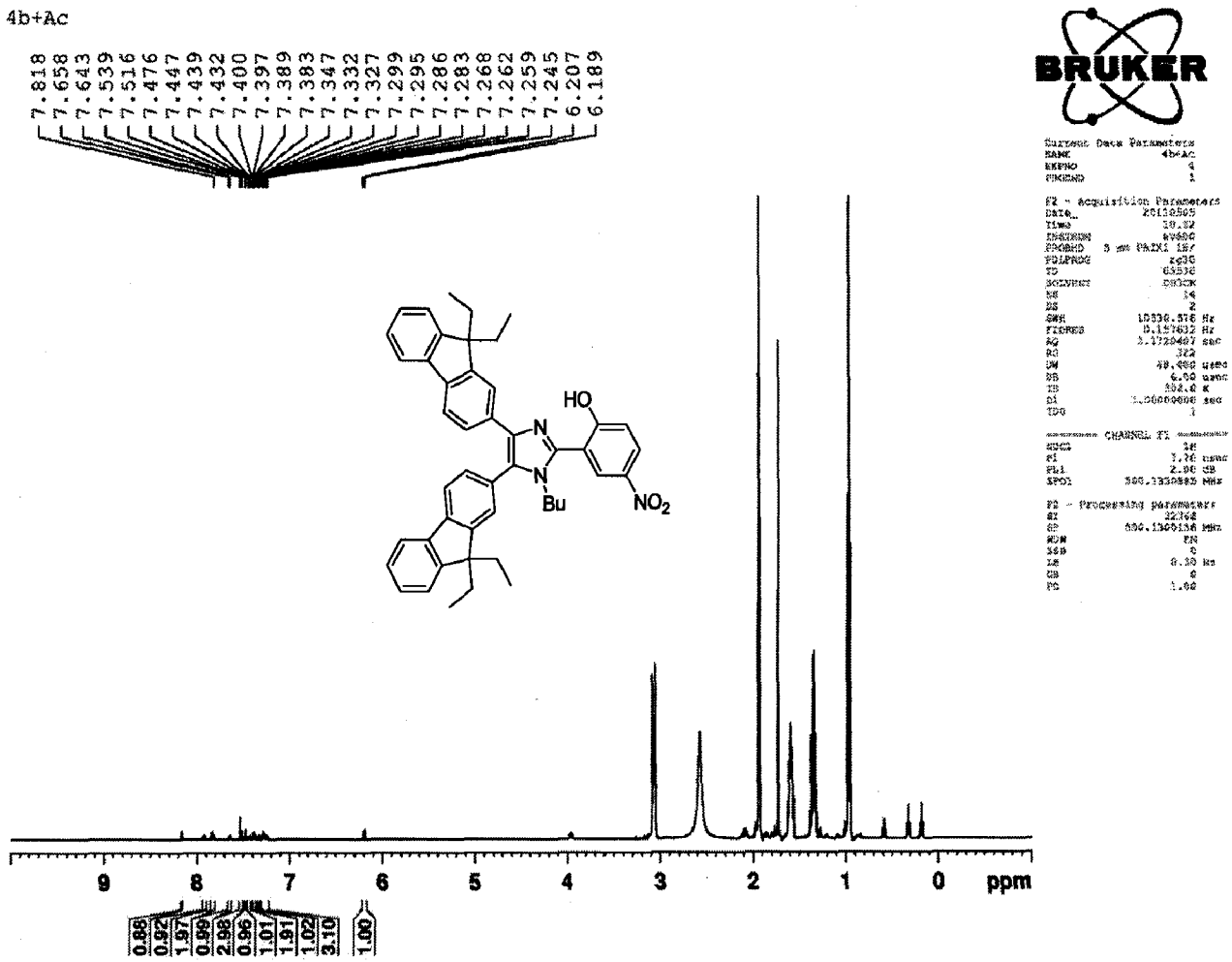

Figure S23. ^{1}H NMR Spectra of **4b+CH_3COO^-** Expansion

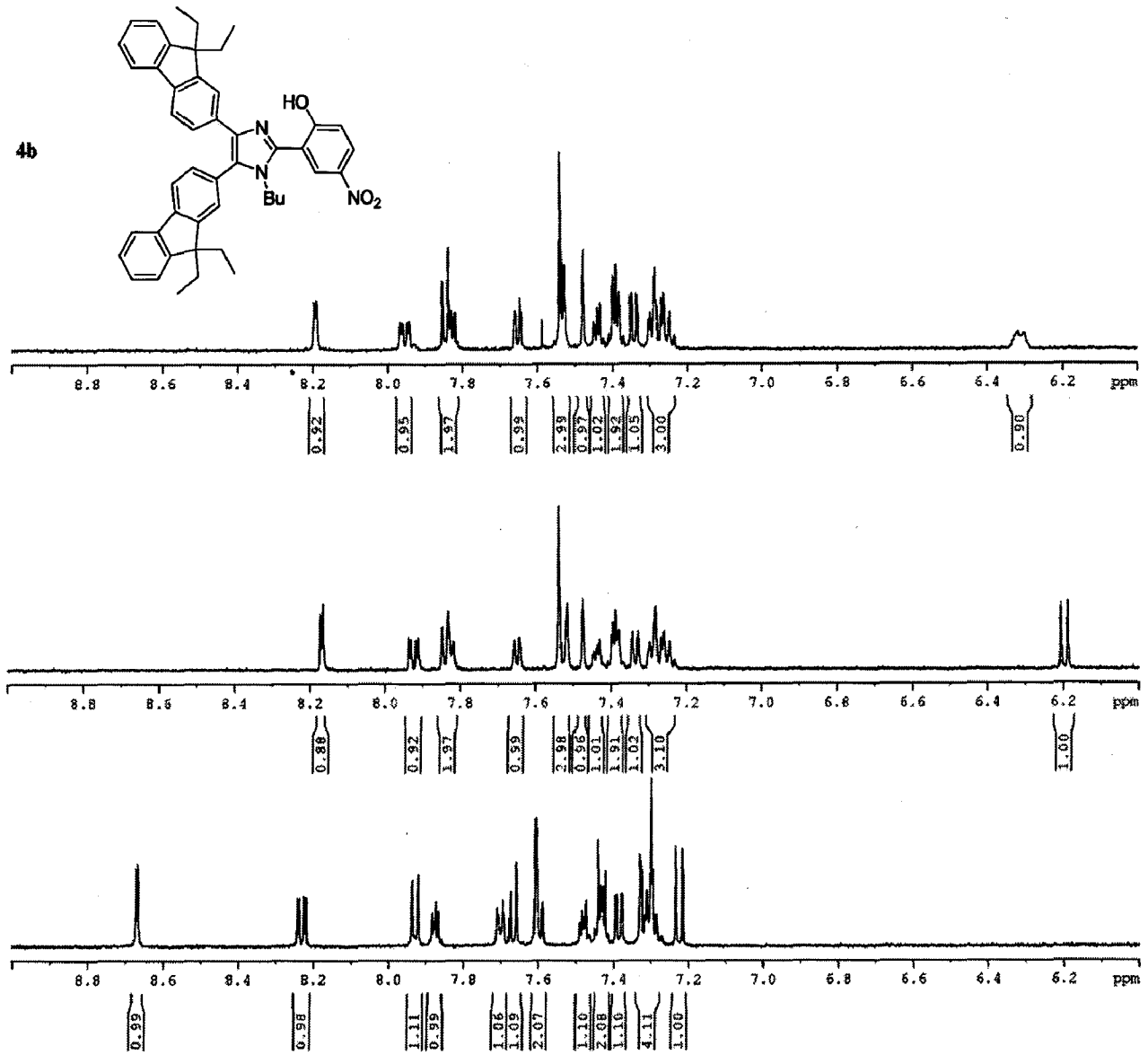

Figure S24. Comparison of ^{1}H NMR Spectra of **4b, 4b+CH_3COO^- and 4b+F^-**

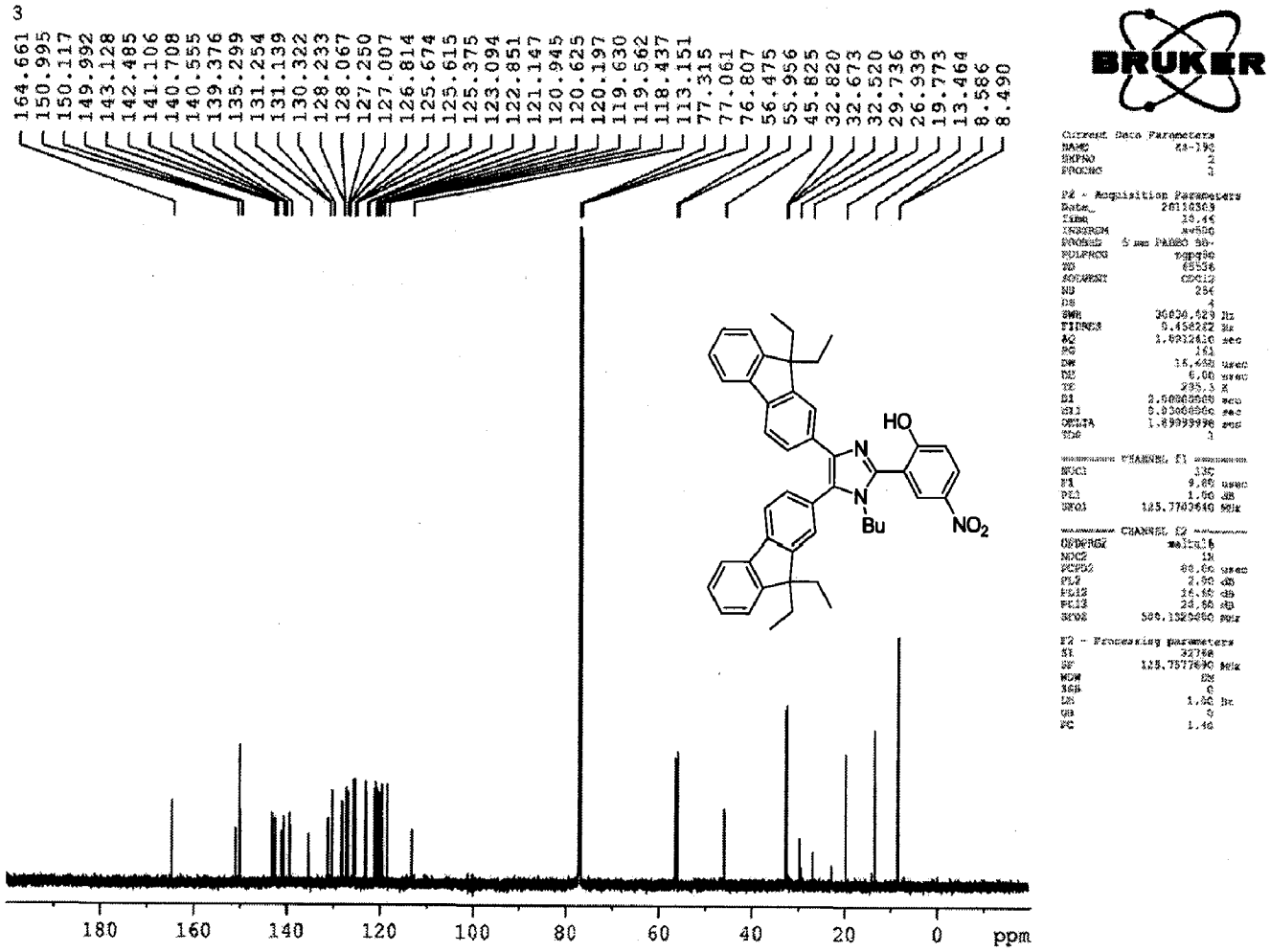

Figure S25. ^{13}C NMR Spectra of **4b**

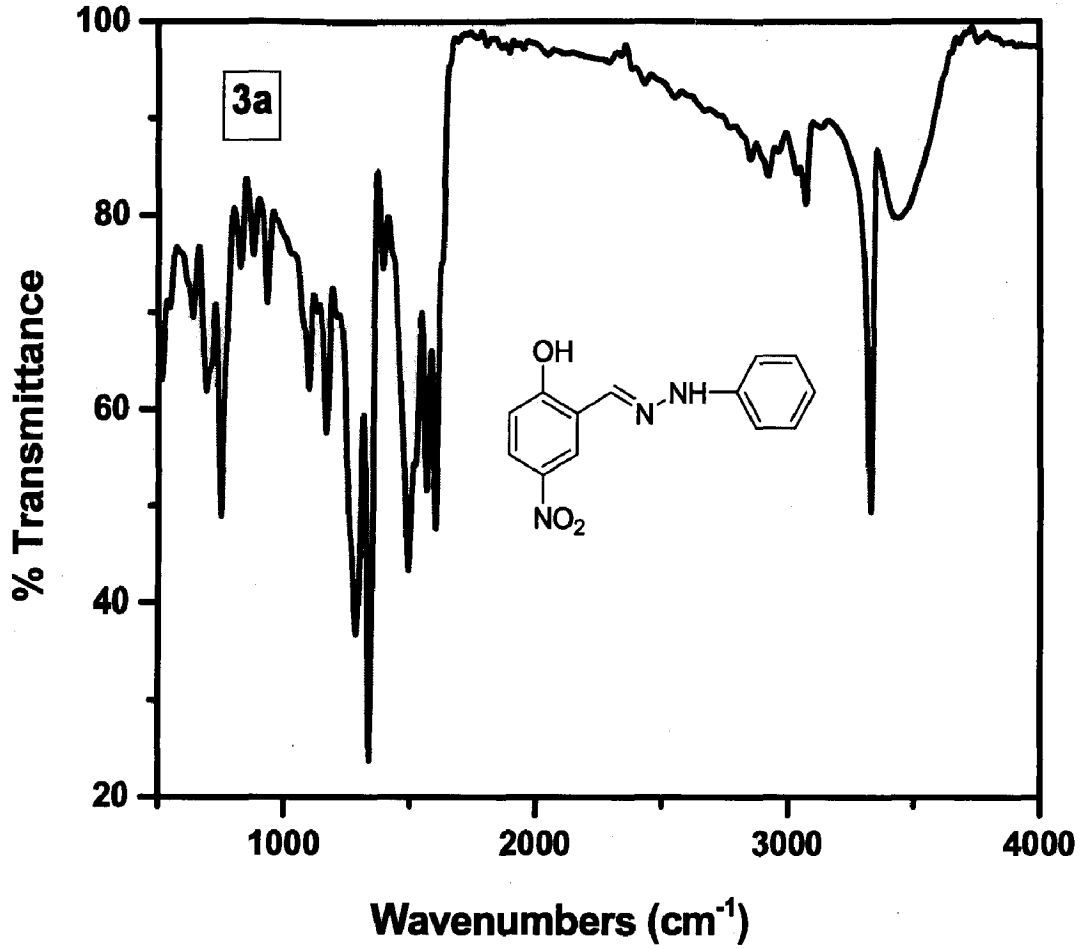

Figure S26. IR Spectra of **3a**

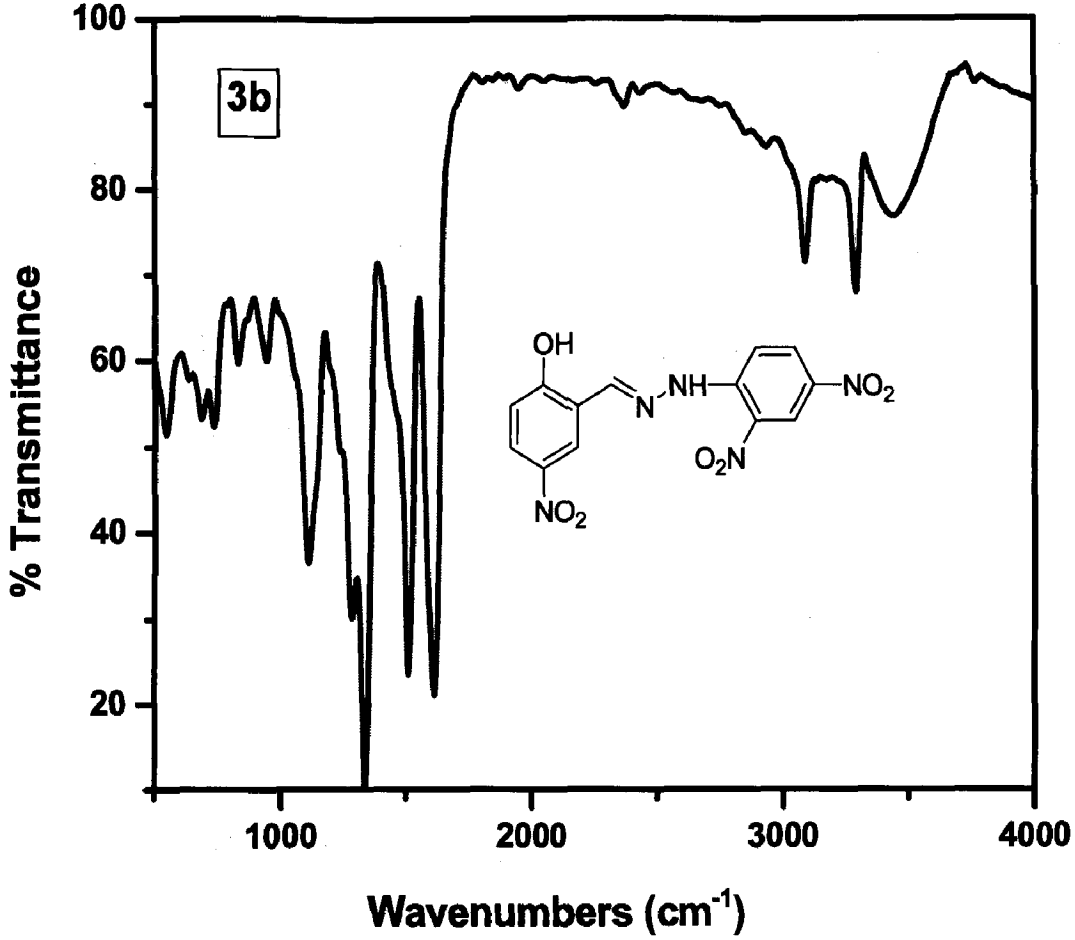

Figure S27. IR Spectra of **3b**

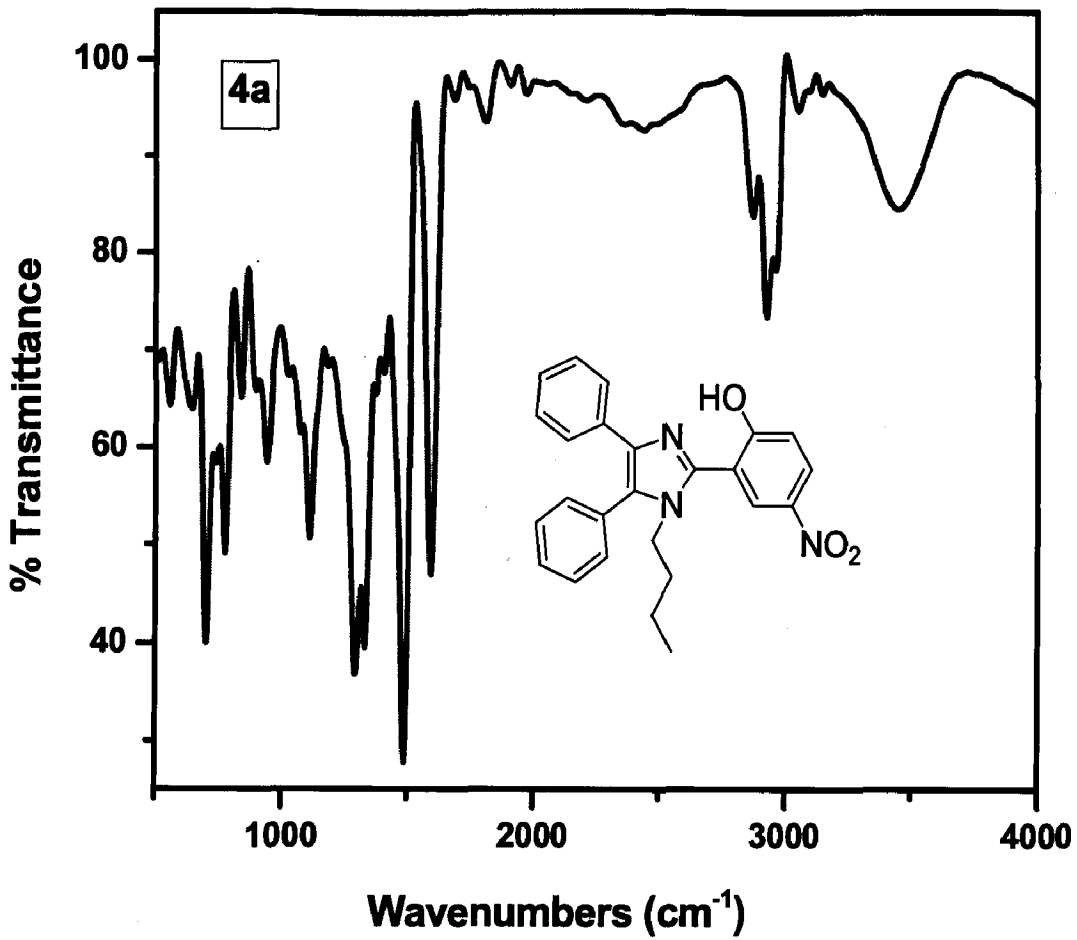

Figure S28. IR Spectra of **4a**

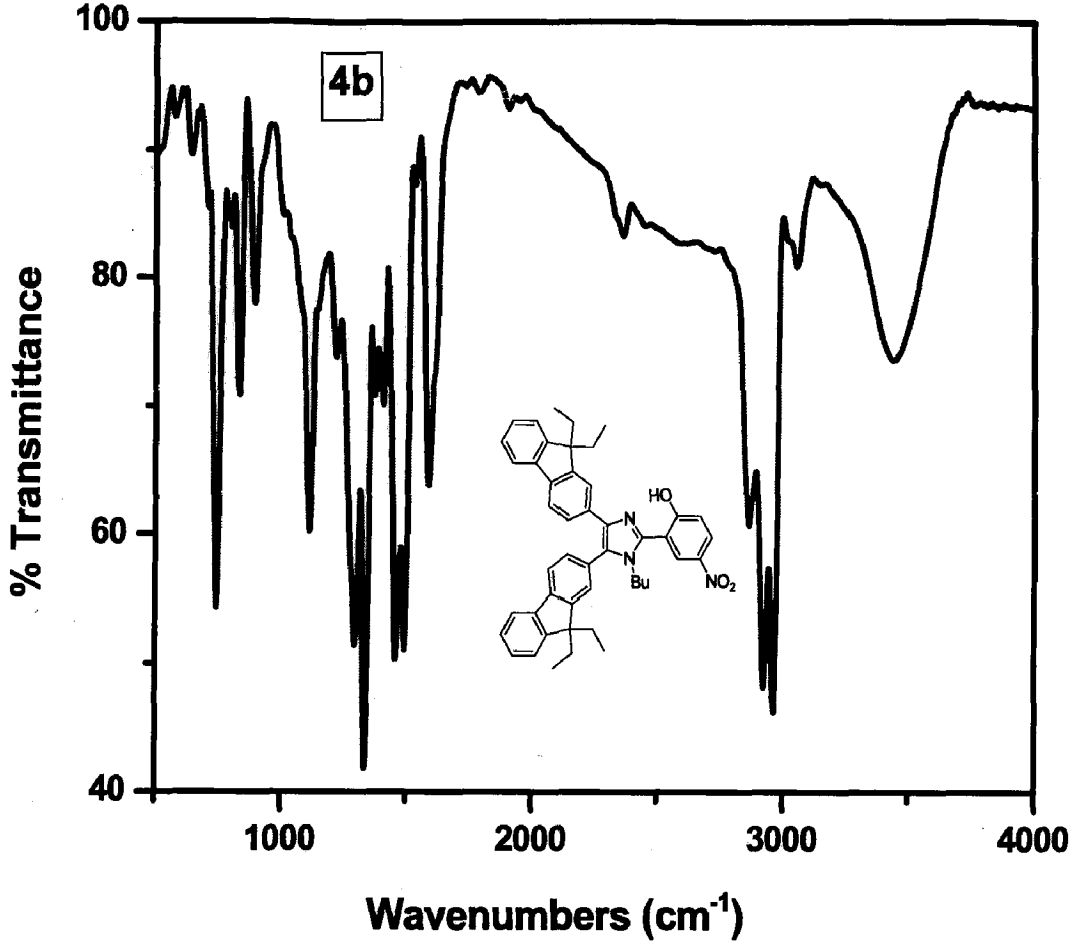

Figure S26. IR Spectra of **4b**